THESIS ON NATURAL AND EXACT SCIENCES B242

Chromatographic Analysis of Cyclohexano-Substituted Hemicucurbiturils and Characterization of their Intermediates with Mass Spectrometry

MARIA FOMITŠENKO

TTÜ PRESS

TALLINN UNIVERSITY OF TECHNOLOGY
School of Science
Department of Chemistry and Biotechnology

This dissertation was accepted for the defence of the degree of Doctor of Philosophy in Chemistry on October 24, 2017

Supervisors: Assoc. Prof. Riina Aav, Department of Chemistry and Biotechnology, School of Science, Tallinn University of Technology, Estonia

Reviewed by: Prof. Mihkel Kaljurand, Department of Chemistry and Biotechnology, School of Science, Tallinn University of Technology, Estonia

Opponents: Assoc. Prof. Michael Pittelkow, Department of Chemistry, University of Copenhagen, Denmark

Assoc. Prof. Koit Herodes, Institute of Chemistry, Faculty of Science and Technology, University of Tartu, Estonia

Defense of the thesis: December 12, 2017

Declaration:

Hereby I declare that this doctoral thesis, my original investigation and achievement, submitted for the doctoral degree at Tallinn University of Technology has not been submitted for doctoral or equivalent academic degree.

/Maria Fomitšenko/

ISSN 1406-4723
ISBN 978-9949-83-181-4 (publication)
ISBN 978-9949-83-182-1 (PDF)

LOODUS- JA TÄPPISTEADUSED B242

Tsükloheksaano-asendatud hemikukurbituriilide kromatograafiline analüüs ning nende vaheühendite mass-spektromeetriline iseloomustamine

MARIA FOMITŠENKO

TTÜ KIRJASTUS

CONTENTS

LIST OF PUBLICATIONS

I Fomitšenko, M.; Shmatova, E.; Öeren, M.; Järving, I.; Aav, R. "New homologues of chiral cyclohexylhemicucurbit[*n*]urils" *Supramolecular Chemistry*, 2014, **16**, 19198-19205.

II Prigorchenko, E.; Öeren, M.; Kaabel, S.; Fomitšenko, M.; Reile, I.; Järving, I.; Tamm, T.; Topic, F.; Rissanen, K.; Aav, R. "Template-controlled synthesis of chiral cyclohexylhemicucurbit[8]uril" *Chemical Communications*, 2015, **51**, 10921-10924.

III Fomitšenko, M.; Peterson, A.; Reile, I.; Cong, H.; Kaabel, K.; Prigorchenko, E.; Järving I.; Aav R. "A quantitative method for analysis of mixtures of homologues and stereoisomers of hemicucurbiturils that allows us to follow their formation and stability" *New Journal of Chemistry*, 2017, **41**, 2490-2497.

Author's Contribution to the Publications

The contributions by the author to the papers included in the thesis are as follows:

I – The author planned and carried out all experiments, which included HPLC screening and optimisation and isolation of 8-membered macrocycle by flash chromatography and was responsible for the experimental part in the manuscript of the article.

II – The author was responsible of analysis part of the reversible macrocyclisation mechanism study, which included HRMS experiments and data interpretation and HPLC analysis. Also wrote the respective part in the manuscript and participated in the final preparation of publication.

III – The author planned and carried out all experiments for calibration, collection of crude samples, isolation of oligomers and UV measurements, except for the synthesis and calibration of unsubstituted hemicucurbiturils. Also wrote the manuscript.

ABBREVIATIONS

AA	acetic acid
ACN	acetonitrile
aq.	aqueous
CB[*n*]	cucurbit[*n*]uril
CD	cyclodextrine
CX	calixarene
cycHC[*n*]	cyclohexanohemicucurbit[*n*]uril
DCC	dynamic covalent chemistry
DCL	dynamic combinatorial library
EIC	extracted ion chromatogram
eq	mol equivalent
ESI-MS	electrospray ionisation mass spectrometry
FA	formic acid
GC	gas chromatography
HC[*n*]	hemicucurbit[*n*]uril
HILIC	hydrophilic interaction liquid chromatography
HPLC	high performance liquid chromatography
HRMS	high resolution mass spectrometry
LoD	limit of detection
LoQ	limit of quantification
MeOH	methanol
NMR	nuclear magnetic resonance
NP	normal phase
RP	reverse phase
SD	standard deviation
TFA	trifluoroacetic acid
TIC	total ion chromatogram
TLC	thin layer chromatography
UV	ultra violet
v/v	volume-to-volume

INTRODUCTION

In 2016 Jean-Pierre Sauvage, Sir J. Fraser Stoddart and Bernard L. Feringa were awarded the Nobel Prize in chemistry "for the design and synthesis of molecular machines"[1], which illustrates the relevance of supramolecular chemistry as the meeting point of technology, biology and chemistry. Synthesized molecular machines are the smallest devices in the world, and can perform different tasks in a controllable manner. The development of such molecular systems as catenanes, rotaxanes and molecular motors, which act as mechanical appliances, opened the way for the design and development of countless movable and programmable nanosystems.[2–5]

Host-guest chemistry, which relies on the phenomenon of molecular recognition, is one of the most influential concepts of supramolecular chemistry. Host-guest complexes describe two or more molecules or ions which are held together by non-covalent interactions. Such connections can include hydrogen bonds, and π-stacking, electrostatic, hydrophobic or van der Waals interactions. Plenty of real-life examples of host-guest systems can be found within living bodies, such as the enzyme-substrate complexes formed through the association of chemically and geometrically suitable chemical compounds with the active sites of proteins. Receptors, ion channels, transport and signal pathways and protein folding are also largely based on host-guest complexation principles. Donald J. Cram, Jean-Marie Lehn and Charles J. Pedersen were awarded the Nobel Prize in chemistry in 1987 for the synthesis and use of molecules that mimic the high selectivity of important biological processes by structure-specific interactions.[6] Their contribution played an important role in the coordination of bio- and organic chemistry, which fueled a new scientific direction that is now known as host-guest chemistry. That's why host-guest chemistry was, and still is, an attractive field of research to study the selectivity of interactions, and the specificity of bindings. Also, it helps to understand how to control each process precisely to develop selective hosts for specific guests and reactions.

One example of host molecules are cucurbiturils (CBs), for which a variety of homologues, derivatives, analogues and congeners are known.[7] The CBs are known in many fields of applications for their ability to form strong and specific complexes with a wide variety of guests, from single ions to large molecules, even including proteins. Generally CBs prefer to bind positively charged species to their portals and hydrophobic compounds within their inner cavities.[8] In addition to CBs, there are many other supramolecular systems which are known cation binders, such as the previously mentioned cyclodextrines or calixarenes. In contrast, the strong binding of anions is still comparatively rare, as specific binding is harder to achieve due to the hydration of anions, their lower charge density and a wide diversity of shapes.[9] Hemicucurbiturils have made progress

in this field[10], where the record for the strongest complexation between host and guest is held by bambusurils[11].
The main focus of this work is on cyclohexano-substituted hemicucurbiturils, mainly the chiral (*R,R*)-cyclohexanohemicucurbiturils, the first entiomerically pure CB family members.
The main focus of this work is on cyclohexano-substituted hemicucurbiturils, mainly the chiral (*R,R*)-cyclohexanohemicucurbiturils, the first entiomerically pure CB family members.
From the synthetic point of view, any CB member can be obtained in a simple one-pot polymerisation reaction, but this fact makes their analysis and isolation difficult. Polymerisation produces a mixture of structurally very similar products, including different sized macrocycles and open chain oligomers, which makes the identification of the composition of the sample, the separation of the desired products, and the determination of their purity exceedingly complicated.
This work focuses on the analysis of cyclohexanohemicucurbiturils (cycHC) by different methods, including HPLC, UV, MS and NMR, but also includes an analysis of unsubstituted hemicucurbiturils, parent cucurbiturils and bioutinuril derivatives. The separation by chromatography and UV absorbance of homologues and isomers of cycHCs and also their oligomeric open-chain derivatives is here examined. A quantitative RP-HPLC method for the fast and easy screening of crude samples has been developed and a contribution to understanding the reversible macrocyclisation mechanism has been made with the help of HRMS analysis.

1 Literature overview

1.1 Comparison of container-macrocycles

Host-guest chemistry is a highly attractive area of science. Its applications can be found in chemistry, biology, medicine, agriculture, food technology, gene therapy, nanomaterials and the textile industry.[12,13] There is no doubt that host-guest complexes will continue to contribute to the advance of new technologies in the future, with progress expected especially in energy-storing systems, self-organizing materials and nanorobotics.

A wide variety of host molecules are known today, many of which are based on the three common molecular scaffolds of calixarenes (CX)[14], cyclodextrines (CD)[15] and cucurbiturils (CB)[13] (See Figure 1), which have attracted a lot of attention in host-guest complexation studies.

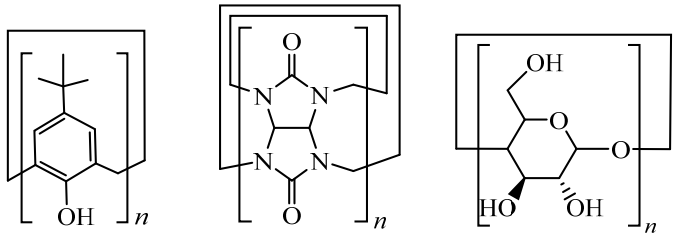

A B C

Figure 1. Structures of monomeric units for A) calixarenes, B) cyclodextrines and C) cucurbiturils, where *n* is the number of repeating units.

The applications for these molecular containers are summed up in Table 1.

Table 1. Applications of the CDs, CBs and CXs.

Molecular biology	Nano-technology	Medicine and pharmacy	Analytical science	Organic chemistry
➢ Caging agents ➢ Biosensors ➢ Receptors ➢ Ion channels ➢ Transporters ➢ Micelles	➢ Nanotubes ➢ Nanoreactors ➢ Rotaxanes ➢ Molecular electronics ➢ Self-organising systems	➢ Drug delivery ➢ Gene transfer ➢ Improving drug bioactivity ➢ Increasing drug solubility	➢ Electro-chemical sensors ➢ Stationary phases ➢ Mobile phase modifiers ➢ Fluorescence spectroscopy	➢ Catalysis ➢ Enantio-selectivity ➢ Supra-molecular building blocks

These three macrocycles have comparable sizes; the inner diameter varies between 4 – 9 Å for CB[5-8][12], 5 – 9 Å for the three main CD homologues[16], and is more variable for CXs, for example the sizes of the lower and upper rim of

sulfonated calix[4]arene are 4 and 10 Å, respectively[17]. All three macrocycles have a hydrophobic cavity, which can accommodate neutral guest molecules. Binding with these hosts is governed by ion-dipole interactions, hydrogen bonding and/or π-staking.

Since the shape, size and flexibility are different between the hosts, this can result in different selectivities and affinities toward the same guests. CBs have tighter portals and are rigid molecules, which leads to more stringent selectivity compared to other macrocycles. On the other hand, CXs have wide openings, which make it possible to encapsulate a variety of guest molecules, but often with low selectivity. The deeper cavities of CDs and CBs, reflected in their larger cavity heights compared to CXs, can increase the complexation strength of host-guest complexes through the complete removal of the guest from the surroundings.

One of the major disadvantages of unfunctionalized CBs and CXs is their relatively low solubility in water compared to CDs. CDs are generally water soluble, except for *β*-CD, which has the relatively low solubility of 18.4 mg/ml compared to its homologues α- and γ-CD, with solubilities of 129.5 and 249.2 mg/ml, respectively.[16] In general the solubility of CBs can be enhanced using additives or by modifying the structure of the macrocycle. For example, less than 1 mg/ml[12] of CB[6] dissolves in water, but its solubility can be increased by the addition of metal salts[18] or formic acid[12,19,20]. Another option is to synthesise substituted derivatives or post-modify the parent macrocycle.[21] The solubility of CXs can also be increased by modifying their structure, most commonly by functionalization on their upper or lower rims with sulfonates, phosphonates, amines, amino acids, peptides or saccharides.[22]

Many comparable studies have shown that among the three macrocyclic hosts CBs often have the highest selectivity and binding constants[23] and also can have the most significant impact on improvement in the fluorescence signal[24] or solubility enhancement of some pharmaceutical compounds. And since the CB family also has members which efficiently bind guests with negative charges[10], they definitely have the greatest opportunity to widen their applications.

Since all three types of the macrocyclic hosts have been intensively investigated in the food and textile industry, in biology and pharmacy - fields that are directly connected to nature and our welfare - it is important to determine the possible toxicity of these macrocycles on living organisms. Given the fact that macrocycles can mask the taste of some food supplements or biologically active medications, by protecting drugs from the environment during delivery they can enhance the solubility or bioactivity of the compound, thereby reducing dosages and side effects. A thorough review of toxicity studies of CDs is given by Stella et al.[25]. Since some CD family members have been approved for use in the food industry and in drug formulation, their metabolism, absorption in the gastrointestinal tract, stability and secretion, distribution and accumulation in the organism, as well as their toxicological effects have been widely studied. Generally CDs are considered to be non-toxic, with lethal doses (LD_{50}) in rats

and mice between 0.3 and 18.8 g/kg depending on the type of cyclodextrin and the type of administration. The most common side effects after treatment with different CD derivatives are diarrhea and cecal enlargement, but these are temporary.[25]

Toxicity among the calixarenes is mostly studied for water soluble sulfonated derivatives. To investigate the haemolytic effect, experiments with human blood have been carried out, and these have showed that sulfonated CXs are totally harmless in concentrations of less than 50 mM.[26] The same CXs have also been injected in mice. No noticeable changes in the behavior of animals have been observed and it was also concluded that macrocycles do not metabolize in the organism since they were rapidly detected in the urine of the mice.[27]

Generally, the toxicity of CBs is assumed to be very low. Uzunova et al.[23] showed that CB[7] is essentially nontoxic when applied in concentrations below 250 mg/kg (or 0.5 mM). Higher dosages of CB[7] and CB[8] were more tolerated when administered orally than intravenously. Hettiarachchi et al.[28] concluded in their studies that CB[7] and CB[5] demonstrated high cell tolerance at concentrations up to 1 mM. Oun et al.[29] studied the neuro-, myo- and cardiotoxicity of CB[6], CB[7] and open-chain cucurbituril-derivative Motor2[28] through *ex vivo* experiments and found no inhibition on the nervous system, but minor muscle contractions.

The limitation of the administration of CBs as medications is probably mostly due to their low solubility rather than their side effects.

1.2 Cucurbituril family

One can divide the CB family into three main parts: acyclic-CB[*n*]s, parent CB[*n*]s, which contain unsubstituted and various substituted family members, and hemiCB[*n*]s, which also have some subclasses (See Figure 2)[7]. A short overview of each main branch, their applications and advances follows, focusing mostly on hemicucurbiturils.

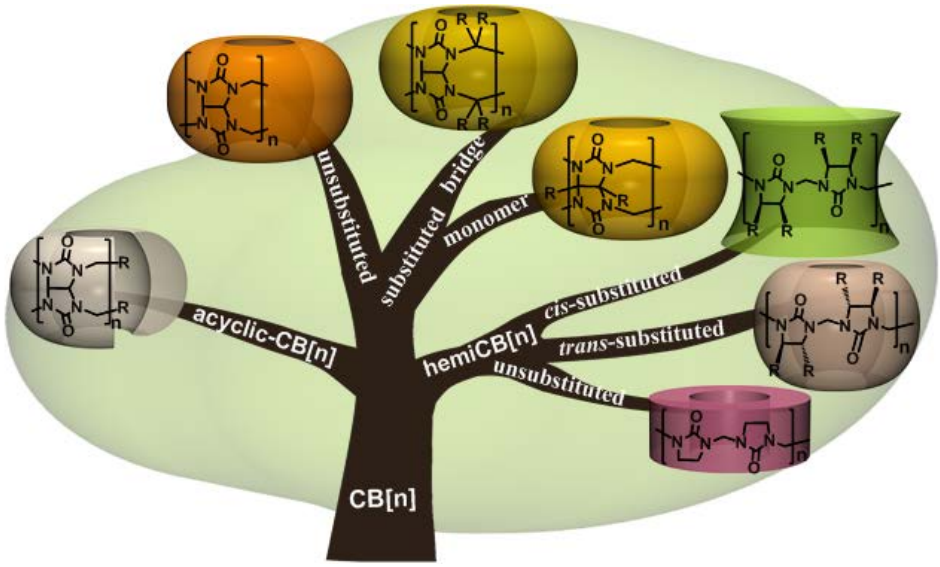

Figure 2. Cucurbituril family tree, consisting of the three main branches of acyclic-CBs, parent CBs and hemiCBs. Reprinted from ref.[7] with permission from Elsevier.

1.2.1 Origin of cucurbiturils

The first macrocyclisation of glycouril monomers was reported in 1905[30], though the structure was established and the compound was named only in 1981 by Mock et al.[31]. This compound was revealed by X-ray crystallography to be a symmetric and hollow molecule which contained six units of glycouril connected to each other through two methylene bridges (see Figure 3). As the given systematic name for that compound was impractical, Mock decided to name the new compound cucurbituril, based on its pumpkin-like shape (*Cucurbitaceae* in Latin).

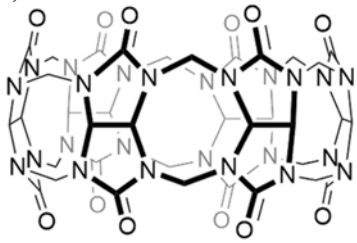

Figure 3. Structure of CB[6]

During the next couple of decades this new cucurbit[6]uril, its physical and chemical properties, binding abilities and some applications[32,33] were studied. After the synthesis and characterisation of new homologues of CB[6][34] the chemistry of cucurbit[*n*]urils started to attract attention from other research groups. Later the CB family grew fast in terms of the number of homologues and

different types of derivatives aimed to improve their solubility and functionalisation.

Substitutions in CBs can be made in three main ways.[7] The first approach is to start with a substituted monomer and perform the usual polymerisation reaction. The second is to use a mixture of building blocks, such as substituted monomers or oligomers, in a polymerization reaction. This approach may lead to very complicated mixtures of isomeric products, due to their similar thermodynamic stabilities. The third way is to add substitutents to the already formed CBs; so far this has only been accomplished through hydroxylation, first demonstrated by Kim et al. [21] in 2003.

The rapid growth of the CB family triggered the members' development into new types of molecular containers and advanced materials, utilizing for example the facts that CB[6] is known to form complexes with alkylammonium ions[35], CB[7] can bind adamantane and aromatic guests with high affinity, and CB[8] can accommodate two aromatic guests. Furthermore, CBs can form complexes with bioactive compounds, such as DNA.[36] Because of the wide range of suitable guests, they have found many applications in very different fields. These macrocycles have been used as catalysts in organic chemistry, and complexation agents and signal enhancers in analytical science. In addition, they are used in biology and medicine due to their ability to act as sensors, receptors, ion channels and transporters. One of the strongest known host-guest systems in water is between the CB[7] and diamantane diammonium ion, with an association constant as high as $7.2 * 10^{17}\,M^{-1}$, which is comparable to the biotin-avidin interaction.[37] Last but not least, CBs can be used to form different supramolecular assemblies and networks, such as nanotubes and –sheets, and they have a very bright future in the field of advanced materials.[38]

1.2.2 Acyclic cucurbituril congeners

One of the subclasses of CBs is the acyclic congeners (see Figure 2). It has been shown that acyclic derivatives can enhance the solubility and bioactivity of several poorly soluble pharmaceuticals up to 2700 times.[28] Acyclic derivatives are more flexible, which increases their ability to bind more and bigger guests than CB macrocycles[39,40], but the binding may be less selective and not as strong. The acyclic oligomeric derivatives of CBs are usually more soluble than macrocycles, as their aromatic terminal groups are easily modified by solubilizing groups (see Figure 4).[41–43]

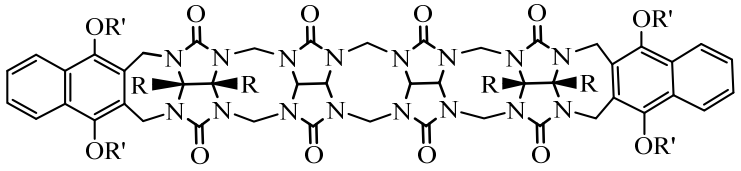

$R = CH_3 \quad R' = (CH_2)_3SO_3Na$

Figure 4. Structure of acyclic-CB derivative Motor2.

Complexation between the acyclic CB analogue with bioactive compounds and drugs can be used to bind anesthetics[44] and, for example, in gene delivery by complexing with DNA[45]. A recent example of promising results for acyclic CB derivative acting as a sensor for opiate determination in urine was published in 2017 by Shcherbakova et al.[46]. Motor2 (See Figure 4) is an acyclic CB family member widely used as a solubilizing agent for poorly soluble or insoluble drugs [28] and progress towards its application as a drug is at the most advanced stage.

1.2.3 Hemicucurbiturils

Hemicucurbiturils (HC) get their name from the fact that they contain exactly half of the CB structure if cut in half at the equator. Since the monomeric units of hemicucurbiturils are connected to each other through single methylene bridges, they can rotate freely and take alternate conformation (see Figure 5).

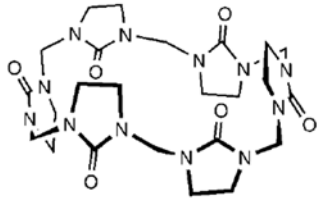

Figure 5. Structure of the hemicucurbit[6]uril.

The alternate arrangement of monomeric units in HCs gives rise to opposite electronic properties compared to CBs. While CBs prefer to bind cations, HCs form complexes with anions[47–49], broadening the possible applications of CB chemistry. This also has an important impact on the field of supramolecular chemistry, because even though there are many cation binding systems based on macrocycles, such as crownethers, cryptands, spherands and cucurbiturils, the number of macrocyclic hosts that form complexes with anions is much smaller. Anion binding, however, is central to many biological processes. Some anion receptors for that purpose have been synthesized, but generally complexation is not as strong.[9]

The first synthesis of HCs was achieved by Miyahara et al.[49] in 2004, when two hemicucurbit[*n*]urils (6- and 12-membered) were isolated. It was shown that these new CB family members can bind anions, as complexes with I^- and SCN^- anions were detected.[47] The binding of hydrophobic aromatic compounds to HCs has also been reported [50–52] and Cucolea et al. [53] recently showed that HCs can be used as transmembrane carriers of amino acid esters. In a liquid membrane extraction, these esters were transported from water to water through a chloroform phase, which contained HC macrocycles.

HC[6] has been shown to also act as a supramolecular catalyst. For example, it displays catalytic activity in the esterification of acids with methanol[54] and in aerobic oxidation reactions of heterocyclic compounds in aqueous solution[55]. Moreover a chemo-selective oxidation of hydroxybenzyl alcohols with 2-

iodoxylbenzoic acid was carried out in the presence of HC[6][56], and Kurane et al.[57] showed catalytic application also on HC[6] surfaces.
Since the synthesis of HC[6] and HC[12], the family of HCs has gained some new members including (*R,S*)-cyclohexanoHC[6][58], its inverted homologue[59] which will be discussed later in this work, the chiral derivative (*R,R*)-cycHC[6,8][60,61] norbornaHCs[62], biotin[6]uril[63] and different 4- and 6-membered bambus[*n*]urils[11,64–69]. Structures of the named macrocycles are presented in Figure 6.
The first enantiomerically pure CB family members - (*R,R*)-cycHC[6,8] - were synthesized in our lab in high yield (85% and 90%, respectively). Our group has shown that these macrocycles can form complexes with anions, carboxylic acids and some neutral compounds and have also shown chiral discrimination between enantiomers of some acids.[60,61,70] CycHCs as the central object of study of this thesis, will be discussed further in the following chapters.

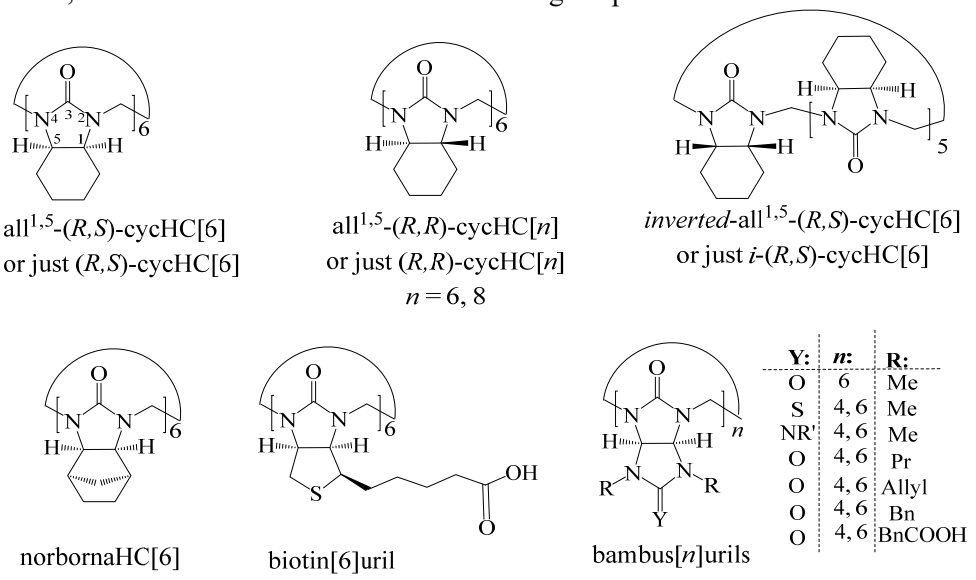

Figure 6. Structures of the substituted hemicucurbiturils

Derivatives of the biotin[6]uril ester have been successfully incorporated into the membranes of micells to perform as ion channels which showed great selectivity for the chloride ion.[71] Complexation with different anions is found to be up to 10^4 M^{-1}.[72] The anion binding of biotinurils can be increased by oxidation at the sulfurs, as biotinsulfon[6]uril and biotinsulfoxide[6]uril show even stronger binding to anions compared to their parent macrocycle, in 2:1 stoichiometry.[73]
Bambusurils (BU) were introduced by Sindelar in 2010.[64] They consist of the same monomeric unit as parent cucurbiturils, but owing to the *N*-subtituents on half of the glycoluril monomers they are connected through one methylene bridge as in hemicucurbiturils. Therefore the monomeric units are also

positioned in alternate forms and the resulting macrocycles prefer to bind anions (see Figure 7).[11,65] Association constants from 10^5 to 10^{10} M^{-1} have been demonstrated for the binding of Cl^-, Br^-, I^-, BF_4^- and TfO^- in different solutions.[68,69,74]

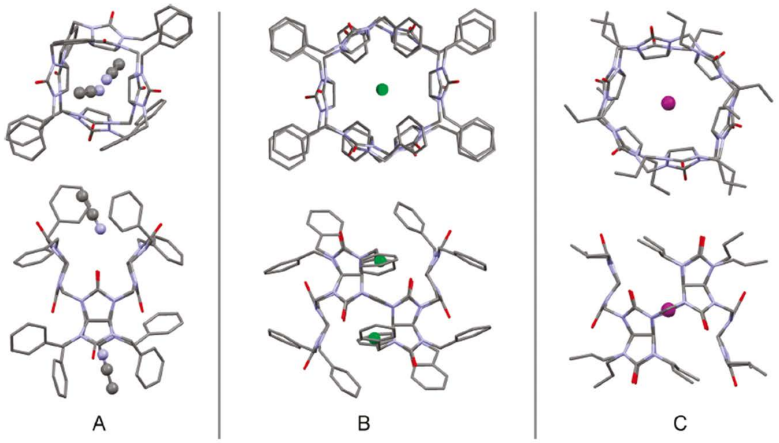

Figure 7. Top and side views of crystal structures for A) $Bn_8BU[4]$:2ACN, B) $Bn_{12}BU[6]$:2Cl^- and C) $Pr_{12}BU[6]$:I^-. Reprinted from ref.[65] with permission from the American Chemical Society.

Larger anions such as those of benzoate or tosylate form 2:1 complexes with $Bn_{12}BU$.[65] Water soluble bambusurils offer competitive binding for anions in aqueous solutions with K_a up to 10^7 M^{-1}.[11,75] From semithio-glycouril monomers, it is possible to synthesise semithiobambusurils (see Figure 6), from which semiazaBU can be made, which have shown the ability to bind three anions simultaneously.[69] BU[6] has also been used to construct crystalline materials demonstrating photo-induced electron transfer, which can greatly contribute to the development of new materials for energy storage or production.[76]

1.3 Analysis of cucurbiturils

Most CBs are formed in a polymerization reaction following the principle of dynamic combinatorial chemistry, which can yield a complex mixture of oligomers and macrocyclic homologues. If more than one starting monomer is used, this mixture may additionally contain various isomers. If the reaction does not clearly favor the formation of a specific product, the resulting complicated mixture can be quite a challenge to analyze and to purify the desired compounds from it. With the approaches of dynamic covalent chemistry, it is possible to influence the composition of product mixture, but to date no conditions have been developed to shift the equilibrium between unsubstituted CBs to some

other macrocycle formation besides the thermodynamically most favorable CB[6].
The CB family is predicted to continue to grow in the near future because of the significant interest in numerous opportunities that CB chemistry can offer to society. Further development is also needed to improve selectivity during synthesis or find better ways to specifically isolate the desired product. Even greater is the need for efficient analytical methods to accurately identify the composition of the product mixture and determine the purity of isolated product. The next sub-chapters highlight the most used methods for the purification and isolation of the macrocycles, the methods for describing the reaction mixture and pure product, common problems and shortcomings in that field.

1.3.1 Isolation of cucurbiturils from crude reaction mixture

The synthesis of CBs, as described by Beherand et al.[30] in 1905, is an acid-catalyzed condensation reaction between formaldehyde and glycouril, which gives a mixture of CB homologues (and oligomers) predominantly consisting of CB[6]. The traditional method for isolating CB homologues is based on their different solubilities in solutions. Odd-numbered homologues are more soluble in aqueous solutions than even-numbered ones. CB[5] and CB[7] can be separated from one another through repeated recrystallisation in a methanol–water or an acetone–water mixture, and CB[8] can be isolated from CB[6] by recrystallisation in sulfuric acid.[34]
Reaction mixtures are commonly purified by simple column chromatography using normal[77] or reversed phase[78] silica gel, ion-exchange resin[79,80], or by gel permeation chromatography[81]. But these methods may have some drawbacks, such as solvent incompatibility, unsatisfactory yields, limited solubility, irreversible adsorption or remaining impurities. For chemically similar compounds, chromatographic separation can be quite time-consuming. The most extreme example is the isolation of twisted-CB[14], which lasted for three months.[80] It was accomplished with an ion-exchange column (5 x 75 cm) using 1:1 AA/H_2O eluent with increasing HCl content from 0.01 to 2 M. The yield of isolated CB[14] was 1.2%. Researchers have struggled to develop more efficient methods for the purification of CBs, as the homologues are similar in structure. A beautiful example of a specific purification procedure for six-membered derivatives is affinity chromatography using aminopentyl-aminomethyl-polystyrene beads, knowing that six membered CBs are bound most strongly to diaminoalkyl chains.[82] An efficient “green” method for isolating cucurbit[*n*]uril homologues (CB[5–8]) has been developed by Dezhi Jiao and Oren A. Scherman (see Figure 8).[83] As was previously mentioned, odd-numbered homologues can relatively easily be separated from even-numbered ones based on their solubility in water. CB[8] and CB[7] can be separated from their respective mixtures by using selective imidazolium salts to improve their water solubility by the formation of inclusion complexes and isolating the less soluble CB[5] and CB[6] from their corresponding mixtures (see Figure 8). This kind of

isolation is recyclable, because the salts can be regenerated and used again several times.

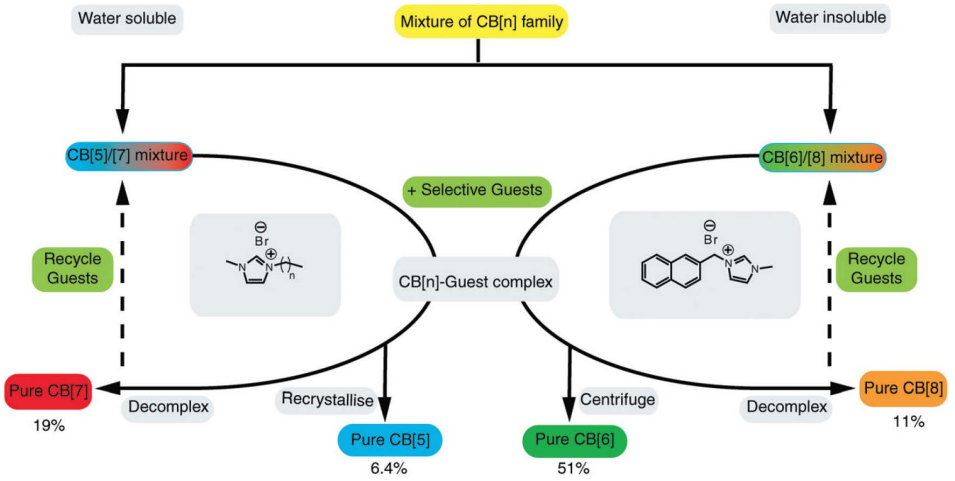

Figure 8. Multiple step isolation procedure for the separation of CB homologues with imidazolium salts. Adapted from ref.[83] with permission from the Royal Society of Chemistry.

1.3.2 Analysis of crude reaction mixture

The following section describes methods used for CB synthesis and the challenges in the analysis of crude reaction mixtures.

TLC is a very easy and fast technique for checking the composition of the reaction mixture, but it is hardly suitable for the analysis of complicated mixtures of structurally similar compounds. It can also prove complicated to analyze such mixtures by NMR spectroscopy, which for pure compounds is a powerful method of determining chemical structure and measuring compound purity. ^{1}H-NMR can often have too many overlapping signals to identify all of the components of the reaction mixture. Studying the formation mechanism with ^{13}C-NMR, which compared to ^{1}H-NMR has a broader window and singlet signals, Day et al.[84] discovered a non-linear correlation between chemical shifts of methylene and methine carbons of repeating units in CB[5-10]. With the help of this correlation, it was possible to predict the shifts for previously unknown CBs, which allowed them to see weak signals for CB[9], though even now the structure of CB[9] has not been characterized. Day also noticed, that the ratios of NMR peak integrals of CB[5] and CB[6] were the same in ^{1}H-NMR and ^{13}C-NMR. Though it was not the case if signals of larger macrocycles were compared to CB[5] or CB[6], integrals of larger macrocycles were smaller than expected. So, the correction factors were found for each larger macrocycle by dividing the expected area by the found area. This technique made it possible to reliably estimate the content of the reaction mixtures.

Another example of misleading results interpreted by NMR was presented by Ayhan et al.[85] in the synthesis of monohydroxylated CB homologues. The method was initially described as a highly efficient way to introduce a single hydroxyl group into the structure of CBs, giving high conversions of 90-100% according to the ^{1}H-NMR of crude product. The apparent efficiency of the method was, however, downgraded after the purification of products by column chromatography. It turned out, that the actual composition of the crude product was a 1:1:1 mixture of CB, CB-OH and CB-OH_2 for each homologue. When the ^{1}H-NMR spectra of the purified fractions were compared, the overlapping peaks for these three products were revealed (see Figure 9). Finally, the real yields were published in a correction to the article[86], where actual yields for the monohydroxylated CB[5], CB[6], CB[7] and CB[8] were 10%, 37%, 20% and 5%, respectively.

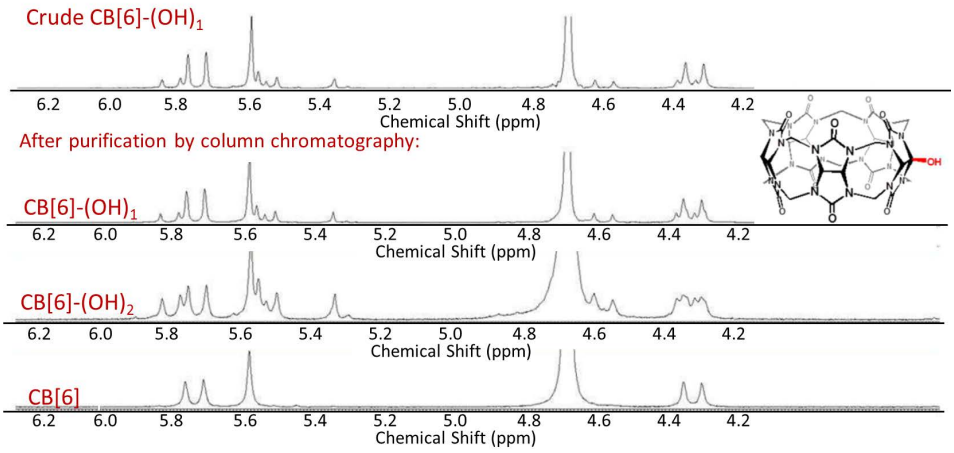

Figure 9. ^{1}H-NMR spectra of a crude reaction mixture and purified products. Adapted from ref.[86] with permission from the American Chemical Society.

Pittelkow et al.[63] used RP-HPLC-ESI-MS to follow the process of the formation of biotin[6]uril (see Figure 10, A and B). The separation was achieved on a Dionex Acclaim RSLC 120 C-18 column, where the products were detected mainly with MS (see Figure 10, A). The calibration of the monomer (biotin), synthesized dimer and biotin[6]uril macrocycle was accomplished by measuring the peak areas from the trace signals received from the UV detection at 209 nm. The calibrations for the trimer, tetramer and pentamer were based on the assumption that the slope of the calibration curve corresponded to the number of chromophores in the analyte structure, as the slope of the monomer proved to be exactly two and six times smaller than the slopes of the dimer and biotin[6]uril, respectively. Following the reactions with developed HPLC-MS methodology, they calculated the fractions of each identified compound during the reaction

and, as they found dimer in the majority, the conclusion was that biotin[6]uril had probably formed by the fusion of the dimeric units (see Figure 10 C).

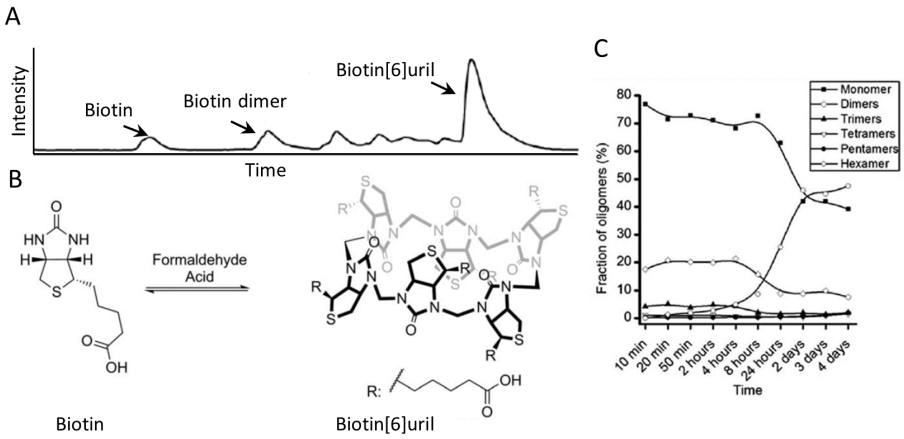

Figure 10. A) HPLC-MS ion chromatogram of a crude reaction mixture, B) Reaction scheme for the synthesis of biotin[6]uril and C) Distribution of oligomers during the reaction. Adapted from ref.[63] with permission from the Royal Society of Chemistry.

Lewin et al.[78] evaluated an analytical technique composed of a phenyl-type RP column coupled with HRMS to quantify the yields and measure the water solubility of synthesized cyclohexano-substituted CB[6] derivatives. The proportionality of the response of the MS with the concentration of CB[6] and CB[7] was confirmed, and latter was used as an internal standard. The peak area ratios of CB[6]/CB[7] were measured from the ion-chromatogram (see Figure 11) to plot them against the ratios of the CB[6]/CB[7] concentrations. So the unknown amount of the CB[6] can be found from the equation of linear regression. In the same way, the content of all substituted CB[6] macrocycles was quantified, though relying on the assumption that unsubstituted and substituted derivatives have equal ionisation ability in MS.

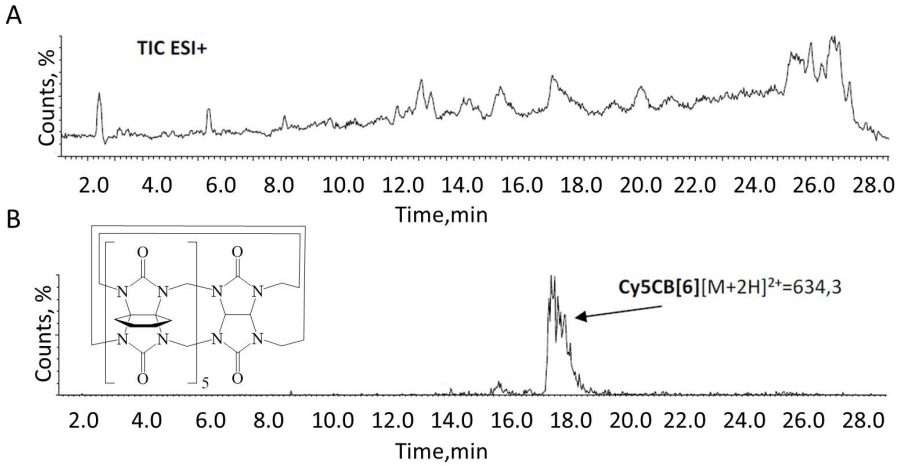

Figure 11. A) RP-HPLC-MS total ion count (TIC) chromatogram from a crude mixture of cyclohexano-substituted CBs. B) Extracted ion chromatogram of m/z = 634.504 from TIC. Adapted from ref.[78] with the permission of John Wiley and Sons.

As can be seen, the analysis of the crude mixture and quantification of cucurbiturils is challenging, which forces chemists to simplify systems and make assumptions through indirect approaches for quantifications.

In the case of other macrocycles, namely cyclodextrines and calixarenes, published analytical methods for simultaneous chromatographic separation and quantification of homologues exist. For example, during the synthesis of calixarenes the reaction rate is followed by the developed HPLC methodology (see Figure 12).

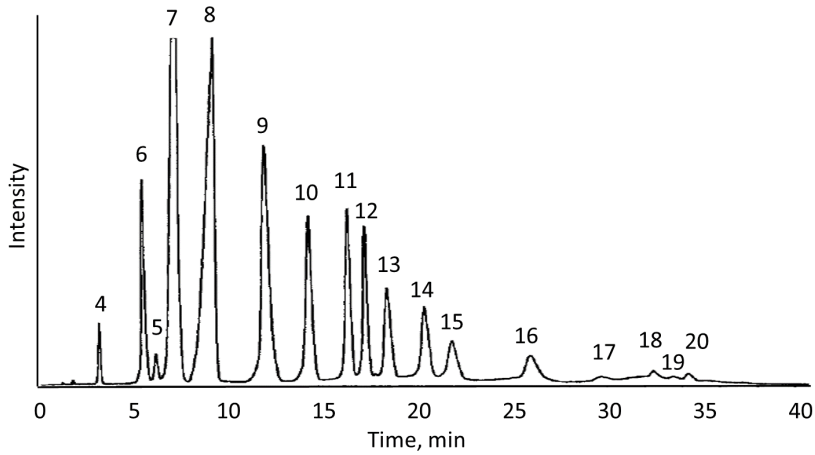

Figure 12. RP-HPLC-UV chromatogram of the separation of calix[4-20]arenes, where 4-20 correspond to numbers of repeating units. Reprinted from ref.[87] with permission from the American Chemical Society.

The separation was achieved on a Merck Hibar RP-18 Lichrospere column (3.9 x 250 mm, 5 μm) with a three-step gradient and very specific eluent system. Eluent A was acetonitrile with 1% of acetic acid and eluent B was a 4:3 mixture of dichloromethane/methyl *tert*-butyl ether with 1% acetic acid. The optimal resolution was obtained by applying an 8 min isocratic run with 80A/20B, a 3 min linear gradient to 65A/35B, followed by a 12 min isocratic run with the same ratio of eluents, and then again a 3 min gradient up to 55A/45B and isocratic for 6 min. The UV/Vis detector was set at 281 nm. With this complicated reaction, the mixture of 4- to 20-membered calixarenes and some short open-chain oligomers (longer ones were separated previously by column chromatography) was resolved in 40 min. The developed system was used to follow the reaction during the optimization procedures for optimal synthesis for larger macrocycles.[87]

A methodology for the separation and quantification of CD homologues[88] has also been developed and used to improve the analysis and therefore the productivity of enzymatic synthesis (see Figure 13). Optimum separation was achieved with a Finepak-NH_2 column (4.6 x 250 mm, 5 μm) with ACN/H_2O (70/30), using a differential refractive index detector.

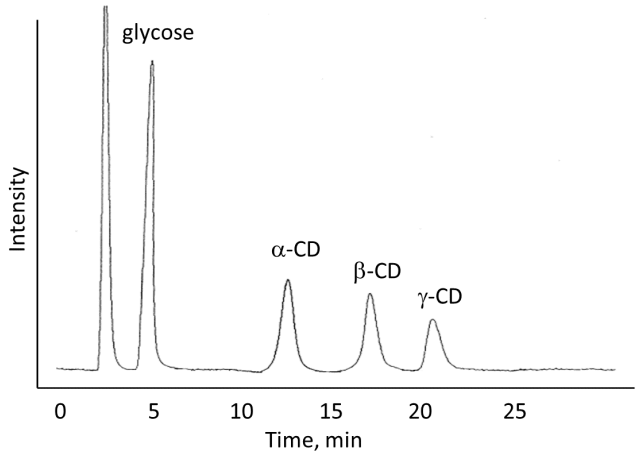

Figure 13. RP-HPLC analysis of a crude mixture of cyclodextrines. Adapted from ref.[88] with permission from Elsevier.

As can be seen, one advantage which led to the development of a methodology for CXs and CDs is the possibility of detecting the compound compared to the CBs. CDs, as sugar derivatives, are detected with a refractive index detector and calixarenes have conjugated structural moiety for simple detection in the UV-Vis region. It is known that chromatographic separation of CBs is challenging due to their low UV absorption[20,78,79]. In that case, separation techniques can be coupled with a mass spectrometer[78].

1.4 Applications of cucurbiturils in analytical chemistry

As was previously shown, there are only a few examples of the quantitative determination of cucurbiturils themselves. However, CBs are widely applied to improve the identification of other analytes via host-guest chemistry. Thanks to the wide range of suitable guests and high affinities, it is possible to develop selective analytical methods to improve the separation or distinction and quantification of the analytes which can act as guests for CBs. For complexation studies, spectroscopic, NMR and ITC titrations are generally used. The next section describes the application of CBs in separation science and in fluorescence spectroscopy.

1.4.1 Cucurbiturils in separation science

CBs have been tested in several ways for their use in separation science, with a few publications describing the use of CBs in capillary electrophoresis and the main body of work devoted to different chromatographic applications. There are examples demonstrating CBs as modifiers of mobile or stationary phases improving the resolution of studied compounds. Huang et al.[89] used CB[7 in the mobile phase to form complexes with adenine derivatives during chromatographic separation and thereby determined the association constants of complexes. A similar approach was made by Chang et al.[90], where again CB[7] was added to a mobile phase to perform a simultaneous determination of structurally very similar palmitine and berberine by RP-HPLC equipped with a fluorescence detector. The achievement was based on the enhancement of the fluorescence of complexed palmitine and berberine in aqueous solution in the presence of cucurbit[7]uril. The same technique is also used in capillary electrophoresis. Wei and Feng used a cucurbit[7]uril-modified phosphate buffer for the rapid and sensitive determination of aristolochic acid I and II in medicinal plants by capillary zone electrophoresis. Wei et al.[91] determined the binding constants of CB[6] and CB[7] complexations with amino compounds in aqueous formic acid.

Some cucurbituril family members have been used as stationary phases. As CBs are quite inert molecules and it is challenging to covalently bind them to silica, dynamic coating was tested in capillary electrophoresis. Xu et al.[92] showed that a CB[7]-coated capillary proved its effectiveness by separating positional isomers of nitrotoluene, nitroaniline and nitrophenol.

When methods for the hydroxylation of CB macrocycles were developed[21] their immobilization on silica was immediately tested. Now several examples of efficient synthesis of CB modified stationary phases are known.[93–97] Generally the examples of CB-modified silica have properties corresponding to the hydrophilic-interaction stationary phase, but its performance as a reversed phase has also been investigated.[95]

Since CBs have excellent thermal stability CB-coated stationary phases are also employed for gas chromatographic separation techniques.[98] Wang et al.[99] mixed

CB[6] with guanidinium ionic liquid and used it as an effective stationary phase in capillary gas chromatography, and Sun et al.[100] tested for the first time the complex-based stationary phase, where they used CB[8] and its coordination complex with Cd(II) as a good material for capillary coating in GC. CB-modified capillaries have non-polar to medium polar natures and they have shown very promising results in separating many analytes, from *n*-alkanes to alcohols prone to give tailing peaks in classic GC.

Such a limited usage of CBs in separation science can be mainly attributed to their poor solubility and incompatibility with ordinary solvents. Given the wide variety of columns and capillaries available on the market, it can be quite challenging to achieve a breakthrough due to market saturation. There might be more opportunities for new achievements in separation science using CBs as mobile phase additives rather than stationary phases by taking advantage of their characteristics and selective binding.

Different approaches in the separation of analytes using bambusurils have been demonstrated by Sindelar et al. $Bn_{12}BU$ attached to a porous hollow fiber was used for the selective separation of Br^- and ClO_4^- anions by the electromembrane extraction technique from tap and sea water, respectively. The same bambusuril was studied for the analysis of mixtures of anions by following the host BU signals in complex with anions.[75] This method showed a spectacular ability to simultaneously distinguish between nine anions and quantify up to five anions (see Figure 14).

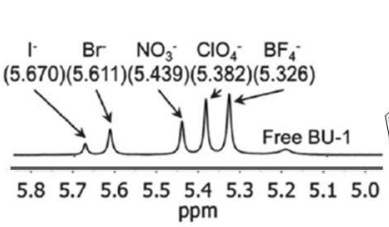

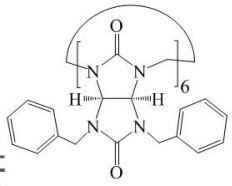

A⁻	$c_{(teor.)}$ [mM]	$c_{(calc.)}$ [mM]	Error [%]
BF_4^-	1.59	1.51	4.8
ClO_4^-	1.31	1.24	5.6
NO_3^-	0.829	0.789	4.8
Br^-	0.571	0.599	4.9
I^-	0.265	0.247	6.6

Figure 14. ^{1}H-NMR spectra of five anions and $Bn_{12}BU[6]$, and a table with theoretical and calculated anion concentrations with errors. Adapted from ref.[75] with the permission of the Royal Society of Chemistry.

1.4.2 Cucurbiturils in fluorescence spectroscopy

Supramolecular analytical applications in fluorescence spectroscopy are becoming more and more common and cucurbiturils play a quite noteworthy role. Mostly they are used to enhance the fluorescence of analytes, but methods using signal quenching have also been developed. A review of applications of CBs in fluorescence spectroscopy has been reported by Elbashir et al.[101]. The first finding that CBs can influence the fluorescence of bound guest molecules was reported by Wagner et al.[102] in 2001, when CB[6] increased the fluorescence intensity of 2,6-anilinonaphtalene-6-sulfonate five fold. After the larger CB

homologues were discovered, which were able to accommodate larger or multiple guests, a number of new studies utilizing fluorescence spectroscopy appeared.[103,104]

An example of extending the fluorescence lifetime of a fluorophore by encapsulation into CB[7] has been reported by Marquez et al.[105] They showed that when 2,3-diazabicyclo[2.2.2]oct-2-ene is encapsulated within a host molecule, which protects it from the environment and various fluorescence quenchers, its emission is prolonged up to 50 times compared to a fluorophore without the host molecule. The emission can last up to 1 microsecond, which is the longest fluorescence lifetime for an organic compound measured in water. This phenomenon can be beneficial to time-resolved fluorescence assays, which are used in biological screenings.

Quenching methods in fluorescence spectroscopy are based on the competitive complexation of a fluorescent probe and a guest compound in the cavity of the host molecule.[106]

In fluorescence spectroscopy studies, the most common host among all CBs is CB[7] because of its good solubility in water and large pool of complexing guests with high affinity.

Interesting applications of analyte-responsible host-fluorophore systems have been shown by Ghale and Nau.[107] They wanted to create a system for the real-time determination of analyte changes during enzymatic reactions. To do this, different systems based on competitive binding assays were developed. The concept of product-selective and substrate-selective tandem enzyme assays is presented in Figure 15. Both assays rely on the fact that cadaverine is selectively bound to CB[7], compared to the organic dye AO (acridine orange). Before the enzyme is added to the solution, the enhanced fluorescent signal of the CB bound dye is measured. When lysine decarboxylase is added and the lysine is converted to cadaverine, the latter will replace the dye in the CB[7] cavity and the fluorescence signal will decrease proportionally to the increase of cadaverine concentration, since this complex does not fluoresce. The substrate-responsible enzyme assay of diamine oxidase is completely opposite to the previous process. Here the fluorescence signal starts increasing, while cadaverine is converted to 1-aminoaldehyde, as more CB[7] becomes available for complexation with the dye AO. The dye-CB[7] fluorescence signal corresponds to a decrease in the cadaverine concentration during the enzymatic oxidation. As can be seen in Figure 15, those two systems can be combined, which increases the ability to analyze two (or more) enzymes and analytes simultaneously in real time.

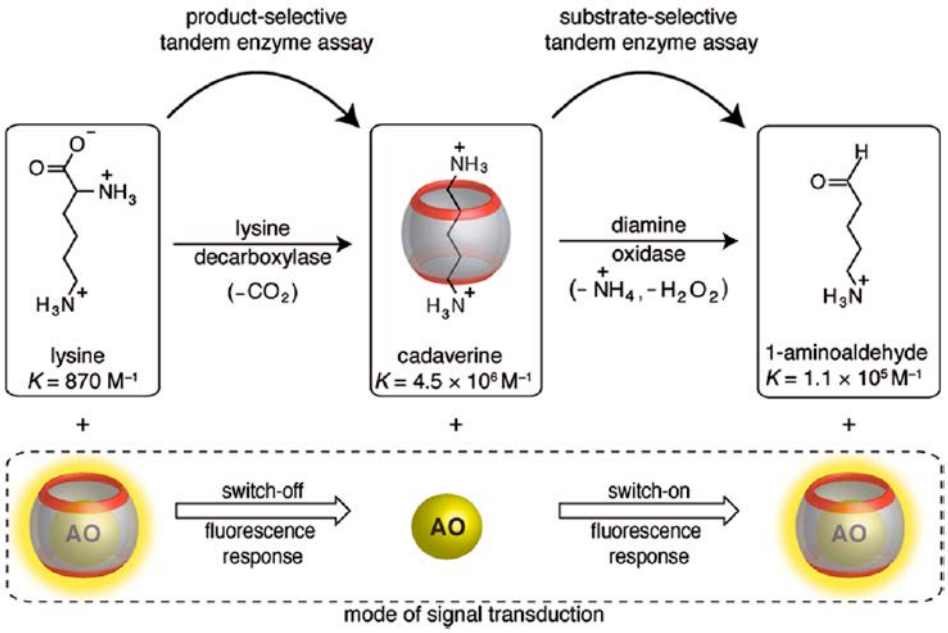

Figure 15. An example of CB application in tandem enzyme assays. Reprinted from ref. [107] with permission of the American Chemical Society.

1.5 Summary of the literature overview

The ability of CB family members to selectively bind a variety of guest molecules will unquestionably continue to inspire researchers in their quest for new applications for CBs.

The synthesis of CBs is a simple polymerization reaction but the analysis of the mixture of formed linear and cyclic CB derivatives is complicated because of the high structural similarity. The development of an analytical method is essential for the reliable estimation of the composition of those mixtures; otherwise there can be underestimation of impurities and overestimation of product yield. With the availability of a reliable analytical method, the synthesis of CBs and development of new members will also be more efficient. So far no analytical chromatographic method has been developed for the simultaneous separation of parent CBs. There is one example of the analysis of biotin[6]uril and its linear oligomers by HPLC and another will be presented in this work.

2 Aims of the present work

The research field of CBs is, in the author's opinion, plagued by a lack of efficient methods for the analysis and separation of complex mixtures of structurally similar homologues, such as those obtained from the polymerization reactions of CB syntheses. Various complications are likely to occur during the isolation of products, in the identification of the composition of crude reaction mixtures and also in the determination of the purity of products. Therefore, there is a great need for a reliable technique for accurate and quantitative identification of these macrocyclic hosts.

Although cyclohexanohemicucurbiturils, the host compounds studied by our group, have only been known for a relatively short period, their ability to selectively bind inorganic anions has been recognized.[66] The rate of further development of these host compounds depends on the existence of accurate and high throughput analytical techniques for their identification. So it is very important to develop a method which can quickly and easily determine all products that are formed in reaction and allow the quantification of their amounts.

The specific aims of this study are to:

- Analyze the UV absorption of cucurbiturils and hemicucurbiturils and find an HPLC methodology for their separation;
- Develop a quantitative analytical method for hemicucurbiturils (HCs);
  - Apply a developed technique to:
    - the analysis of crude reaction mixtures to calculate the yields of produced cycHCs;
    - study the mechanism of reversed macrocyclisation of cycHCs;
    - analyze the stability of HCs.

3 Experimental

The procedures not presented here are described in corresponding articles and are cited in the discussion.

For analysis and identification, two equipment sets (**set A** and **set B**) were used, and minor deviations in the setup are outlined in the text:

Set A – HPLC-UV: Agilent Technologies HPLC 1200 system with a multiple wavelength detector generally with Kinetex C18 column (2.1 x 100 mm, 2.6 µm). Eluents A (acetonitrile) and B (water) were used in a 10-minute gradient from 50/50 to 100/0, unless otherwise stated. The column temperature was set at 30 °C, the flow rate at 0.25 ml/min and the injection volume at 5 µl.

Set B – HPLC-MS: The Agilent 6540 UHD Accurate-Mass Q-TOF LC/MS system with AJ-ESI ionization was used for analyte identification. The system was equipped with a Zorbax Eclipse Plus C18 column (2.1 x 150 mm, 1.8 µm), and eluents C (acetonitrile with 0.1% of formic acid and 1.0% water) and D (water with 0.1% of formic acid) were used for elution. The flow rate was 0.4 ml/min, the temperature was 30 °C and the injection volume was varied depending on the concentration of analytes. Direct injection without the chromatographic separation was also used. Thorough optimisation of the MS methodology was not performed, as the variation of gas flow and temperature did not affect the apparent composition of the sample; only the intensity was affected.

Analysis of the cucurbiturils.

UV analysis of CB[5-8] was performed on a Jasco V-730 spectrophotometer. Type S15-UV-10 quartz cuvettes were used. Saturated solutions of each homologue were made in ACN and H_2O. Heterogeneous samples were centrifuged and the UV spectra from 190 to 300 nm of clear solutions were measured. Measurements were referenced to the respective solvent absorbance. Since the spectra of all CB homologues were very similar, including when compared in different solvents, only CB[6] spectra in ACN are presented in the results section as examples.

Cucurbit[6]uril hydrate was purchased from Sigma Aldrich. The sample preparation for HPLC analysis required its dissolution in a concentration of ~1 mg/ml, which was achieved in acidified water, where HCl and TFA were used. The columns used in this analysis were Kinetex C18 column (2.1 x 100 mm, 2.6 µm), Agilent Eclipse XDB-C18 (4.6 x 150 mm, 5 µm), Kinetex HILIC column (2.1 x 100, 2.6 µm) and C8 column Ultra Amino (4.6 x 200 mm, 5 µm) from Restek.

The CB kit was purchased from Strem Chemicals Inc. For the HPLC analysis, the samples of CB[5-8] were prepared separately and then mixed together. The samples of CB[5] and CB[7] were prepared in water with concentrations of ~0.05 and ~0.06 mg/ml, respectively. Samples of CB[6] and CB[8] were prepared in water containing about 20% acetic acid (~0.05 mg/ml). Homologues were mixed together before the chromatographic analysis. Hexafluoroisopropanol was added to the samples to test its effect on the solubility and resolution of CBs, but it didn't affect any of them, and therefore its use was abandoned. The columns used in the analysis of the CB kit were Kinetex C18 column (2.1 x 100 mm, 2.6 μm), Agilent Eclipse XDB-C18 (4.6 x 150 mm, 5 μm), HILIC Kinetex (4.6 x 50 mm, 2.6 μm) and YMC-Triart Diol-HILIC (2.0 x 100 mm, 1.9 μm). When using RP columns, different ratios and gradient lengths with water (or acidified water with 0.05% of TFA) and acetonitrile moving from polar to unpolar were tried out. For the HILIC columns, 0.1 M ammonium acetate (pH = 7) was also used as an eluent instead of water with different gradients, from an unpolar to a polar solvent system. The detection of CBs was tested on several wavelengths.

Optimization of the RP-HPLC-UV technique for the separation of the cycHCs.

For the optimization of the chromatographic separation and spectroscopic detection, the following parameters were varied: the wavelengths at 200, 210, 250, 254 and 280 nm, eluent composition with gradient modes from 70/30 to 40/60 of ACN/H_2O or ACN/0.05% TFA, and solvents for the sample preparation, which were acetonitrile, methanol, formic acid, acetic acid, trifluoroacetic acid and chloroform in pure form or as mixtures, were compared.

Synthetic procedure for mixing (R,S)-cyclohexa-1,2-diylurea and biotin.

The synthesis of (*R,S*)-cyclohexaneurea was repeated in our laboratory according to the literature procedure.[58] An analysis was done on a chosen reaction with a fixed ratio of starting materials. Namely, in a 5:1 mixture of biotin (87 mg; 0.36 mmol) and (*R,S*)-cyclohexaneurea (10 mg; 0.07 mmol) paraformaldehyde (13 mg; 0.43 mmol) and 7 M aq. HCl (5 ml) were added. The mixture was heated for three days at 60°C. After that it was cooled in an ice bath, water (18 ml) was added, it was centrifuged, and the solution was decantated. This procedure was repeated three times. Methanol was added and the mixture was mixed over night and concentrated HCl was added the next day. An analysis was performed with the RP-HPLC-UV method with the set A with some changes, which are detailed in the corresponding section of the discussion. An HRMS analysis was done for the identification of compounds.

Calibration of inverted-(R,S)-cycHC[6].

The calibration of this macrocycle was not published with the others[108], but the procedure is similar to that described. Briefly, to calibrate the signal against the macrocycle content, two six-point calibration curves were created using linear regression analysis. The concentration range chosen was from the LoD to 200 µg/ml. Stock solutions were made by weighing the macrocycle and dissolving it in $CHCl_3$. Dilutions were made with MeOH. Standard solutions were made directly before analysis. Each solution was prepared in three parallels, which were measured once. The parallels were used to calculate the standard deviations of the peak areas. The accuracies for standard solutions were calculated by the square root of the sum of the squares of accuracies corresponding to weights or syringes during preparation. The LoD and LoQ were found experimentally by diluting samples until the signal to noise ratio was 3 and 10, respectively.
The purity of the compounds that were used for calibration was determined by ^{1}H-NMR, following a known procedure, and this is described in Article III. The purities of macrocycles used for the UV signal calibrations are listed in Table 2.

Table 2. Purities of the macrocycle measured by ^{1}H-NMR.

Macrocycle	**Purity ± SD**[a]
(*R,R*)-cycHC[8]	84.4 ± 0.7%
(*R,R*)-cycHC[6]	85.2 ± 0.7%
(*R,S*)-cycHC[6]	87.7 ± 0.6%
i-(*R,S*)-cycHC[6]	79.8 ± 0.1%

[a] $n = 3$

The general procedure to prepare HPLC samples from reaction mixtures was to take 20 µl of the reaction mixture and dilute it in a $CHCl_3$/MeOH (1 : 4) mixture. The concentrations were found using the y = ax + b equation from the calibration curves.

4 Results and discussion

This thesis focuses on the chromatographic and mass spectrometric analysis of cucurbiturils and hemicucurbiturils, with a focus on the cyclohexano-substituted hemicucurbiturils. The first of the following chapters describes our attempts to analyze parent cucurbiturils. The second chapter covers the optimization of the RP-HPLC methodology to analyze different batches of crude reaction mixtures of (*R,R*)-cycHC[6]. The third part focuses on the mechanistic studies of the reversible macrocyclization between (*R,R*)-cycHC homologues. The fourth describes the analysis of substituted HCs from mixed monomers of cyclohexadiylurea and biotin. Unsubstituted hemicucurbiturils are analyzed in the fifth chapter and the final sixth chapter describes the calibration procedure and UV analysis of cycHCs.

4.1 Analysis of cucurbiturils

As mentioned in the literature part, the detection of CBs with UV is troublesome. Although CBs have carbonyl group chromophores, two per monomer, isolated from each other and therefore unable to form a conjugated system, the signal in the lower UV-Vis region should still be visible. The carbonyl group should give two possible absorption bands corresponding to $\pi \rightarrow \pi^*$ and $n \rightarrow \pi^*$ electron transitions.[109] The first transition has a maximum under 190 nm, but it should still be seen at 200 or 210 nm, since the inherent extinction coefficient is around 1000 $M^{-1}cm^{-1}$. The second transition has its maximum around 270-280 nm, but as its absorptivity is very low ($\varepsilon \sim 10\ M^{-1}cm^{-1}$), we did not expect to observe it.

From the UV measurements on the UV spectrophotometer, it was clear that CB[6] has its absorbance maximum at a lower wavelength than 190 nm (see Figure 16 A), but a signal was observed at up to 210 nm. The spectra looked the same for all CB homologues and showed the same tendency in both solvents tested (ACN and H_2O). Solvents were chosen considering further analysis of CBs on HPLC system, where ACN and water were the main eluents used in the RP- and HILIC techniques.

The first measurements on HPLC were recorded on several chosen wavelengths (see Figure 16, B) to check the applicability range of UV detection in the HPLC system; for further experiments, detection was carried out only at 200 nm.

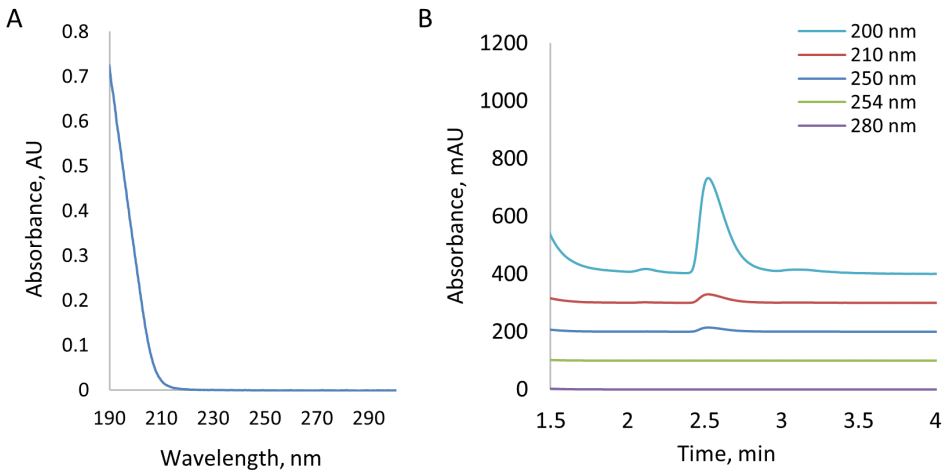

Figure 16. Absorbance of CB[6] measured with A) UV-spectrofotometer and B) HPLC equipped with a multiple wavelength detector. Experimental conditions for spectrophotometric analysis: a saturated solution of CB[6] in ACN was prepared and centrifuged, and the clear solution was measured; for HPLC-UV analysis: ~1 mg/ml of CB[6] was dissolved in 0.1 M aq. HCl. Kinetex Hilic column, isocratic elution with 20/80 ACN/ H_2O at 0.25 ml/min.

The solubility of CBs is low in common organic solvents. To improve the solubility, formic acid can be used[19]. CB[5] and CB[7] are known to have better solubility in water, so their respective samples were prepared in pure water (around 0.05 mg/ml). Based on the choice of solvents used for the CB sample preparation, normal phase (NP) separation was not considered for the analysis of CBs; instead, reverse phase (RP) HPLC and HILIC techniques were seen as possible options.

The chromatographic separation of a six-membered homologue was approached first. After optimization of the eluting system on both C18 columns (see details in the experimental section), the signal corresponding to CB[6] was still not separated on the Kinetex C18 column from the wide solvent peak (see Figure 17).

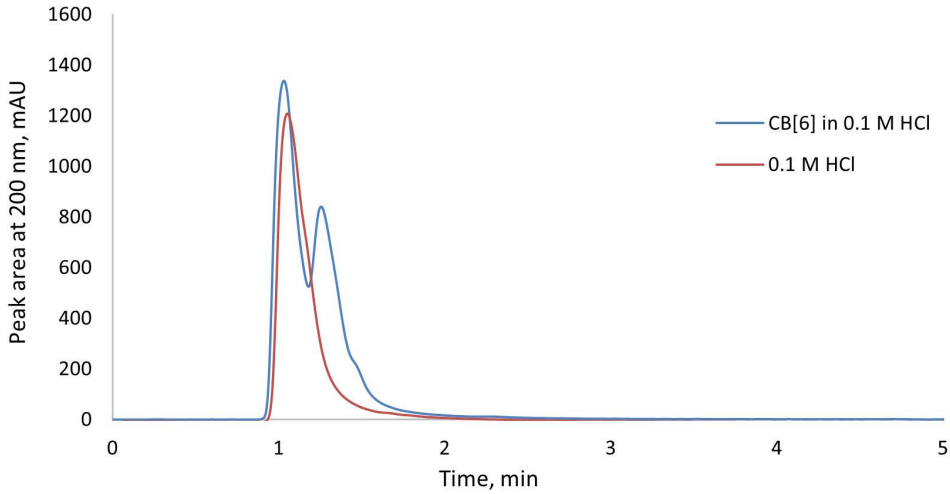

Figure 17. Separation of CB[6] in 0.1 M aq. HCl solution under experimental conditions named in set A, with 1/99 ACN/H_2O isocratic elution.

Observing that the signal of CB[6] appeared at such short retention times in these chromatograms, it was concluded that CBs must be too polar to be separated by RP-HPLC. Therefore, we switched to the HILIC technique, in essence a combination of RP- and NP-HPLC, which is most suitable for polar compounds. In HILIC mode, a polar stationary phase is used in combination with reverse phase eluents. The most common solvent for elution is ACN consisting of a small amount of water. Retention would be stronger for a more polar compound, so less polar analytes will elute first. Using a HILIC column, it was possible to separate CB[6] from the solvent signal (see Figure 18).

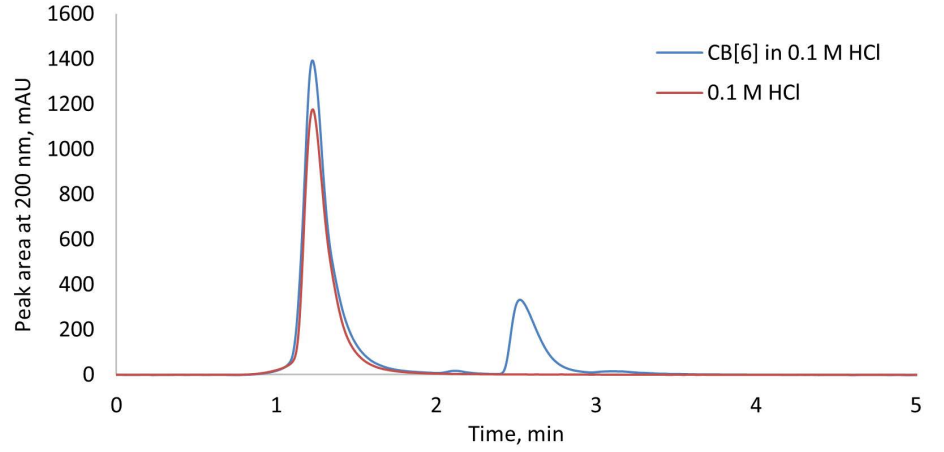

Figure 18. Separation of the CB[6] sample dissolved in 0.1 M aq. HCl solution on Kinetex Hilic column with 20/80 ACN/H_2O isocratic elution at 0.25 ml/min.

After the detection of CB[6], its 5-, 7- and 8-membered homologues were added to the same sample. Unfortunately, after several attempts at the optimization of

eluent compositions and gradients modes on different column types, C18, C8 and HILIC, the separation of CBs was still not accomplished, and probably all homologues coeluted.

4.2 Analysis of cyclohexanohemicucurbiturils with RP-HPLC

4.2.1 Crude mixture of (*R,R*)-cyclohexanocucurbit[6]uril

By the time I started my PhD studies, the structure and properties of (*R,R*)-cycHC[6] had already been characterized and the properties were identified well enough to consider analysis of this macrocycle on RP-HPLC using UV detection. The macrocycle has a barrel-like shape, it is unpolar in the portals, it has a polar belt, and the cavity is hydrophobic (see Figure 19). Chiral cycHC[6] can form complexes with some anions, such as halids and carboxylic acids.[61]

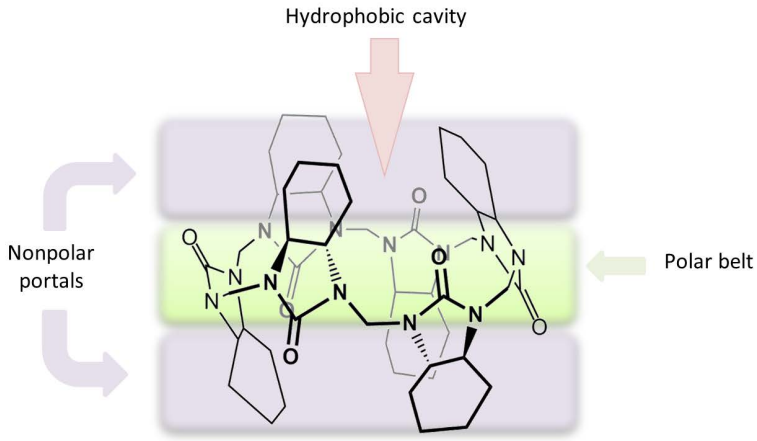

Figure 19. Illustrative structure of (*R,R*)-cycHC[6].

According to the structure of cycHC[6], it has enough hydrophobic interaction sites for the C18 stationary phase.
(*R,R*)-cycHC[6] is soluble in chlorinated solvents, which is not a very suitable solvent for RP-HPLC. Close to zero water solubility also complicates the analysis. Fortunately this macrocycle dissolves in a small amount of methanol and acetonitrile, which is compatible with RP-HPLC analysis. To increase the solubility of the crude sample, a larger portion (10-20% v/v) of chloroform or acid (AA or FA) was used to prepare the sample for injection into HPLC.
The UV absorbance of cycHC[6] had not been studied previously. But considering that CBs were detected at wavelengths below 210 nm, the signal of HCs was also expected to be present, though at a lower intensity, as HCs have less chromophoric groups, compared to CBs.

The spectrum of the (*R,R*)-cycHC[6] measured with a UV spectrophotometer is shown in Figure 20 A, and detection with HPLC-UV at different wavelengths in Figure 20 B.

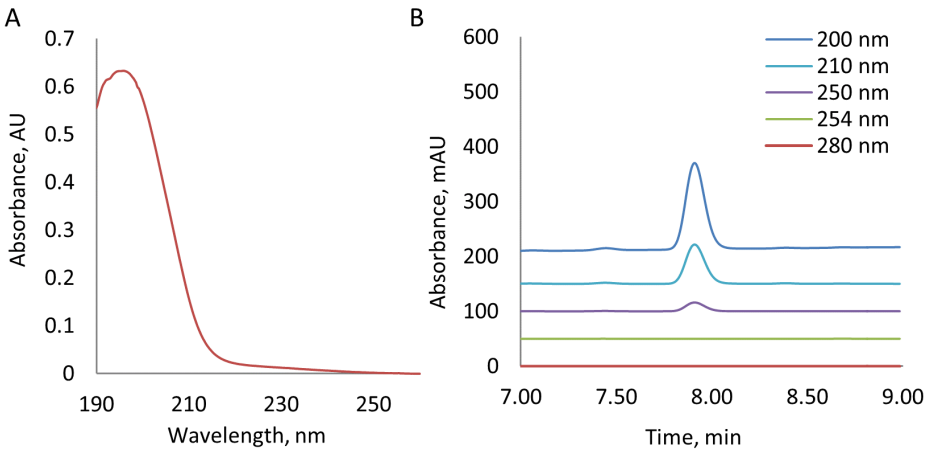

Figure 20. Absorbance of (*R,R*)-cycHC[6] measured with A) UV spectrophotometer and B) HPLC with a multiple wavelength detector at different wavelengths. Experimental conditions for UV analysis: cycHC[6] was dissolved in ACN; a detailed description can be found in Article III; and for HPLC analysis: set-A, about 1 mg/ml of cycHC[6] was dissolved in 1:9 v/v $CHCl_3$/ACN mixture.

As was expected, the strongest signal was observed around 200 nm. At 210 nm the signal was also present and even at 250 a residue signal was observed through the HPLC-UV system. Since wavelength 200 nm is near the limit of the detector and also the baseline fluctuates more due to absorbance by the solvents of eluent, 210 nm was chosen for further experiments.
Elution with ACN/H_2O and ACN/0.05% TFA didn't affect the resolution or effectiveness much (see Figure 21). Since it was slightly faster to use acidified water for elution, it was chosen for further use at first, but after discovering that macrocycles were not stable in acids, we switched to the ACN/H_2O eluent system (pH = 7) to avoid any changes through reactions in acidic aqueous media during the run.

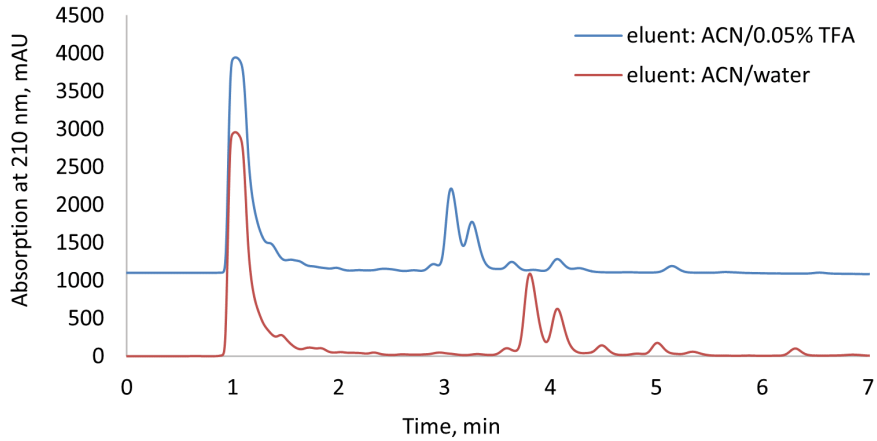

Figure 21. Analysis of a crude sample of (*R,R*)-cycHC[6] with two different eluents in set A, with a 60/40 eluent system.

Studying the aspects that affect chromatographic behavior (retention, absorption or precipitation during run) in different solvent systems for sample preparation, one observation was made: using formic acid as an additive for preparation, a gradual increase in a new compound in the sample was detected (see Figure 22), which is described in the next section.

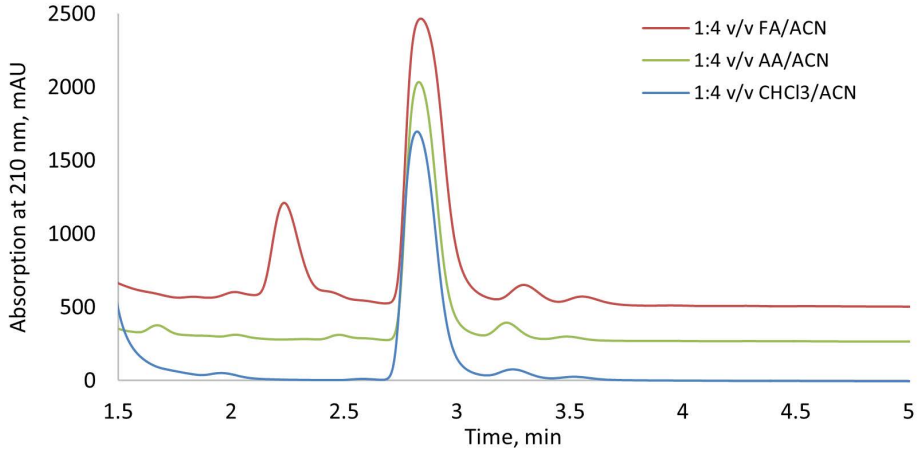

Figure 22. Analysis of (*R,R*)-cycH[6] in different sample preparation solvents in set A with 70/30 ACN/TFA.

4.2.2 Isolation of (*R,R*)-cycHC[8]

The first (*R,R*)-cycHC[8] macrocycle was prepared starting with enantiopure (*R,R*)-cyclohexadiylurea, according to the pathway shown in Scheme 1.

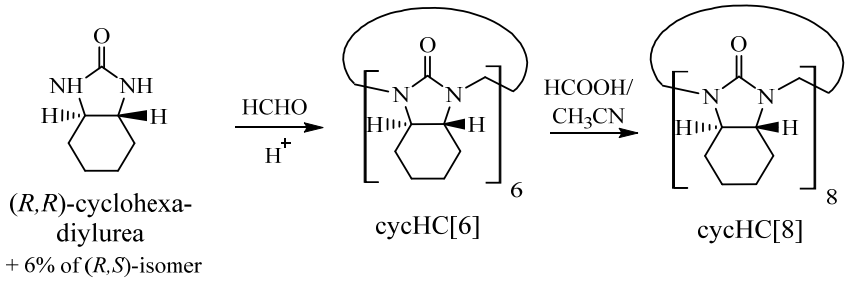

(*R,R*)-cyclohexa-diylurea
+ 6% of (*R,S*)-isomer

cycHC[6]

cycHC[8]

Scheme 1. Synthesis of (*R,R*)-cycHC[8].

High resolution mass spectrometric analysis of (*R,R*)-cycHC[6] sample dissolved in FA/ACN showed that the new peak corresponded to an 8-membered macrocycle, where $[M+Na]^+$ was the most intensive peak in the mass spectrum. The adducts $[M+H]^+$ and $[M+K]^+$ were also present (see Figure 23).

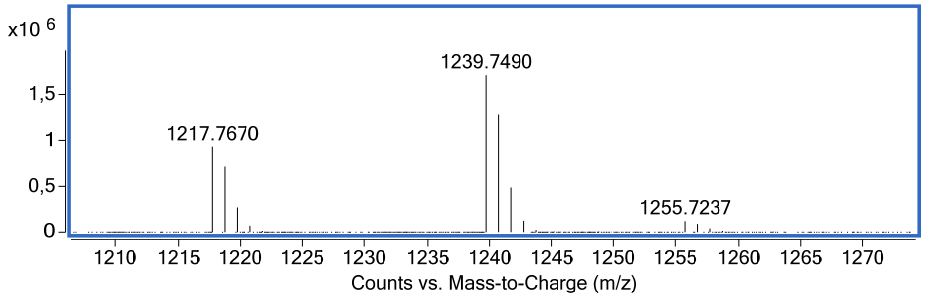

Figure 23. Mass spectrum of (*R,R*)-cycHC[8]. Experimental: set B. Theoretical m/z values for adducts with H^+, Na^+ and K^+ are 1216.7670, 1239.7489 and 1255.7229, respectively.

Also the presence of 7-, 9- and 10-membered homologues were detected in the same sample, although in trace amounts (see Figure 24).

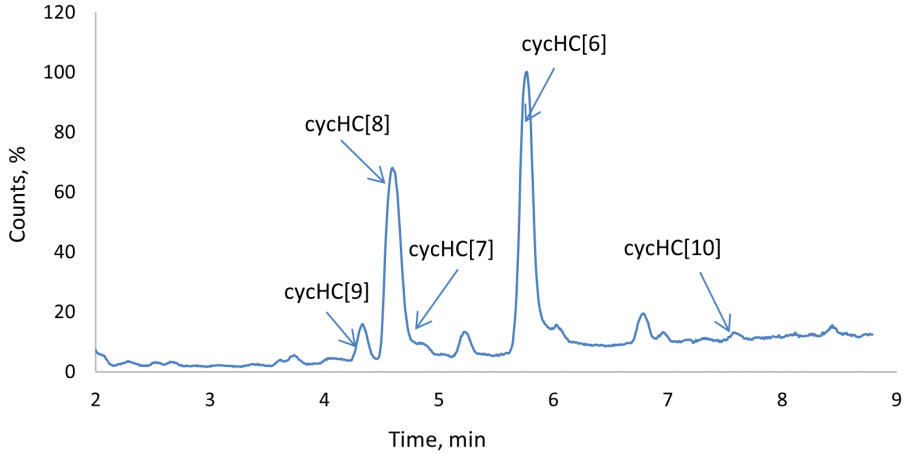

Figure 24. TIC from the HPLC-MS chromatogram of the cycHC[6] sample dissolved in 1:9 FA/ACN solution. Experimental: set B.

The RP-HPLC-MS analysis showed the elution order for the macrocycles to be cycHC[9], cycHC[8] and cycHC[7], which were not baseline resolved, followed by cycHC[6] and cycHC[10], further apart. It is not exactly known how the macrocycles interacted with the stationary phase. The resolution could have been affected by shape, size and polarity. Trying to understand more about the detected macrocycles, the computational calculations were done by Mario Öeren in our group to view the geometries of all new macrocyles (see Article I and Figure 25).

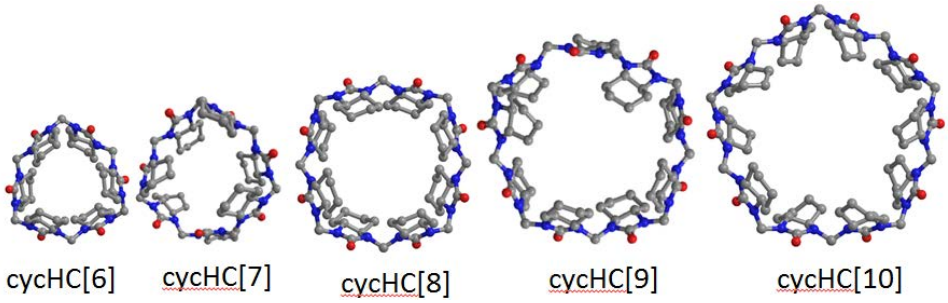

Figure 25. DFT modeled structures of cycHC[6-10].

As expected, all even numbered hosts were symmetrical, showing triangular, tetragonal and pentagonal cavity shapes for 6-, 8- and 10-membered homologues, respectively. Odd numbered macrocycles were not as symmetrical since all monomers could not adopt alternate conformation and two monomers oriented their carbonyl groups in the same direction, but the general shape was still barrel-like, with different sizes for the cavity. The dimensions and structures are shown in Article I.

The mass spectrometric analysis was also done in negative mode and it was interesting to observe that the overall ionisation of cycHC[6] was much smaller compared to its ionisation in positive mode (see Figure 26).

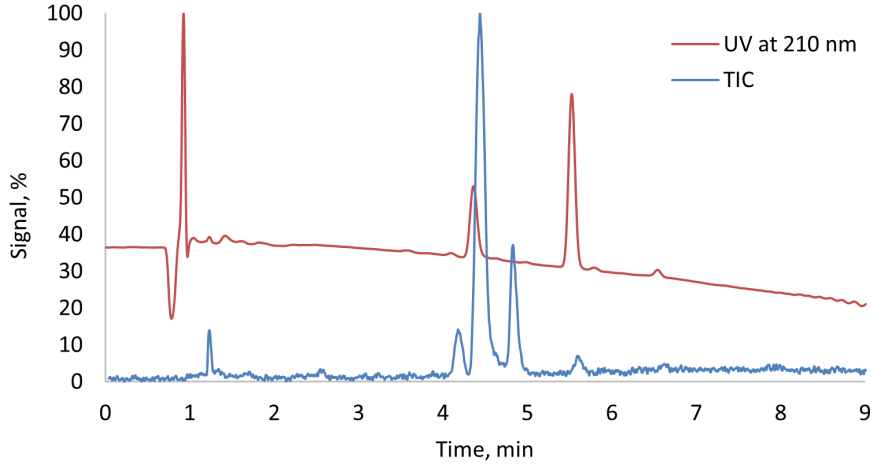

Figure 26. HPLC-UV and -ESI(-)-HRMS analysis of cycHC[6] in 1:9 FA/ACN solution. Experimental: set B.

Generally it is known that the intensities in negative mode of electrosprayionisation are lower compared to in positive mode. It is also common that halogenides can suppress the ionisation. Considering the fact that cycHC[6] forms an inclusion complex with a chloride anion and the [cycHC[6] + Cl]$^-$ adduct was detected with HRMS (see Figure 27), this could be the reason for the very weak signal. Generally, in negative mode, the dominant adducts were usually formed with formate as [M+HCOO]$^-$ (see Figures 27 and 28), where the source of formate was formic acid added to the sample or to the eluent in RP-HPLC. No other macrocycles beside cycHC[6] and cycHC[8] were detected during the mass spectrometric analysis in negative mode.

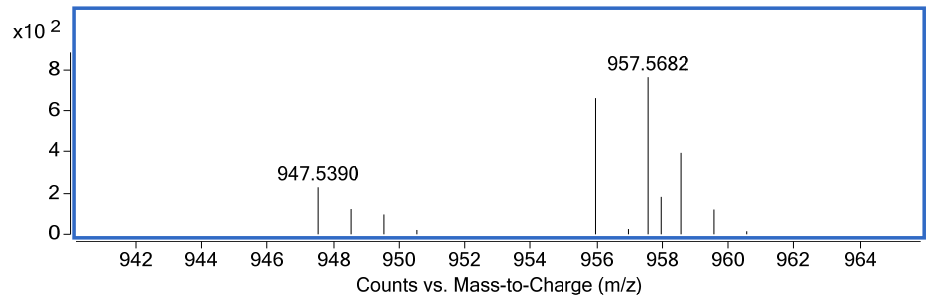

Figure 27. Mass spectrum of (*R,R*)-cycHC[6] from ESI(-)-HRMS. Experimental: set B. Theoretical m/z values for adducts with Cl$^-$ and HCOO$^-$ are 947.5392 and 957.5680, respectively.

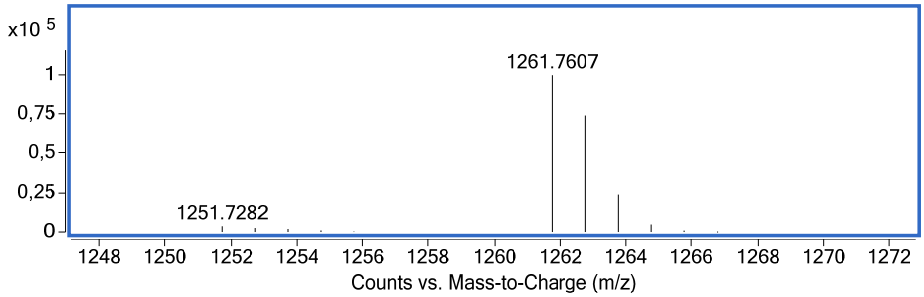

Figure 28. Mass spectrum of (*R,R*)-cycHC[8] from ESI(-)-HRMS. Experimental: set B. Theoretical m/z values for adducts with Cl^- and $HCOO^-$ are 1251.7291 and 1261.7579, respectively.

In order to have a better understanding and the opportunity to characterize the new 8-membered macrocycle, flash chromatography was performed. A crude reaction mixture of cycHC[6], which was dissolved in FA and ACN, was used for separation. As a result, from 200 mg of cycHC[6] 21 mg of 8-membered macrocycle (details can be seen in Article I) was obtained. Isolated product was characterized by IR, NMR, melting point and optical rotation, though the isolated fraction contained some additives. It can be seen in the HPLC-UV chromatogram (see Figure 29) and NMR spectra (see Figure 30) that the isolated fraction contains mainly (*R,R*)-cycHC[8], but also some other isomers of an 8-membered macrocycle and also a small portion of six-membered cycHC isomers. Additives were identified by HPLC-HRMS.

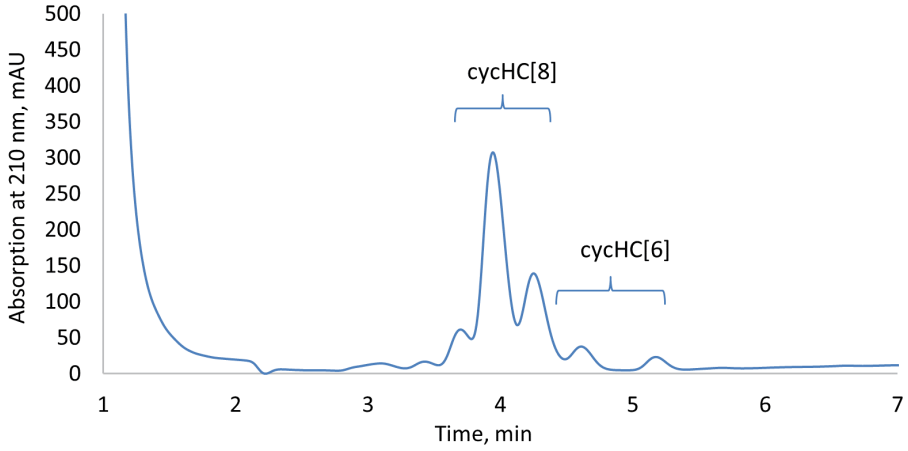

Figure 29. HPLC chromatogram of the first isolated cycHC[8]. Experimental: set A with 60/40 ACN/H_2O.

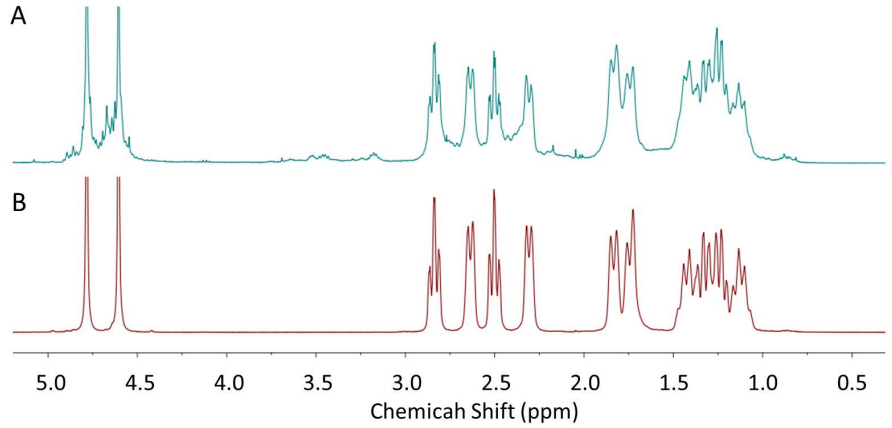

Figure 30. ^{1}H-NMR spectra of (1) pure (*R,R*)-cycHC[8] and (2) the first isolated fraction of (*R,R*)-cycHC[8].

Later it was established by NMR of the starting material, the (*R,R*)-cyclohexa-1,2-diylurea (see Scheme 1), that besides enantiopure *trans*-isomer it contained 6% *cis*-isomer, which caused the formation of diastereomeric isomers of cycHC[6] and cycHC[8].

At the same time, a deeper investigation was started to find out why and in what cases the 6-membered macrocycle turned into an 8-membered one and what happened during that transformation. This is covered in Article II and described in the next section.

4.2.3 (*R,S*)-cyclohexanohemicucurbit[6]uril

In addition to chiral cycHCs, the synthesis of achiral (*R,S*)-cyclohexano-hemicucurbit[6]uril was performed in our laboratory by Anastassia Baškir, Madli Trunin and Elena Prigorchenko. The effect of acids on the stability of (*R,S*)-cycHC[6] was also investigated, and its chromatographic analysis was developed. To compare the interaction of cycHCs with the C18 stationary phase, a mixture of 6- and 8-membered (*R,R*)- and 6-membered (*R,S*)-derivatives was simultaneously analyzed. It turned out that (*R,S*)-cycHC[6] is the most polar and its retention time is even shorter than that of an 8-membered macrocycle (see Figure 31).

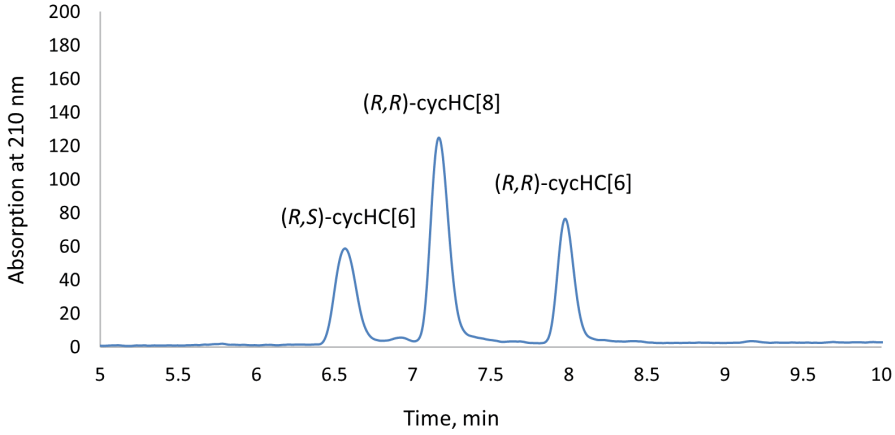

Figure 31. RP-HPLC-UV chromatogram of (*R,S*)-cycHC[6], (*R,R*)-cycHC[8] and (*R,R*)-cycHC[6]. Experimental: set A.

After the resolution was established, (*R,S*)-cycHC[6] was dissolved 1:1 in FA (300 eq)/ACN (~40 mg/ml heterogeneous), 1:1 in TFA (177 eq)/ACN (~33,3 mg/ml) and $NaPF_6$ (50 eq) and 1:1 in AA (183 eq)/ACN (~43,5 mg/ml), similarly to how it was done previously for (*R,R*)-cycHC[6][60]. The content of (*R,S*)-cycHC[6] was followed with RP-HPLC. In the case of (*R,R*)-cycHC[6] in the FA/ACN solution, the 8-membered macrocycle was in the majority in 24 hours. Compared to the chiral isomer, the (*R,S*)-macrocycle was quite stable and even after a couple of days its UV signal had decreased only by one quarter. Some small peaks were noticed close to the (*R,S*)-cycHC[6] peak on the first day of analysis, but this signal didn't increase significantly later. At first it was suspected that this signal belonged to an 8-membered homologue, and therefore the sample was analyzed by HRMS.

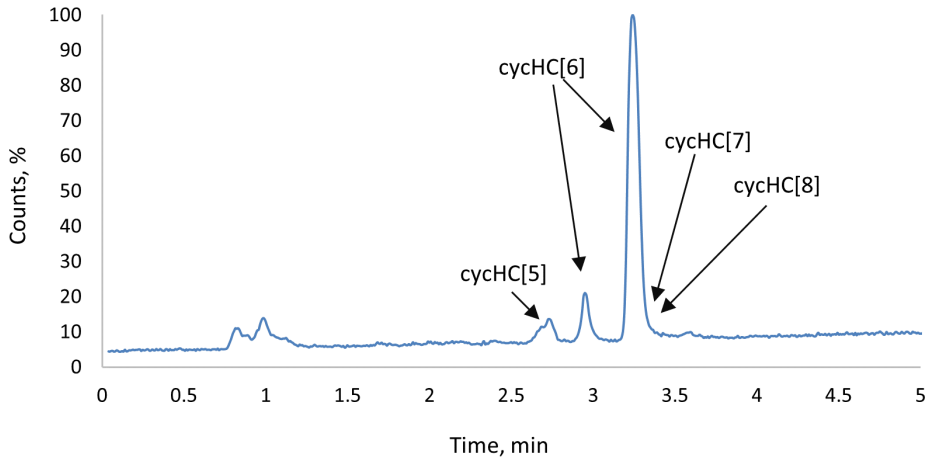

Figure 32. TIC from HPLC-MS of (*R,S*)-cycHC[6] sample dissolved in 1:1 FA/ACN and measured after 48 hours. Experimental: set B.

It turned out that the new peak was another 6-membered homologue of cycHC. All these samples contained two 6-membered cycHCs and also traces of 5-, 7- and 8-membered homologues (see Figure 32 and Figure 33).

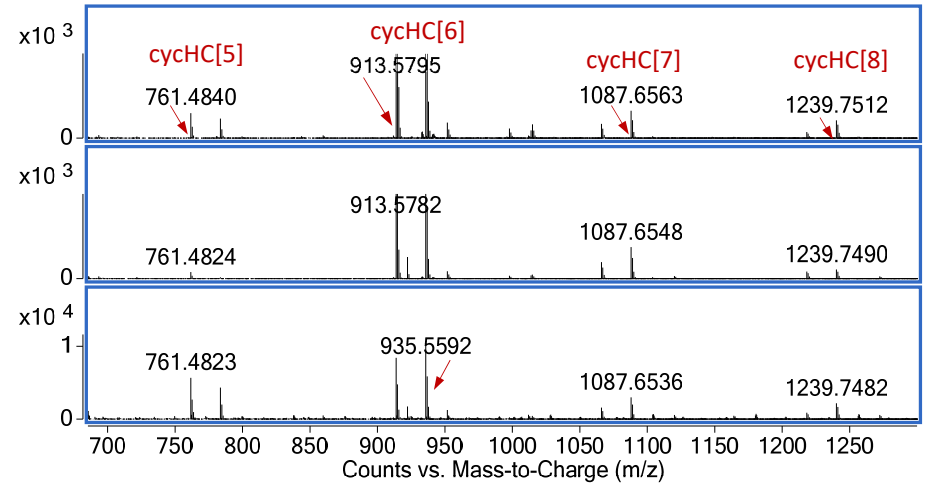

Figure 33. Mass-spectra of the crude solution of (*R,S*)-cycHC[6] in A) FA/ACN (48 h), B) in $NaPF_6$/AA/ACN (48 h) and C) in TFA/ACN (1 h). Experimental: set B. The calculated m/z value for the $[cycHC[5] + H]^+$ adduct is 761.4821; the $[cycHC[6] + H]^+$ and $[cycHC[6] + Na]^+$ adducts are 913.5771 and 935.5590; the $[cycHC[7] + Na]^+$ adduct is 1087.6540; the $[cycHC[8] + Na]^+$ adduct is 1239.7489.

About 2/5 of the (*R,S*)-cycHC[6] was degraded in a $NaPF_6$/AA/ACN solution after 48 hours. In a TFA/ACN solution, more than half of the macrocycle degraded within 1 hour.

Later, in 2017, it was confirmed that the new six-membered macrocycle was *inverted*-(*R,S*)-cycHC[6], which will be discussed in section 4.4.1.

4.3 HPLC and MS analysis of cycHCs for uncovering reversible macrocyclisation mechanism

After the first realization that one macrocycle can be turned into another, we focused on finding the optimal conditions for the synthesis of 8-membered (*R,R*)-cycHC either from a monomer or cycHC[6] homologue. We also attempted to determine the mechanism for this reversible macrocyclisation.
Lisbjerg et al.[63] proposed that biotin[6]uril formation proceeds through trimerisation of dimers. Using HPLC-MS, they quantitatively followed the reaction mixtures, showed that dimers are the major intermediates and concluded that biotin[6]uril is formed through the connection of dimeric units. It was interesting to determine how the reversible macrocyclisation proceeded from cycHC[6] to cycHC[8], as they differ by exactly a dimer unit. For this purpose, a 1:1 mixture of cycHC[6] and labeled cycHC[6] (consisting of ^{13}C-labelled methylene bridges) was dissolved in a 1:1 deuterated FA/ACN mixture and followed with ^{13}C-NMR for two days; then it was also analyzed with HRMS (see Figure 34).

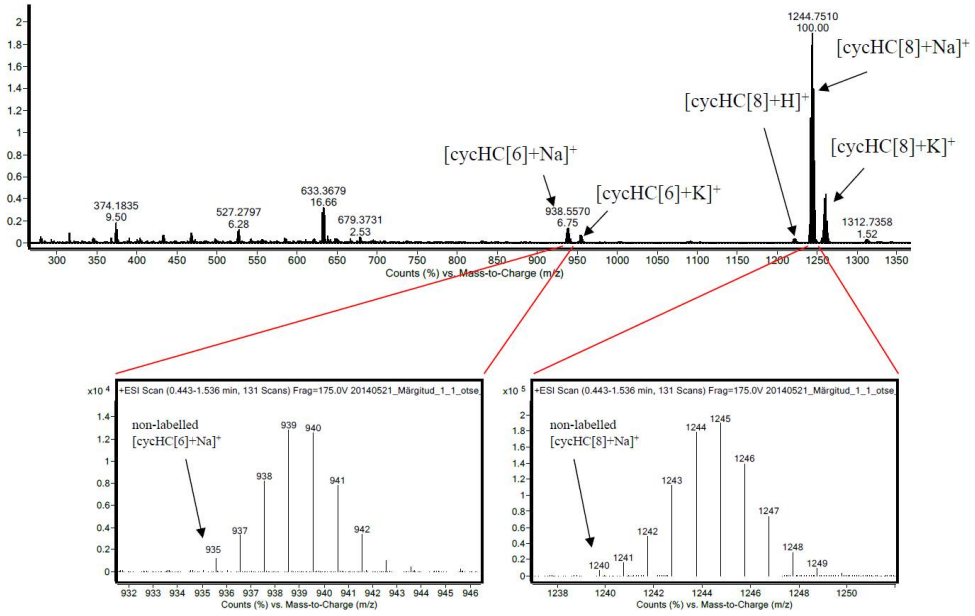

Figure 34. HRMS spectra of the reaction mixture of labeled and unlabeled (*R,R*)-cycHC[6] in a 1:1 FA/ACN solution measured after 48 hours. Experimental: set B. Reprinted from ref.[60] with permission from the Royal Society of Chemistry.

As can be seen, the shape of the isotopic distribution for the Na^+ complexes for cycHC[6] and cycHC[8] followed the normal distribution, which means that

degradation and propagation of the chain proceeded by adding a monomeric unit instead of a dimer, as was first expected.

The influence of different acids (AA, FA and TFA) and solvents (water, methanol and acetonitrile) on the formation of (*R,R*)-cycHC macrocycles, and on the previously formed and isolated oligomers was intensively studied. About 40-50 reactions were performed for the whole study, and all were followed up with a developed HPLC method and HRMS analysis (see Article II). As a result of this study, it was concluded that dynamic covalent chemistry (DCC) is operative in cycHCs formation (see Scheme 2). The synthesis of macrocycles proceeds through dynamic combinatorial library (DCL), which represents the equilibrium of different sized linear and cyclic oligomers. Applying the right conditions (template) to the mixture of DCL, it is possible to affect the selectivity of the products in the desired direction.

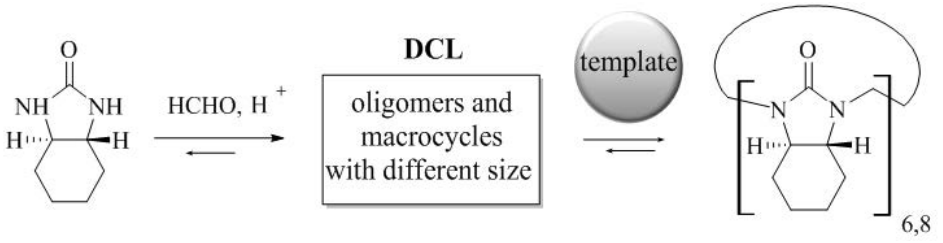

Scheme 2. Macrocycle formation through DCL.

In Figure 35 all of the detected and identified oligomers are shown, and their m/z values, which were used for identification, are shown in the supporting information of Article II. Each type of oligomer is discussed below.

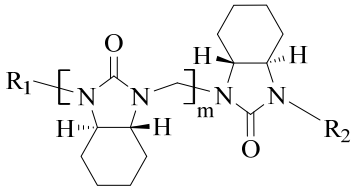

a: m=0
b: m=1
c: m=2
d: m=3
e: m=4
f: m=5
g: m=6
h: m=7
i: m=8
j: m=9

1: R_1=R_2: -H
2: R_1: -H; R_2: -CH_2OCHO
3: R_1=R_2: -CH_2OCHO
4: R_1: -H; R_2^+: =CH_2
5: R_1: -H; R_2: -CH_2OH
6: R_1=R_2: -CH_2OH
7: R_1: -H; R_2: -CH_2OCH_3
8: R_1=R_2: -CH_2OCH_3

Figure 35. Structures of oligomers detected with HRMS during a reversible macrocyclisation process.

The results of the HPLC-MS analysis of cycHCs in different acids showed that in acetic acid reversible macrocyclisation did not occur, but since some open-chain oligomers **1** were observed it was concluded that this weak acid was strong enough to break the methylene bonds between the monomeric units in the macrocycle, though with a very low reaction rate. The formed oligomers were not seen in the chromatogram, but were identified by HRMS; usually no longer

than 6-membered oligomers (**1b-f**) were formed in samples containing acetic acid. The same acid was later used together with a suitable non-acidic template, $NaPF_6$, which actually gave the best yield for the formation of an 8-membered (*R,R*)-cycHC from a 6-membered homologue (see Article II).
Mixtures of higher complexities were usually formed in any formic acid solution. They often contained, besides macrocycles, many open-chain oligomers (see Figure 36), whose structures were often not identified. The oligomers **1a-j, 4a-h** and sometimes **5a-g** were identified using HRMS.

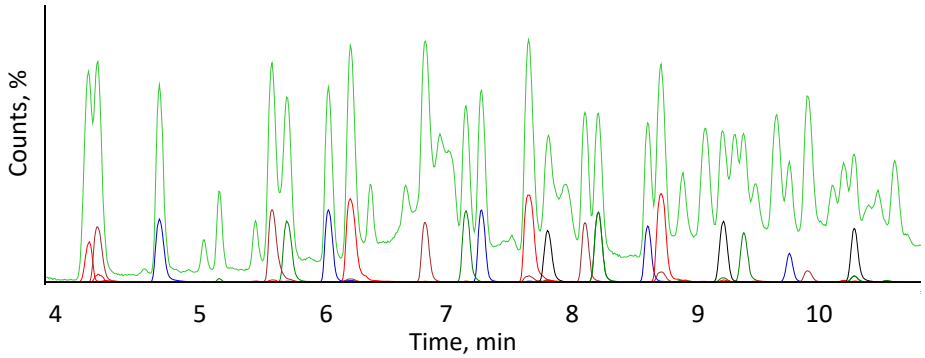

Figure 36. The HPLC-HRMS chromatogram of the (*R,R*)-cycHC[8] solution in 1:4 FA/ACN. Color explanation: light green: TIC, red and black: EIC of unknown oligomers, brown: EIC of hydroxyl-terminated oligomers (**6c-f**, from Figure 35), blue: EIC of hydrogen-terminated oligomers (**1c-g,** from Figure 35), and dark green: EIC of formate-terminated oligomers (**4c-f,** from Figure 35).

The oligomeric fractions of solutions that contained formic acid were usually detected in the chromatogram by UV (see Figure 37), which means that they made up the major part of the products.

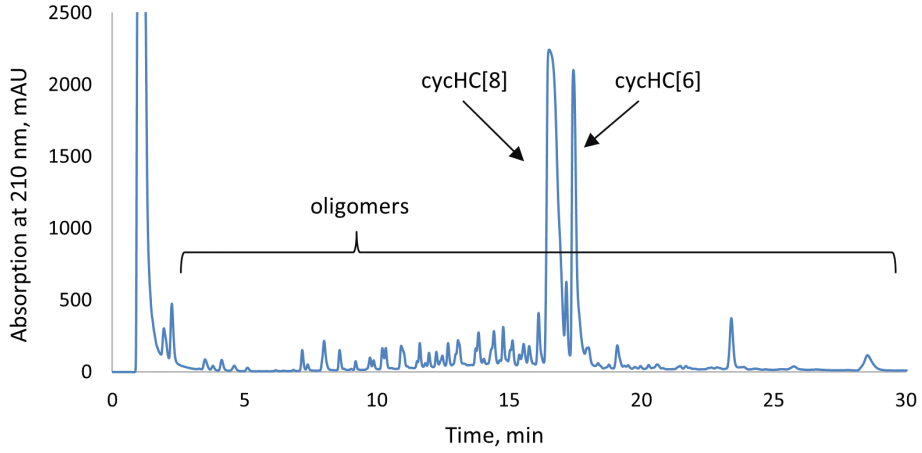

Figure 37. The HPLC-UV chromatogram of the (*R,R*)-cycHC[8] sample in 1:4 FA/ACN, measured after a week. Experimental: set A with 20 min gradient from 20/80 to 100/0 of the ACN/ H_2O eluent system.

Compared to samples prepared in the presence of FA, the samples containing TFA were interesting in that there were not many side products, and 8-membered (*R,R*)-cycHC formed fast in a good yield either from monomers, oligomers or a 6-membered macrocycle. It was concluded that besides acid-catalyzed breakage of the methylene bridges, TFA acted as a template for the 8-membered macrocyle, and thus the reaction was fast and oligomers **1** were usually detected in small amounts. Oligomers withCH_2OCOCF_3 terminal groups were not detected.

In an analysis of samples in negative mode and, extracted from the MS spectra, the complexes of the 8-membered macrocycle with conjugated bases of the used acids, only $[M+HCOO]^-$ was detected as a major ion. Neither $[M+CF_3COO]^-$ nor $[M+CH_3COO]^-$ were detected in our study, though $[M+CF_3COO]^-$ and $[M+PF_6]^-$ can be formed and observed by MS.[70]

Oligomers **2** and **6** (the structures are given in Figure 35) were also often observed in crude reaction mixtures. Later it was confirmed that samples which were treated with methanol mainly contained oligomers **7** and **8**.

Figure 38 presents the mass spectrum of oligomers which were formed from monomers in a mixture of FA and ACN, isolated by flash chromatography and diluted in $CHCl_3$/MeOH for the HPLC-MS analysis. Oligomers **1**, **2**, **5**-**8** were identified.

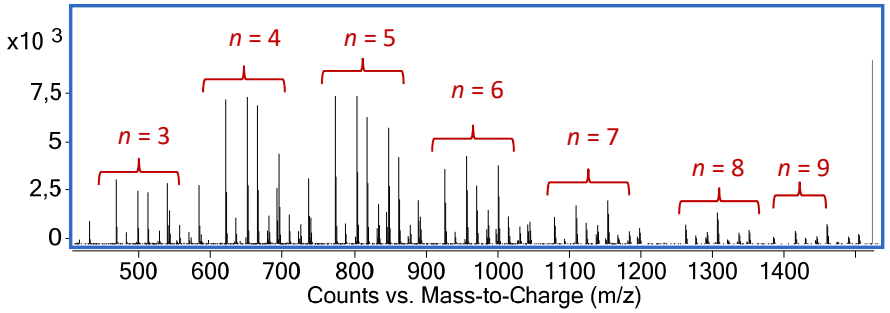

Figure 38. HRMS spectrum of a directly injected solution of *n*-membered oligomers in a 1:9 $CHCl_3$/MeOH mixture.

The formation of all previously mentioned oligomers should proceed via the iminium form of oligomers (see Scheme 3).

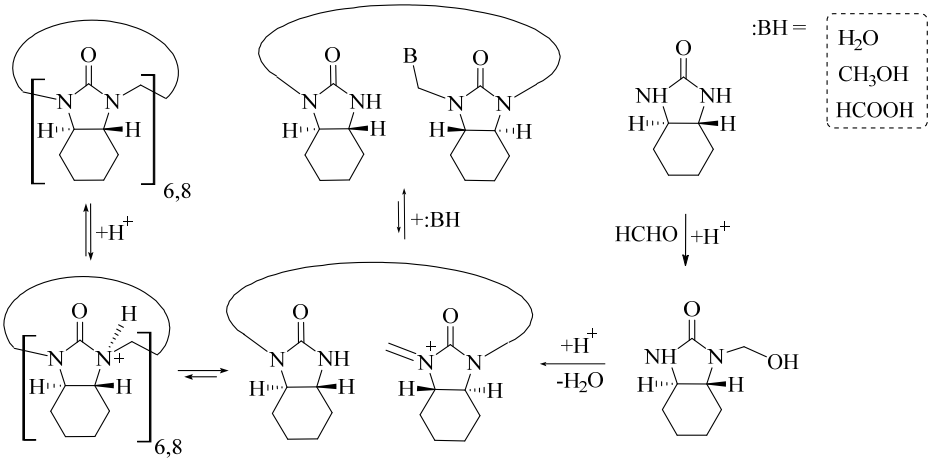

Scheme 3. Formation of oligomers with different terminal groups form macrocycles and monomers.

Searching for iminium ions with the HRMS was problematic. Firstly, they have the same m/z values as respective macrocycle $[M+H]^+$ ions and, secondly, since iminium is quite reactive, it normally reacts with nucleophiles during sample preparation. Therefore, only in cases where there were $[M+Na]^+$ and $[M+K]^+$ adducts besides protonated ones was it stated that this was the macrocycle and not the open-chain iminium. Also it was assumed that iminium ions were formed during the mass spectrometric analysis by the fragmentation of any compound.
More details about performed reactions using different starting materials, namely monomers, oligomers and macrocycles, and a discussion of the tunability of the DCL is provided in Article II. The main conclusions are the following: it is possible to synthesize cycHC[6] and cycHC[8] from each other, from monomers and from oligomers via dynamic covalent chemistry (see

Scheme 2). The size of a template dictates the size of the macrocycle, and the rate of the reaction is dependent on the acidity of the media.

4.4 Analysis of other cyclohexano-substituted hemicucurbiturils

Analyzing different batches of crude samples from the synthesis of (*R,R*)-cycHC[6] in one sample, two peaks with equal intensities (peaks 3 and 4 in Figure 39 A) were observed. Both observed peaks corresponded to six-membered macrocycles according to HRMS (see Figure 39 B). Treating this sample with formic acid, both of the cycHC[6] isomers turned into 8-membered ones (see Figure 39 A and C, peaks **1** and **2**).

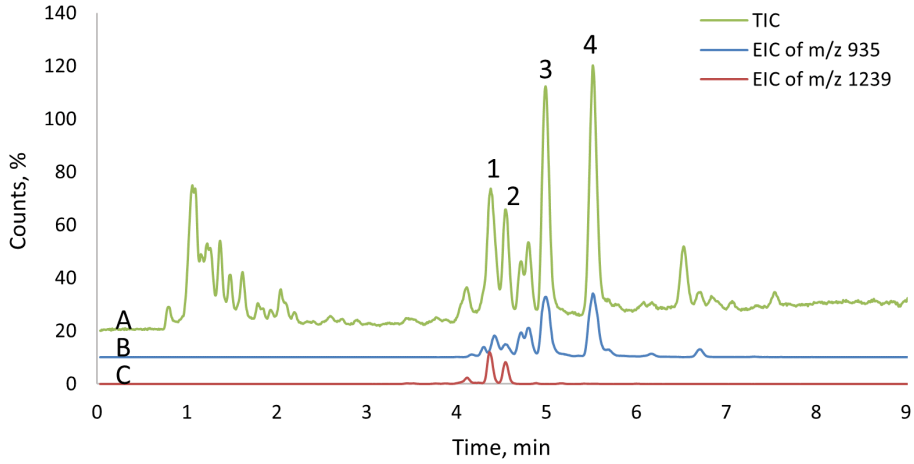

Figure 39. HPLC-HRMS analysis of a crude sample of cycHC[6] dissolved in FA/ACN. A) TIC, B) extracted ion chromatography for $[cycHC[6] + Na]^+$ adduct and C) extracted ion chromatogram for $[cycHC[8] + Na]^+$ adduct. Compounds **1** and **2** are cycHC[8] and **3** and **4** are cycHC[6]. Experimental: set B.

This observation encouraged our group to study the synthesis of macrocycles from diastereoisomeric monomer units, though this particular case (see Figure 39) was connected with impure starting material. Later it was determined that the starting material used for the (*R,R*)-cycHC[6] synthesis contained 94% (*R,R*)-cyclohexa-1,2-diylurea and 6% (*R,S*)-isomer; therefore the formation of diastereomers was possible.

4.4.1 Diastereomeric cycHC macrocycles

The synthesis of diastereoisomeric cycHCs was attempted in our group[110] and as a starting material a mixture of (*R,S*)- (*R,R*)- and (*S,S*)-isomers was used (see Scheme 4).

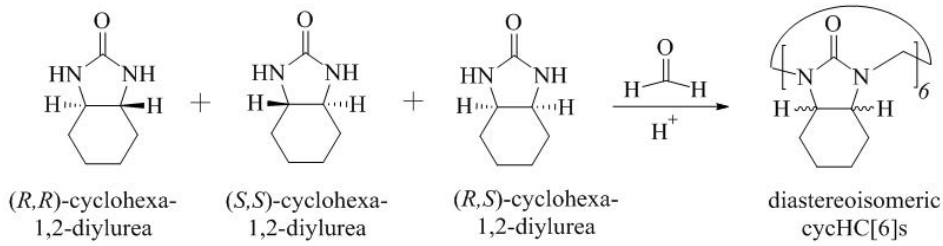

Scheme 4. Synthesis of diastereoisomeric cycHC[6]s.

As expected, the formed mixtures were very diverse and complicated to analyze (see Figure 40 A). However, it was noted that by increasing the amount of (*R,S*)-monomer relative to racemic-isomer it was possible to distinguish four major peaks in the chromatogram (see Figure 40 B-D).

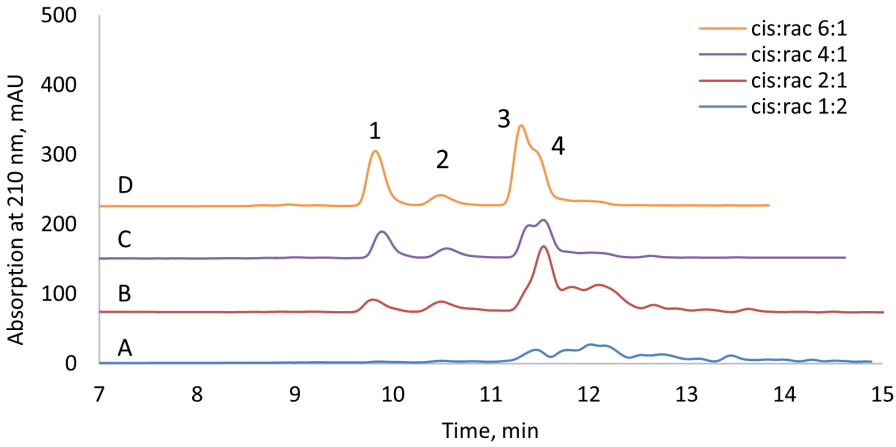

Figure 40. Chromatograms of crude samples synthesized from a mixture of *cis*- and *rac-trans*-cyclohexa-1,2-diylurea with ratios of the starting isomers of A) 1:2, B) 2:1, C) 4:1 and D) 6:1. Compound **1** is *inverted*-(*R,S*)-cycHC[6]; **2** is unknown cycHC[6]; **3** is cycHC[6] consisting of five *cis*- and one *trans*-cyclohaxaneurea units and compound **4** is (*R,S*)-cycHC[6]. Experimental: set A with 10 min gradient from 45/55 to 60/40 ACN/H_2O.

HRMS analysis showed that all of the formed macrocycles were six-membered. It was not possible to identify using MS which isomeric forms of cyclohexanourea were incorporated into the macrocyclic structures. All of the isomers of the studied building blocks had exactly the same m/z ratio, though it was possible to determine the number of monomers in the macrocycles. The (*R,S*)-cycHC[6] (compound **4** in Figure 40) was a known compound (viide) and its retention time coincided with the reference sample synthesized in our lab. Compound **3** was isolated in column chromatography as a mixture with (*R,S*)-cycHC[6] under the peak **4.** The macrocycle **3** was identified using NMR by

Madli Trunin to contain five *cis*- and one *trans*-cyclohaxaneurea unit.[110] Compounds **1** and **2** coeluted in flash chromatography, and NMR analysis confirmed that this sample contained several macrocycles, but it was possible to extract signals of compound **1** from ^{1}H and ^{13}C spectra of this mixture. Compound **1** was determined using NMR by other group members to be a macrocycle which contained a symmetry plane (a molecule with 6 bridging methylene groups and 6 carbonyl groups had in the ^{13}C spectra methylene signals with 3 chemical shifts and 4 carbonyl signals, of which two had double intensity). As the starting material consisted of a mixture of *cis*- and racemic *trans*-monomers, it was expected that all diastereomeric monomers would be incorporated into this new macrocycle, as shown in Figure 41, structures A, B and C. Firstly, the proposed macrocycles had one or two *cis*-monomers along with *trans*-monomers in their structures; the proposed structures contradicted the observation from the cycHCs interaction with the stationary phase of RP-HPLC (see Figure 40), where macrocycles from enantiomerically pure *trans*-monomers of (*R,R*)-cycHC[6] had much longer retention times compared to the (*R,S*)-cycHC[6] formed from *cis*-monomers (see Figure 41 D). Later the structure of compound **1** was identified as *inverted*-(*R,S*)-cycHC[6] (see Figure 41, structure D). All monomers were in *cis*-configuration, where five of them were pointing with the methine hydrogens inside the macrocycle and one (*R,S*)-cyclohexaneurea unit was directed the opposite way. Because of that, it was called an *inverted*-(*R,S*)-cycHC[6], analogously to *inverted*-CB[6] and *inverted*-CB[7][111].

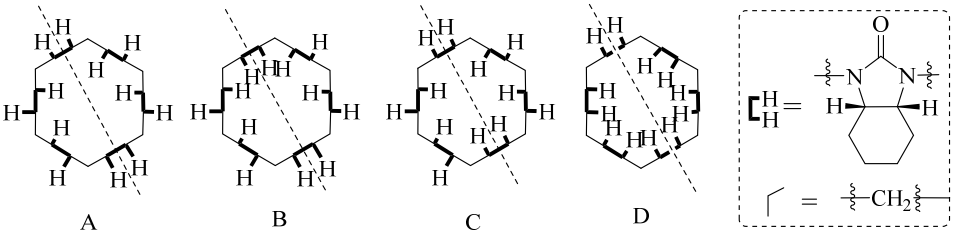

Figure 41. Structures of the possible diastereoisomeric cycHC[6]s having symmetry plane.

An analysis of crude reaction mixtures by HPLC revealed that *inverted*-(*R,S*)-cycHC[6] was also formed in reactions where only *cis*-monomer was used as starting material[59], along with the previously known (*R,S*)-cycHC[6][58] (see Figure 42).

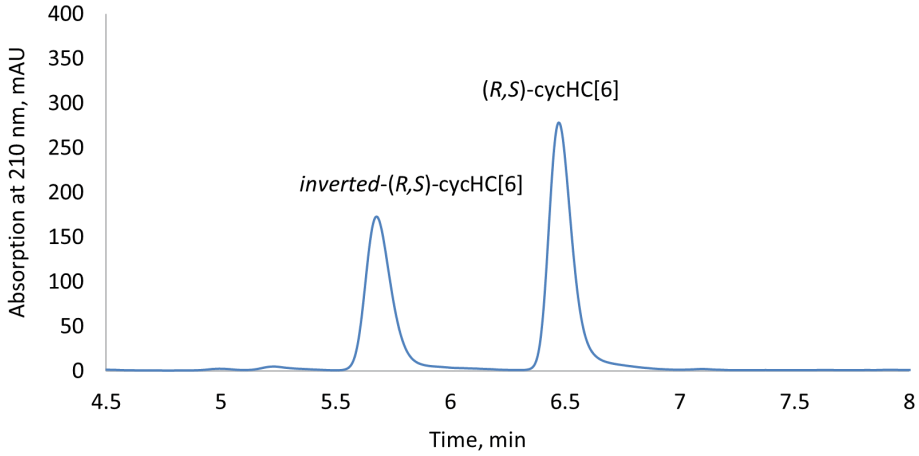

Figure 42. HPLC-UV chromatogram of a sample from the reaction mixture containing *i*-(*R,S*)-cycHC[6] and (*R,S*)-cycHC[6]. Experimental: Set A.

The structure of *inverted*-(*R,S*)-cycHC[6] was also confirmed by crystallographic analysis performed by Sandra Kaabel.

4.4.2 CycHCs containing biotinuril incorporated in the structure

An attempt was also made to synthesize a macrocycle which would contain biotin as one monomeric unit in the structure (see Scheme 5). In this case there was an effort to make the macrocycle more water soluble and modify it through the carboxylate functionality. Many reactions were performed while varying the ratios between biotin **B** and cyclohexa-1,2-diylurea **C**, and the best results were achieved with a 5:1 ratio, where macrocycles with different amounts of cyclohexaneurea **C** and methylated biotin **Met-B** units were identified.

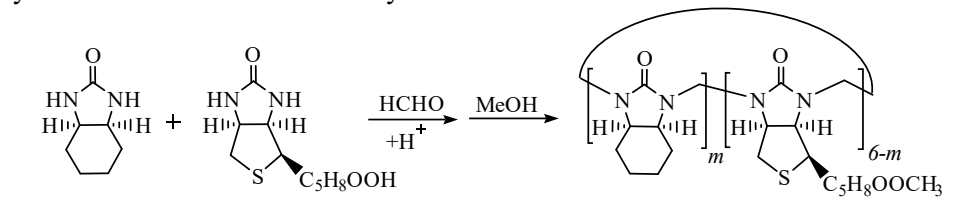

cis-cyclohexadiylurea **C** + biotin **B**

m=1 1**C**+5**Met-B**
m=2 2**C**+4**Met-B**
m=3 3**C**+3**Met-B**

Scheme 5. Synthesis of the 6-membered macrocycles with monomers **C** and **B** in ratio 1:5.

The mixtures of formed macrocycles were usually very complicated. It was impossible to find good conditions to achieve baseline separation. The chromatogram of the reaction mixture is given in Figure 43.

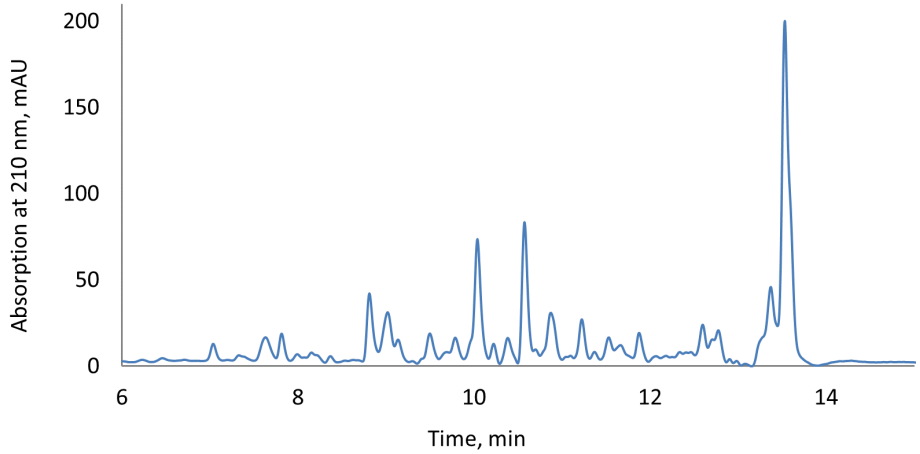

Figure 43. HPLV-UV chromatogram of the macrocyclisation reaction of mixed monomers shown in Scheme 5. Experimental conditions: set A with gradient 10/90 to 100/0 of ACN/H_2O.

As it was hard to identify products using NMR, HRMS was a good choice, since it can distinguish between used monomers. Analyzing mixtures by ESI(+)-HRMS, it was possible to identify some 6-membered macrocycles containing both cyclohexaneurea and methylated biotin incorporated in the structures. Additionally, (*R,S*)-cycHC[6], methylated biotin[6]uril and biotin[4]uril, and some oligomers formed from methylated biotin were also identified (see Figure 44).

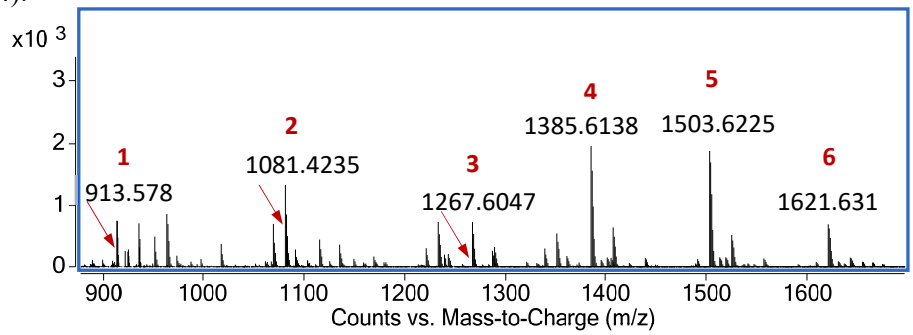

Figure 44. Mass spectra of the crude sample of the reaction shown in Scheme 5. Experimental: set B. Compound **1** is cycHC[6] (calculated m/z value for $[cycHC[6]+H]^+$ = 913.5771); compound **2** is methylated biotin[4]uril (calculated m/z value for H^+ adduct is 1081.4225); compound **3**, **4** and **5** are 3**C**+3**Met-B**, 2**C**+4**Met-B** and 1**C**+5**Met-B**, respectively (calculated m/z values for H^+ adducts are 1267.6036, 1385.6125 and 1503.6213, respectively); compound **6** is methylated biotin[6]uril (calculated m/z value for H^+ adduct is 1621.6332).

From the reactions with the biotin and (*R,R*)-cyclohexaneurea as building blocks, it was concluded that mixed macrocycles formed during the reaction. HPLC-MS analysis showed that all new mixed six-membered macrocycles had

chromatographic behavior similar to methylated biotin[6]uril since they all eluted next to each other. Also it was seen that the more cyclohexaneurea units a macrocycle had, the shorter the retention time.
To conclude this section, it was clear that mixed macrocycles formed, but not in a selective way as in the case of *cis*- and *rac-trans*-isomers of the cyclohexaneurea mixtures, in 6:1 ratio respectively, where only four major peaks were observed.

4.5 Analysis of HC[6] and HC[12]

Studying the reversible macrocyclisation in the case of cycHCs and their degradation in strong acids also increased our desire to analyze unsubstituted hemicucurbiturils in the same way, knowing from the literature that they are used as catalysts in acidified environment[55]. So macrocycles HC[6] and HC[12] were obtained from Dr. H. Cong (Guizhou University, China). We were interested in analyzing their stability in acids and whether they were prone to reversible macrocyclisation.
At first there was a need to evaluate the optimal conditions for the separation of these two macrocyles and to see if they were detectable at chosen wavelengths. Acidified and neutral water and different gradient modes were tested. The order of elution was HC[6] and HC[12], as shown in Figure 45.

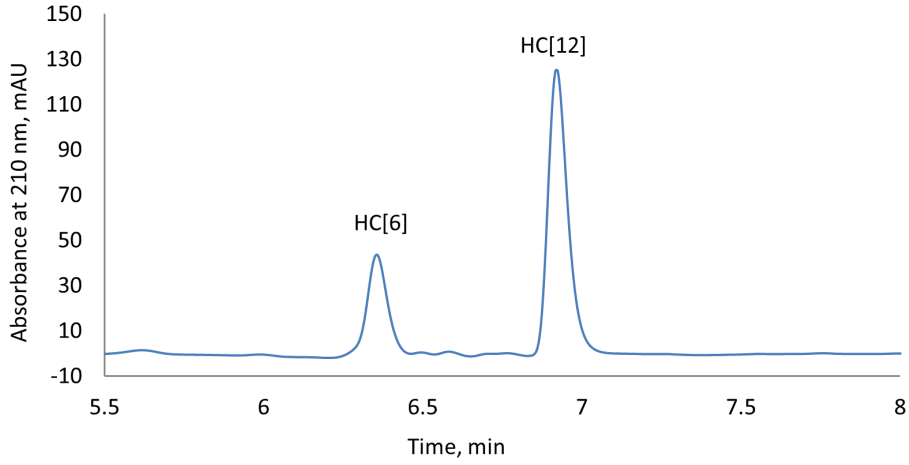

Figure 45. RP-HPLC-UV chromatogram of HC[6] and HC[12]. Experimental: set A, with 0.05% TFA instead of water as an eluent, gradient from 5% ACN to 100%.

The preliminary experiments on the stability of HC[6] and HC[12] in FA and AA showed that both of the macrocycles degraded in those acids, but the samples were stable in chloroform/methanol mixtures.
For stability analysis, it was decided to perform experiments in conditions similar to those used in the literature as catalysts in 0.1 M aq. HCl. First, the UV signals of macrocycles were calibrated using a developed HPLC-UV technique.

Acidified additives were not included in preparing calibration samples, since previous experiments showed their instability even in AA. 0.05% of TFA was still used in the eluent, but it was confirmed that peak areas did not depend on the TFA concentration in the eluent and stayed the same during parallel runs. Unsubstituted HCs had low solubility in most of the solvents, which was mentioned by Miyahara in 2004. For HC[12], solubility was achieved only in ethylene glycol by heating it over 100 °C, which actually created a gel-like solution.[49] The solvents tested in this work were chloroform, dichloromethane, ethylacetate, dimethylsulfoxide, methanol, water and mixtures of these solvents. Standard solutions of HC[6] were prepared in $CHCl_3$/MeOH (generally 1:9) solution and a standard solution of the HC[12] in $CHCl_3$/MeOH with 5% DMSO. Even those solvent mixtures were not ideal since macrocycles started to precipitate after several hours; therefore analysis was performed within that time limit.

The stability of macrocycles was investigated with HPLC and ^{1}H-NMR. Detailed results are given in Article III.

Since the reliable calibration for a 12-membered macrocyle was not achieved, probably because of very poor solubility, the quantitative analysis was done only for 6-membered HC to measure the rate of its degradation. Unexpectedly, the calibration of the HC[6] was non-linear in the same range tested for the cycHCs. This might have been caused by the aggregation of HC[6] in larger concentrations.

A qualitative analysis of HC[6] and HC[12] in 0.1 M aq. HCl solutions showed that both macrocycles degraded to the same oligomers, which was detected in ^{1}H-NMR, HRMS and also in HPLC (see Article III SI). HC[12] was usually less stable, which was evidenced by the faster degradation in acidified media. HC[6] fully degraded in three hours at elevated temperature.

A quantitative analysis for a homogeneous solution of HC[6] (0.14 mg/ml) showed that the degradation rate constant at 65 °C in 0.1 M aq. HCl was 1.15 ± 0.02 h^{-1}.

To compare the stability of HC[6] with the literature examples, where heterogeneous solutions of HC[6] and HC[12] were generally used, saturated solutions of HC[6] and HC[12] (2.6 and 3.1 mg/ml, respectively) were made in 0.1 aq. HCl. An analysis showed that in that case only half of the 6-membered macrocycle degraded in 3 hours. The slower degradation in the heterogeneous mixture can be explained by the continuous dissolution of the solid material into the solution, which turned out to be a slower process than depolymerisation.

The conclusions for that work are that HC[6] and HC[12] degraded, but very slowly at room temperature, and at elevated temperatures their degradation was relatively fast. However, they can be used as solid phase catalysts. No reversible macrocyclisation was detected in the studied conditions.

Analyzing HC[12] with HRMS, it was noticed that the ionization of this host was low. At concentrations below 0.0025 mg/ml of HC[12] in acidified solution,

compound was not detected by MS, though it gave a clear signal by HPLC-UV. (see Figure 46).

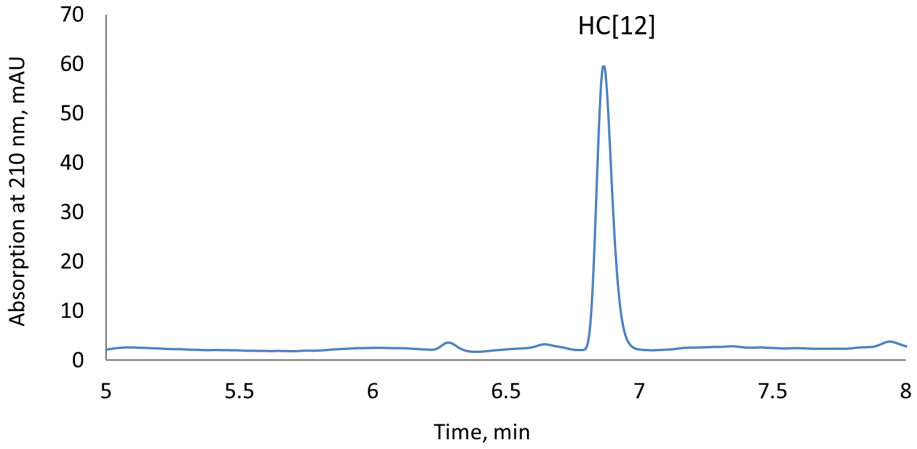

Figure 46. RP-HPLC-UV chromatogram of 0.0025 mg/ml of HC[12] dissolved in HCl aq. solution. The experimental conditions were the same as in Figure 45.

4.6 Quantitative analysis of cycHCs by HPLC

4.6.1 Calibration of cycHC[6] and cycHC[8]

The RP-HPLC calibration procedure of cycHCs, except for *inverted*-(*R,S*)-macrocycle, are described in Article III. Calibration was done for four macrocycles, and slopes for the two monomers were also found to compare their proportionality with macrocycles. We were curious whether the slope of the monomer would correlate with the slope of the macrocycle, as was the case with biotin[6]uril[63].

Macrocycles can all be analyzed with the same gradient mode, but not monomers, since they coelute with the solvent peaks. So for monomers optimal conditions for separating both *cis*- and *trans*-isomers needed to be found. Several more polar gradients were tested for this purpose and an optimal resolution is shown in Figure 47. Monomers were soluble in a variety of solvents and there was no need for chloroform.

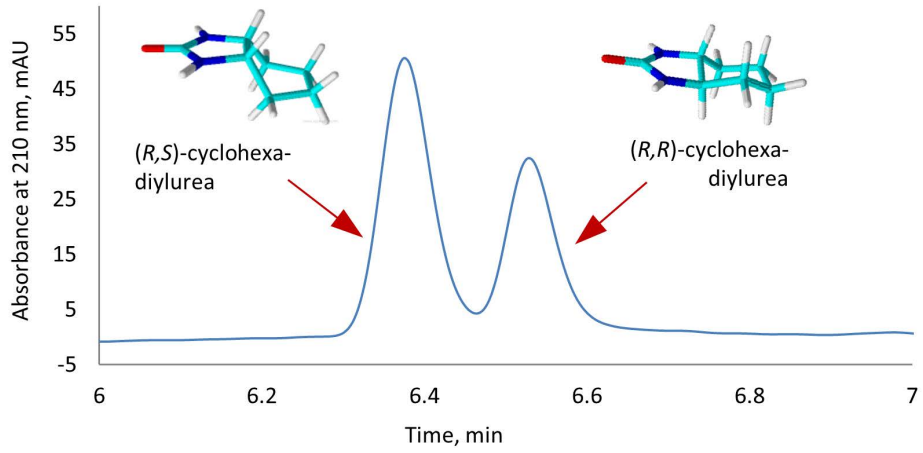

Figure 47. RP-HPLC-UV chromatogram of (*R,S*)- and (*R,R*)-cyclohexa-1,2-diylurea sample dissolved in 1:9 $CHCl_3$/MeOH (46 and 62 µg/ml, respectively). Experimental: set A with 5 min gradient from 1/99 to 80/20 ACN/H_2O. Adapted from ref.[108] with permission from the Royal Society of Chemistry.

The mixture of macrocycles was also analyzed utilizing the same gradient as mentioned in Figure 47 to verify that the peak areas did not depend on the gradient system.

In analyzing cycHCs, it was noted that the absorptions of 6- and 8-membered macrocycles were not proportional to their number of monomeric units. And furthermore, it was interesting to see that all six-membered diastereomeric macrocycles also had different absorbances. To confirm this observation, careful quantitative HPLC-UV analysis of cycHCs was performed.

One would expect that the same amount of the chromophoric unit (carbonyl group) should give the same absorption regardless of whether it was incorporated into the macrocycle as a monomer or monomeric unit. But this wasn't the case, as can be seen in Figure 48 and Table 3. Absorption was different for each of the compounds and even *cis*- and *trans*-isomers of monomers had large differences in absorptivity.

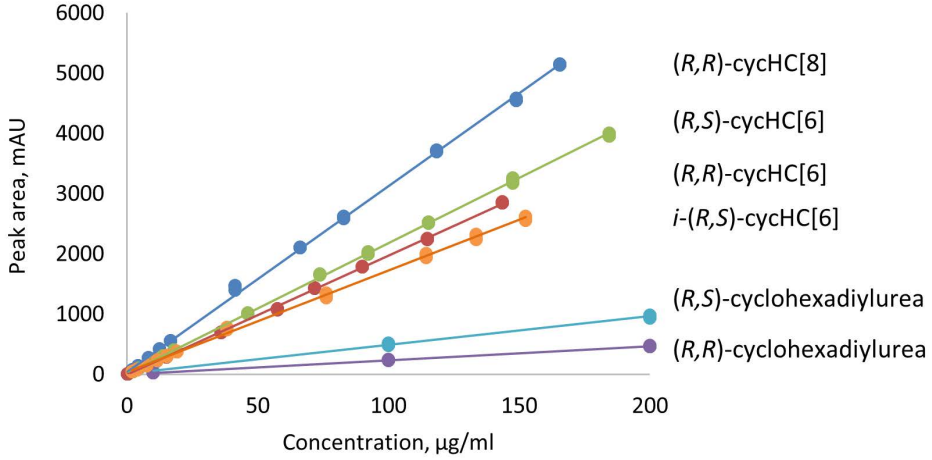

Figure 48. Calibration curves for macrocycles and monomers.

Table 3. Calibration parameters measured with developed HPLC-UV technique

Compound	Equation	R^2	LoD	LoQ
(*R*,*R*)-cycHC[8]	y = (30.2 ± 0.1)x + (40 ± 10)	0.9993	0.149 ± 0.004	0.50 ± 0.01
(*R*,*S*)-cycHC[6]	y = (21.7 ± 0.1)x + (13 ± 6)	0.9997	0.446 ± 0.003	1.49 ± 0.01
(*R*,*R*)-cycHC[6]	y = (19.73 ± 0.07)x – (1 ± 4)	0.9996	0.274 ± 0.004	0.91 ± 0.01
i-(*R*,*S*)-cycHC[6]	y = (16.8 ± 0.1)x + (42 ± 9)	0.9986	1.91 ± 0.06	6.3 ± 0.2
(*R*,*S*)-cyclohexa-1,2-diylurea	y = (4.79 ± 0.09)x + (10 ± 10)	0.9977	-	-
(*R*,*R*)-cyclohexa-1,2-diylurea	y = (2.33 ± 0.03)x + (3 ± 4)	0.9987	-	-

As can be seen, the 8-membered macrocycle has the largest value of slope of calibration plot, and (*R*,*S*)-cycHC[6] has the highest absorption among 6-membered isomers per same unit. Also the slopes of *cis*- and *trans*-monomers differ almost two fold.
The reason may lie in their geometrical shapes (see Figure 49), as this might affect the distribution of the electron density of the molecules.

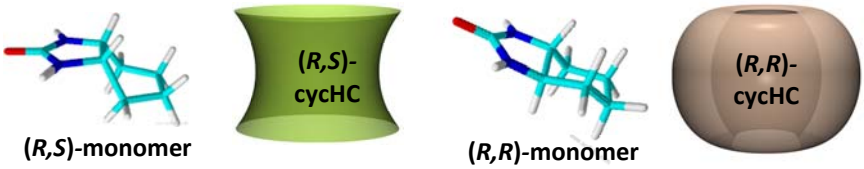

Figure 49. 3D structures of (*R,S*)- and (*R,R*)-cyclohexadiylureas and cartoon illustrations of relevant macrocycles.

This observation leads us to a more detailed UV analysis of the compounds.

4.6.2 UV-analysis of monomers, macrocycles and oligomers

Differences in the slopes measured during the calibration procedure encouraged us to analyze the UV absorbance of macrocycles and monomers more deeply to gain additional insight into the UV absorption of oligomers. For that purpose it was necessary to isolate at least some of the individual oligomers (see Article III). Isolation of oligomers was accomplished on the analytical HPLC apparatus, as shown in Picture 1.

Picture 1. Isolation of oligomers by collecting the fractions from the HPLC apparatus.

Collecting fractions directly after detection was achieved by knowing the inner diameter of tubes and the length of capillaries and the flow rate, making it possible to calculate when the fraction collection should start. Fortunately, it was only about 0.40 seconds, so it was reliable to collect the fraction after it appeared on the screen. Collected fractions were analyzed by HRMS and it was decided to go further with the UV-analysis with three isolated oligomers, which are shown in Figure 50.

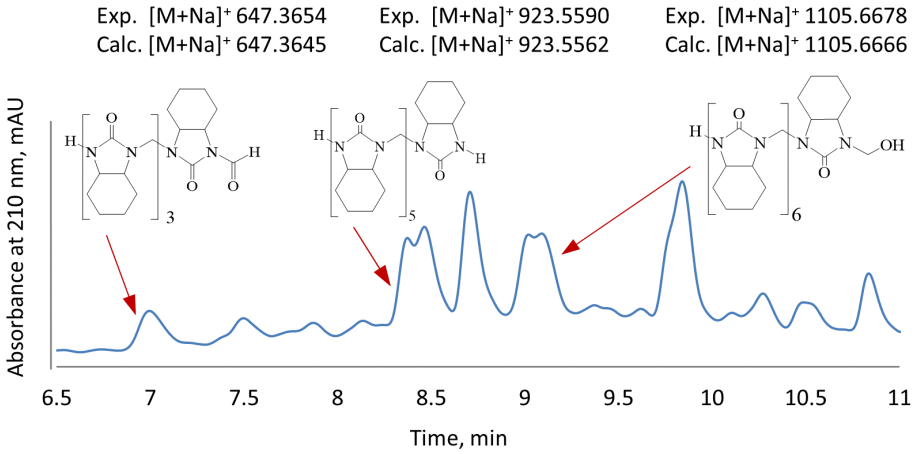

Figure 50. RP-HPLC-UV chromatogram of a mixture of oligomers, and structures of isolated oligomers determined by HRMS.

Acetonitrile was chosen as a solvent to measure the UV absorbances of cycHCs cyclohexadiylureas and oligomers. From the measured data the absorption coefficients were obtained. Acetonitrile is suitable for analyzing analytes at 210 nm since its cutoff range is at 190 nm. Also, it is similar to the HPLC eluent system and it is suitable for dissolving monomers, oligomers and macrocycle in low concentrations. The extinction coefficients of each analyzed compound are presented in Figure 51 and in Table 6. Though it was very problematic to dissolve (*R,S*)-macrocyle, a saturated solution was made and centrifuged, and the supernatant was taken and injected into the HPLC system to calculate the concentration according to calibration.

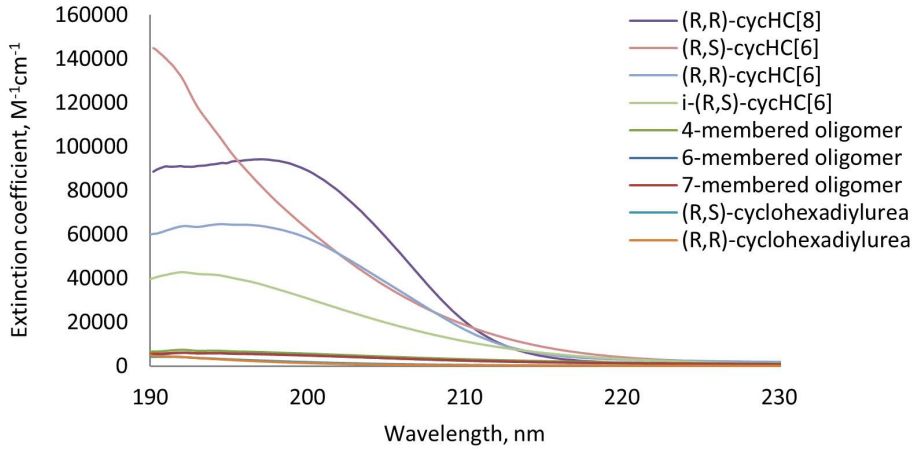

Figure 51. UV spectra of studied compounds.

Table 4. Absorption maximum (λ_{max}) and extinction coefficients (ε_λ) of cycHCs, oligomers and cyclohexa-1,2-diylureas at λ_{max} and λ_{210}

No	Compound	λ_{max} (nm)	$\varepsilon_{\lambda max}$ ($M^{-1}cm^{-1}$) × 1000 [a]	ε_{210} ($M^{-1}cm^{-1}$) × 1000 [a]
1	(*R,R*)-cycHC[8]	197	94.2 ± 0.2	19.2 ± 0.4
2	(*R,R*)-cycHC[6]	196	64 ± 4	17 ± 2
3	(*R,S*)-cycHC[6]	n.d.[b]	145.0 ± 0.2 [c]	18.4 ± 0.2
4	*i*-(*R,S*)-cycHC[6]	192	43 ± 1	11.3 ± 0.2
5	4-membered oligomer	192	7 ± 4	3 ± 2
6	6-membered oligomer	192	6 ± 2	2 ± 1
7	7-membered oligomer	192	6 ± 3	3 ± 1
8	(*R,R*)-cyclohexa-1,2-diylurea	191	4.3 ± 0.4	0.33 ± 0.07
9	(*R,S*)-cyclohexa-1,2-diylurea	191	4.1 ± 0.4	0.5 ± 0.1

[a] Values are given with standard deviation of ε determined at 5 different concentrations (see SI of Article III). [b] The maximum was out of the range of measurement, i.e. below 190 nm. [c] Determined at 190 nm.

At lower wavelengths some fluctuations were observed (see Figure 52). This might have been caused by light scattering or by some instrumental limitations. The fluctuations in signals were especially pronounced in the spectra of the oligomeric samples. In the case of (*R,S*)-cycHC[6], it was impossible to measure the maximum of the absorption. The interference could have been caused by some solid particles from the saturated solution, since the solution was not filtered.

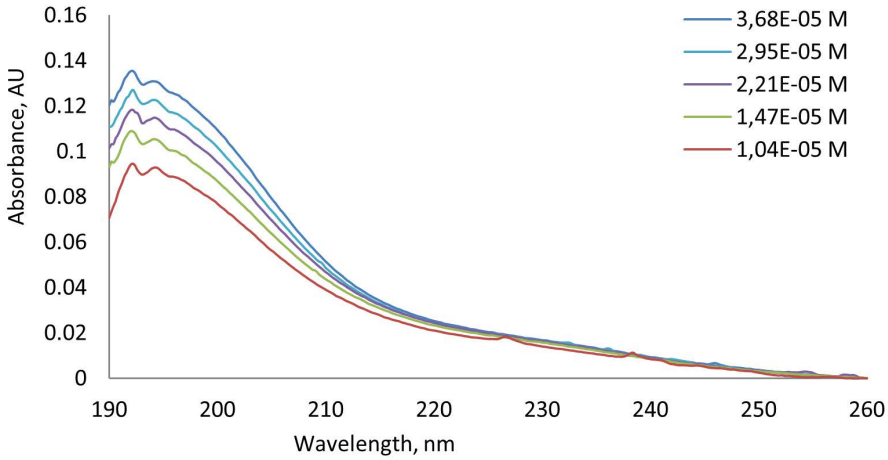

Figure 52. UV spectra of an isolated 6-membered oligomer in ACN. Experimental conditions as described in Article III. Reprinted from ref.[108] with permission from the Royal Society of Chemistry.

This study confirmed the results from the calibration analysis with HPLC-UV. Disproportionality between the chromophoric units and absorbance was observed. UV analysis showed that the absorbance of the macrocycles was higher than that of linear open-chain oligomers by about one order of magnitude (see Table 4, rows 2 and 6). This may have been caused by the rigidity of the repeating units in the macrocycle. Therefore, it can be concluded that in the studied linear and cyclic oligomeric analogues the correlation between the number of chromophores in repeating units and UV absorbance was not proportional and a separate calibration is necessary for every compound of interest. This phenomenon should also be considered in other classes of polymeric macrocycles.

CONCLUSIONS

The main aim of this work was to analyze HCs and develop a quantitative analytical method to determine compounds in mixture quickly and easily. The summary of the achievements of this work is as follows:

- CB[6] was analyzed with the HPLC using RP- and HILIC columns, where CB[6] was detected at 200 nm in both cases. The mixture of CB[5-8] was also analyzed using the same technique, but homologues coeluted.
- The RP-HPLC-MS analysis of the crude reaction mixture of (*R,R*)-cycHC[6] in formic acid/acetonitrile solution revealed the formation of a new 8-membered macrocycle, which was isolated in 11% yield for the first time.
- A quantitative RP-HPLC method was developed for the analysis of two (*R,R*)-cycHC homologues.
- This methodology was used for the study of reversible macrocyclisation between (*R,R*)-cycHC[6] and (*R,R*)-cycHC[8]. With HRMS, open-chain oligomers and new macrocycles were identified in reaction mixture, which helped to determine factors affecting the dynamic combinatorial library.
- The developed technique for quantitative analysis of macrocycles made it possible to estimate their yield and perform the optimization of reaction conditions in mg scale.
- The developed RP-HPLC technique for the analysis of (*R,S*)-cycHC[6] assisted in the discovery of the *inverted*-(*R,S*)-cycHC[6].
- Mixtures of macrocycles containing different substituted ethyleneureas as monomers ((*R,S*)-, (*R,R*)-, (*S,S*)-cyclohexadiylurea and biotin) were followed by developed RP-HPLC analysis. The macrocyclisation reaction in hydrochloric acid was non-selective when biotin and cyclohexadiylureas were used together as monomers. Some selectivity was observed when an excess (*R,S*)-cyclohexadiylurea was used in the presence of its *trans*-diastereomers.
- The qualitative analysis of the unsubstituted HC[6] and HC[12] in 0.1 M aqueous HCl solution revealed that both macrocycles degraded to the same oligomers. The degradation was faster in the case of HC[12].
- A quantitative analysis was developed for the HC[6], which allowed us to calculate the rate of degradation in 0.1 M aqueous HCl.
- No reversible macrocyclisation of unsubstituted HCs was observed in the studied conditions and low stability in the presence of such acids as acetic acid, formic acid and trifluoroacetic acid was noted.
- The calibration procedure of the cycHC macrocycles revealed disproportionality between UV absorbance and the number of chromophoric units. The UV-analysis of macrocycles and open-chain oligomers showed that the extinction coefficient of the latter is about one order of magnitude lower than the macrocycle coefficients.

REFERENCES

(1) "The Nobel Prize in Chemistry 2016". Nobelprize.org. Nobel Media AB 2014. Web. <http://www.nobelprize.org/nobel_prizes/chemistry/laureates/2016/> (accessed May 30, 2017).

(2) Eelkema, R.; Pollard, M. M.; Vicario, J.; Katsonis, N.; Ramon, B. S.; Bastiaansen, C. W. M.; Broer, D. J.; Feringa, B. L. *Nature* **2006**, *440* (7081), 163–163.

(3) Kudernac, T.; Ruangsupapichat, N.; Parschau, M.; Maciá, B.; Katsonis, N.; Harutyunyan, S. R.; Ernst, K.-H.; Feringa, B. L. *Nature* **2011**, *479* (7372), 208–211.

(4) Badjić, J. D.; Balzani, V.; Credi, A.; Silvi, S.; Fraser, J. *Science* **2004**, *303* (5665), 1845–1849.

(5) Liu, Y.; Flood, A. H.; Bonvallet, P. A.; Vignon, S. A.; Northrop, B. H.; Tseng, H. R.; Jeppesen, J. O.; Huang, T. J.; Brough, B.; Baller, M.; Magonov, S.; Solares, S. D.; Goddard, W. A.; Ho, C. M.; Fraser Stoddart, J. *Journal of the American Chemical Society* **2005**, *127* (27), 9745–9759.

(6) "The Nobel Prize in Chemistry 1987". Nobelprize.org. Nobel Media AB 2014. Web. <http://www.nobelprize.org/nobel_prizes/chemistry/laureates/1987/> (accessed May 30, 2017).

(7) Aav, R.; Kaabel, S.; Fomitšenko, M. *Comprehensive Supramolecular Chemistry II* **2017**, *3*, 203–220.

(8) Barrow, S. J.; Kasera, S.; Rowland, M. J.; Del Barrio, J.; Scherman, O. A. *Chemical Reviews* **2015**, *115* (22), 12320–12406.

(9) Langton, M. J.; Serpell, C. J.; Beer, P. D. *Angewandte Chemie - International Edition* **2016**, *55* (6), 1974–1987.

(10) Lisbjerg, M.; Pittelkow, M. *Comprehensive Supramolecular Chemistry II* **2017**, *3*, 221–236.

(11) Yawer, M. A.; Havel, V.; Sindelar, V. *Angewandte Chemie - International Edition* **2015**, *54* (1), 276–279.

(12) Masson, E.; Ling, X.; Joseph, R.; Kyeremeh-Mensah, L.; Lu, X. *RSC Advances* **2012**, *2* (4), 1213–1247.

(13) Chernikova, E. Y.; Fedorov, Y. V.; Fedorova, O. A. *Russian Chemical*

Bulletin **2012**, *61* (7), 1363–1390.

(14) Rebek Jr., J. *Chemical Communications* **2000**, 637–643.

(15) Chen, G.; Jiang, M. *Chemical Society reviews* **2011**, *40* (5), 2254–2266.

(16) Sabadini, E.; Cosgrove, T.; Egídio, F. D. C. *Carbohydrate Research* **2006**, *341* (2), 270–274.

(17) Atwood, J. L.; Dalgarno, S. J.; Hardieb, M. J.; Colin L. Raston. *Chemical Communications* **2005**, 337–339.

(18) Jeon, Y. M.; Kim, J.; Whang, D.; Kim, K. *Journal of the American Chemical Society* **1996**, *118* (40), 9790–9791.

(19) Buschmann, H. J.; Jansen, K.; Meschke, C.; Schollmeyer, E. *Journal of Solution Chemistry* **1998**, *27* (2), 135–140.

(20) Buschmann, H.-J.; Cleve, E.; Jansen, K.; Schollmeyer, E. *Analytica Chimica Acta* **2001**, *437* (1), 157–163.

(21) Jon, S. Y.; Selvapalam, N.; Oh, D. H.; Kang, J.; Kim, S.; Jeon, Y. J.; Lee, J. W.; Kim, K. *Journal of the American Chemical Society* **2003**, *125*, 10186–10187.

(22) Saluja, V.; Sekhon, B. S. *Journal of Pharmaceutical Education and Research* **2013**, *4* (1), 16–25.

(23) Guo, D.-S.; Uzunova, V. D.; Assaf, K. I.; Lazar, A. I.; Liu, Y.; Nau, W. M. *Supramolecular Chemistry* **2015**, *28*, 384–395.

(24) Liu, Y.; Li, C.-J.; Guo, D.-S.; Pan, Z.-H.; Li, Z. *Supramolecular Chemistry* **2007**, *19* (7), 517–523.

(25) Stella, V. J.; He, Q. *Toxicologic Pathology* **2008**, *36* (1), 30–42.

(26) Da Silva, E.; Shahgaldian, P.; Coleman, A. W. *International Journal of Pharmaceutics* **2004**, *273* (1-2), 57–62.

(27) Coleman, A. W.; Jebors, S.; Cecillon, S.; Perret, P.; Garin, D.; Marti-Battle, D.; Moulin, M. *New Journal of Chemistry* **2008**, *32* (5), 780.

(28) Ma, D.; Hettiarachchi, G.; Nguyen, D.; Zhang, B.; Wittenberg, J. B.; Zavalij, P. Y.; Briken, V.; Isaacs, L. *Nature Chemistry* **2012**, *4* (6), 503–510.

(29) Oun, R.; Floriano, R. S.; Isaacs, L.; Rowan, E. G.; Wheate, N. J. *Toxicology Research* **2014**, *3* (6), 447–455.

(30) Behrend, R.; Meyer, E.; Rusche, F. *Annalen der Chemie* **1905**, *339* (1), 1–37.

(31) Freeman, W. A.; Mock, W. L.; Shih, N.-Y. *Journal of the American Chemical Society* **1981**, *103* (24), 7367–7368.

(32) Mock, W. L.; Shih, N.-Y. *Journal of Organic Chemistry* **1986**, *51* (6), 4440–4446.

(33) Mock, W. L.; Shih, N.-Y. *Journal of the American Chemical Society* **1988**, *110* (4), 4706–4710.

(34) Kim, J.; Jung, I. S.; Kim, S. Y.; Lee, E.; Kang, J. K.; Sakamoto, S.; Yamaguchi, K.; Kim, K. *Journal of the American Chemical Society* **2000**, *122* (3), 540–541.

(35) Burton, D. J.; Naae, D. G.; Flynn, R. M. *Journal of Organic Chemistry* **1983**, *48*, 3618–3619.

(36) Lagona, J.; Mukhopadhyay, P.; Chakrabarti, S.; Isaacs, L. *Angewandte Chemie International Edition* **2005**, *44* (31), 4844–4870.

(37) Cao, L.; Šekutor, M.; Zavalij, P. Y.; Mlinarič-Majerski, K.; Glaser, R.; Isaacs, L. *Angewandte Chemie - International Edition* **2014**, *53* (4), 988–993.

(38) Liu, J.; Lan, Y.; Yu, Z.; Tan, C. S. Y.; Parker, R. M.; Abell, C.; Scherman, O. A. *Accounts of Chemical Research* **2017**, *50* (2), 208–217.

(39) Ma, D.; Zavalij, P. Y.; Isaacs, L. *Journal of Organic Chemistry* **2010**, *75* (14), 4786–4795.

(40) Zhang, M.; Sigwalt, D.; Isaacs, L. *Chemical Communications* **2015**, *51*, 6–9.

(41) Burnett, C. A.; Witt, D.; Fettinger, J. C.; Isaacs, L. *Journal of Organic Chemistry* **2003**, *68* (16), 6184–6191.

(42) Lu, X.; Isaacs, L. *Organic letters* **2015**, *17*, 4038–4041.

(43) Burnett, C. A.; Lagona, J.; Wu, A.; Shaw, J. A.; Coady, D.; Fettinger, J. C.; Day, A. I.; Isaacs, L. *Tetrahedron* **2003**, *59* (11), 1961–1970.

(44) Ma, D.; Glassenberg, R.; Ghosh, S.; Zavalij, P. Y.; Isaacs, L. *Supramolecular Chemistry* **2012**, *24* (5), 325–332.

(45) Sigwalt, D.; Ahlbrand, S.; Zhang, M.; Vinciguerra, B.; Briken, V.; Isaacs,

L. *Organic Letters* **2015**, *17* (23), 5914–5917.

(46) Shcherbakova, E. G.; Zhang, B.; Gozem, S.; Minami, T.; Zavalij, P. Y.; Pushina, M.; Isaacs, L.; Anzenbacher, P. *Journal of the American Chemical Society* **2017**, *139* (42), 14954–14960.

(47) Buschmann, H.-J.; Cleve, E.; Schollmeyer, E. *Inorganic Chemistry Communications* **2005**, *8*, 125–127.

(48) Buschmann, H. J.; Zielesny, A. *Computational and Theoretical Chemistry* **2013**, *1022*, 14–22.

(49) Miyahara, Y.; Goto, K.; Oka, M.; Inazu, T. *Angewandte Chemie - International Edition* **2004**, *43* (38), 5019–5022.

(50) Jin, X. Y.; Wang, F.; Cong, H.; Tao, Z. *Journal of Inclusion Phenomena and Macrocyclic Chemistry* **2016**, *86* (3-4), 241–248.

(51) Jin, X. Y.; Wang, F.; Cong, H.; Tao, Z. *Journal of Inclusion Phenomena and Macrocyclic Chemistry* **2016**, *86* (3-4), 249–254.

(52) Xiang, D.-D.; Geng, Q.-X.; Cong, H.; Tao, Z.; Yamato, T. *Supramolecular Chemistry* **2014**, *27* (1-2), 37–43.

(53) Cucolea, E. I.; Buschmann, H.-J.; Mutihac, L. *Supramolecular Chemistry* **2016**, *28* (9-10), 727–732.

(54) Cong, H.; Yamato, T.; Feng, X.; Tao, Z. *Journal of Molecular Catalysis A: Chemical* **2012**, *365*, 181–185.

(55) Cong, H.; Yamato, T.; Tao, Z. *Journal of Molecular Catalysis A: Chemical* **2013**, *379*, 287–293.

(56) Cong, H.; Yamato, T.; Tao, Z. *New Journal of Chemistry* **2013**, *37* (11), 3778–3783.

(57) Kurane, R.; Bansode, P.; Khanapure, S.; Kale, D.; Salunkhe, R.; Rashinkar, G. *Catalysis Letters* **2016**, *146* (12), 2485–2494.

(58) Li, Y.; Li, L.; Zhu, Y.; Meng, X.; Wu, A. *Crystal Growth & Design* **2009**, *9* (10), 4255–4257.

(59) Baškir, A. Bachelor thesis, Diastereoisomers of 6-membered cyclohexanohemicucurbiturils, Tallinn University of Technology, 2017.

(60) Prigorchenko, E.; Oeren, M.; Kaabel, S.; Fomitsenko, M.; Reile, I.; Jarving, I.; Tamm, T.; Topic, F.; Rissanen, K.; Aav, R. *Chemical*

Communications **2015**, *51*, 10921–10924.

(61) Aav, R.; Shmatova, E.; Reile, I.; Borissova, M.; Topic, F.; Rissanen, K. *Organic Letters* **2013**, *15* (14), 3786–3789.

(62) Fiala, T.; Sindelar, V. *Synlett* **2013**, *24* (18), 2443–2445.

(63) Lisbjerg, M.; Jessen, B. M.; Rasmussen, B.; Nielsen, B. E.; Madsen, A. Ø.; Pittelkow, M. *Chemical Science* **2014**, *5* (7), 2647–2650.

(64) Svec, J.; Necas, M.; Sindelar, V. *Angewandte Chemie International Edition* **2010**, *49* (13), 2378–2381.

(65) Havel, V.; Svec, J.; Wimmerova, M.; Dusek, M.; Pojarova, M.; Sindelar, V. *Organic Letters* **2011**, *13* (15), 4000–4003.

(66) Rivollier, J.; Thuéry, P.; Heck, M. P. *Organic Letters* **2013**, *15* (3), 480–483.

(67) Havel, V.; Sindelar, V.; Necas, M.; Kaifer, A. E. *Chemical Communications* **2014**, *50* (11), 1372–1374.

(68) Singh, M.; Solel, E.; Keinan, E.; Reany, O. *Chemistry - A European Journal* **2015**, *21* (2), 536–540.

(69) Singh, M.; Solel, E.; Keinan, E.; Reany, O. *Chemistry - A European Journal* **2016**, *22* (26), 8848–8854.

(70) Kaabel, S.; Adamson, J.; Topić, F.; Kiesilä, A.; Kalenius, E.; Öeren, M.; Reimund, M.; Prigorchenko, E.; Lõokene, A.; Reich, H. J.; Rissanen, K.; Aav, R. *Chemical Science* **2017**, *8* (3), 2184–2190.

(71) Lisbjerg, M.; Valkenier, H.; Jessen, B. M.; Al-Kerdi, H.; Davis, A. P.; Pittelkow, M. *Journal of the American Chemical Society* **2015**, *137* (15), 4948–4951.

(72) Lisbjerg, M.; Nielsen, B. E.; Milhøj, B. O.; Sauer, S. P. a; Pittelkow, M. *Organic & biomolecular chemistry* **2015**, *13* (2), 369–373.

(73) Pittelkow, M.; Lisbjerg, M. *The 5th International Conference on Cucurbiturils* **2017**.

(74) Révész, Á.; Schröder, D.; Svec, J.; Wimmerová, M.; Sindelar, V. *Journal of Physical Chemistry A* **2011**, *115* (41), 11378–11386.

(75) Havel, V.; Yawer, M. A.; Sindelar, V. *Chemical Communications* **2015**, *51*, 4666–4669.

(76) Fiala, T.; Ludvikova, L.; Heger, D.; švec, J.; Slanina, T.; Vetrakova, L.; Babiak, M.; Necas, M.; Kulh??nek, P.; Klan, P.; Sindelar, V. *Journal of the American Chemical Society* **2017**, *139* (7), 2597–2603.

(77) Lin, J.; Zhang, Y.; Zhang, J.; Xue, S.; Zhu, Q.; Tao, Z. *Journal of Molecular Structure* **2008**, *875* (1-3), 442–446.

(78) Lewin, V.; Rivollier, J.; Coudert, S.; Buisson, D. A.; Baumann, D.; Rousseau, B.; Legrand, F. X.; Kouřilová, H.; Berthault, P.; Dognon, J. P.; Heck, M. P.; Huber, G. *European Journal of Organic Chemistry* **2013**, 3857–3865.

(79) Huang, W.-H.; Zavalij, P. Y.; Isaacs, L. *Journal of the American Chemical Society* **2008**, *130* (26), 8446–8454.

(80) Cheng, X. J.; Liang, L. L.; Chen, K.; Ji, N. N.; Xiao, X.; Zhang, J. X.; Zhang, Y. Q.; Xue, S. F.; Zhu, Q. J.; Ni, X. L.; Tao, Z. *Angewandte Chemie - International Edition* **2013**, *52* (28), 7252–7255.

(81) Isobe, H.; Sato, S.; Nakamura, E. *Organic Letters* **2002**, *4* (8), 1287–1289.

(82) Sasmal, S.; Sinha, M. K.; Keinan, E. *Organic letters* **2004**, *6* (8), 1225–1228.

(83) Jiao, D.; Scherman, O. A. *Green Chemistry* **2012**, *14* (9), 2445–2449.

(84) Day, A.; Arnold, A. P.; Blanch, R. J.; Snushall, B. *Journal of Organic Chemistry* **2001**, *66* (24), 8094–8100.

(85) Ayhan, M. M.; Karoui, H.; Hardy, M.; Rockenbauer, A.; Charles, L.; Rosas, R.; Udachin, K.; Tordo, P.; Bardelang, D.; Ouari, O. *Journal of the American Chemical Society* **2015**, *137* (32), 10238–10245.

(86) Ayhan, M. M.; Karoui, H.; Hardy, M.; Rockenbauer, A.; Charles, L.; Rosas, R.; Udachin, K.; Tordo, P.; Bardelang, D.; Ouari, O. *Journal of the American Chemical Society* **2016**, *138* (6), 2060.

(87) Stewart, D. R.; Gutsche, C. D. *Journal of the American Chemical Society* **1999**, *121* (17), 4136–4146.

(88) Kinalekar, M. S.; Kulkarni, S. R.; Vavia, P. R. *Journal of Pharmaceutical and Biomedical Analysis* **2000**, *22* (4), 661–666.

(89) Huang, Y.; Xue, S. F.; Zhu, Q. J.; Zhu, T. *Supramolecular Chemistry* **2008**, *20* (3), 279–287.

(90) Chang, Y. X.; Qiu, Y. Q.; Du, L. M.; Li, C. F.; Wu, H. *Journal of Liquid Chromatography & Related Technologies* **2011**, *34* (20), 2629–2639.

(91) Wei, F.; Liu, S.-M.; Xu, L.; Cheng, G.-Z.; Wu, C.-T.; Feng, Y.-Q. *Electrophoresis* **2005**, *26* (11), 2214–2224.

(92) Xu, L.; Liu, S.-M.; Wu, C.-T.; Feng, Y.-Q. *Electrophoresis* **2004**, *25* (18-19), 3300–3306.

(93) Won, J. C.; Joung, H. G.; Yoon, S. B.; Sung, S. K.; Nagarajan, E. R.; Selvapalam, N.; Young, H. K.; Kim, K. *Bulletin of the Korean Chemical Society* **2008**, *29* (10), 1941–1945.

(94) Liu, S.; Xu, L.; Wu, C.; Feng, Y. *Talanta* **2004**, *64*, 929–934.

(95) Ma, L.; Liu, S. M.; Yao, L.; Xu, L. *Journal of Chromatography A* **2015**, *1376*, 64–73.

(96) Ma, L.; Liu, S.; Wang, Q.; Yao, L.; Xu, L. *Journal of Separation Science* **2015**, *38* (7), 1073–1262.

(97) Nagarajan, E. R.; Oh, D. H.; Selvapalam, N.; Ko, Y. H.; Park, K. M.; Kim, K. *Tetrahedron Letters* **2006**, *47* (13), 2073–2075.

(98) Zhang, P.; Qin, S.; Qi, M.; Fu, R. *Journal of Chromatography A* **2014**, *1334*, 139–148.

(99) Wang, L.; Wang, X.; Qi, M.; Fu, R. *Journal of Chromatography A* **2014**, *1334*, 112–117.

(100) Sun, T.; Ji, N.; Qi, M.; Tao, Z.; Fu, R. *Journal of Chromatography A* **2014**, *1343*, 167–173.

(101) Elbashir, A. A.; Aboul-Enein, H. Y. *Critical Reviews in Analytical Chemistry* **2015**, *45* (10), 52–61.

(102) Wagner, B. D.; Fitzpatrick, S. J.; Gill, M. A.; MacRae, A. I.; Stojanovic, N. *Canadian Journal of Chemistry* **2001**, *79* (7), 1101–1104.

(103) Li, C. F.; Du, L. M.; Zhang, H. M. *Spectrochimica Acta - Part A: Molecular and Biomolecular Spectroscopy* **2010**, *75* (2), 912–917.

(104) Li, C. F.; Du, L. M.; Wu, W. Y.; Sheng, A. Z. *Talanta* **2010**, *80* (5), 1939–1944.

(105) Marquez, C.; Huang, F.; Nau, W. M. *IEEE Transactions on Nanobioscience* **2004**, *3* (1), 39–45.

(106) Wu, W. Y.; Yang, J. Y.; Du, L. M.; Wu, H.; Li, C. F. *Spectrochimica Acta - Part A: Molecular and Biomolecular Spectroscopy* **2011**, *79* (3), 418–422.

(107) Ghale, G.; Nau, W. M. *Accounts of Chemical Research* **2014**, *47*, 2150–2159.

(108) Fomitšenko, M.; Peterson, A.; Reile, I.; Cong, H.; Kaabel, S.; Prigorchenko, E.; Järving, I.; Aav, R. *New Journal of Chemistry* **2017**, *41*, 2490–2497.

(109) Skoog, D. A.; Holler, F. J.; Crouch, S. R. *Principles of Instrumental Analysis, 7th Edition*; Boston, Mass.: Cengage Learning, 2016.

(110) Trunin, M. Master's thesis, Synthesis of the substituted hemicucurbiturils, Tallinn University of Technology, 2016.

(111) Isaacs, L.; Park, S.; Liu, S.; Ko, Y. H.; Selvapalam, N.; Kim, Y.; Kim, H.; Zavalij, P. Y.; Kim, G.; Lee, H.; Kim, K. *Journal of the American Chemical Society* **2005**, *127*, 18000–18001.

Publication I

Fomitšenko, M.; Shmatova, E.; Öeren, M.; Järving, I.; Aav, R. "New homologues of chiral cyclohexylhemicucurbit[n]urils" *Supramolecular Chemistry*, 2014, **16**, 19198-19205.

Supramolecular Chemistry, 2014
Vol. 26, No. 9, 698–703, http://dx.doi.org/10.1080/10610278.2014.926362

Taylor & Francis
Taylor & Francis Group

New homologues of chiral cyclohexylhemicucurbit[*n*]urils

Maria Fomitšenko, Elena Shmatova, Mario Öeren, Ivar Järving and Riina Aav*

Department of Chemistry, Tallinn University of Technology, Akadeemia tee 15, 12618 Tallinn, Estonia

(*Received 21 February 2014; accepted 16 May 2014*)

The existence of new 7-, 8-, 9- and 10-membered homologues of chiral cyclohexylhemicucurbituril is reported. The barrel-shaped (*all-R*)-cyclohexylhemicucurbit[8]uril ((*all-R*)-cycHC[8]) was isolated and its complexes with anions were detected in negative ion mode MS. Here, 7-, 9- and 10-membered homologues were detected by HPLC–HRMS. Geometries of all reported macrocycles were calculated using quantum chemical methods, which showed that even-numbered homologues were barrel-shaped and odd-numbered homologues were asymmetrical barrel-shaped with unequal dimensions of the openings. The size of the ((*all-R*)-cycHC[8]) cavity was comparable to CB[8] and it probably can serve as a chiral host.

Keywords: hemicucurbiturils; cucurbiturils; chiral macrocycles; NMR; host–guest complex

Introduction

Hemicucurbiturils are members of the cucurbituril (*1*) family, which has grown enormously in this century (*2*, *3*). There are several homologues (*4–6*) of normal cucurbiturils and a wide variety of analogues (*7–13*). In general, glycoluril monomers in these macrocyclic compounds are joined together by two methylene bridges and form strong host–guest pairs with cationic ammonium compounds (*3*, *14*, *15*). In hemicucurbiturils, on the other hand, monomers are linked together via one bridge, causing a zigzag orientation of the urea functionalities (*16–18*). This structural change, compared with the normal cucurbiturils, drastically influences the electronic structure of macrocycles and allows complexation of anions inside the cavity (*19*, *20*). The zigzag orientation of the single-bridged glycoluril monomers in bambusurils (*21*) exhibits similar anion binding properties (*22–24*). Presently, the ring sizes of cucurbituril family macrocycles range from 4-membered bambusurils (*25*) to 14-membered twisted normal cucurbituril (*26*). The most widely applied normal cucubituril homologues have six to eight monomers joined together and the inner dimensions of these macrocycles allow for selective complexation of a large number of useful small molecules (*2*, *3*, *14*). Until now, only 6- and 12-membered hemicucurbiturils have been isolated. Ten years ago, Miyahara et al. (*16*) reported that, in strongly acidic conditions, ethyleneurea, in the presence of formalin, can selectively produce two homologues of unsubstituted hemicucurbiturils in very high yields. Hemicucurbit[6]uril (HC[6]) is formed in concentrated HCl at lower temperatures and hemicucurbit[12]uril (HC[12]) in diluted acid at higher temperatures (Figure 1). It has been shown that unsubstituted hemicucurbituril can catalyse organic reactions (*27–29*). The structure of the first substituted hemicucurbituril – achiral *meso*-cyclohexylhemicucurbit[6]uril (*meso*-cycHC[6]) – was reported by Li et al. (*17*) and, due to introduced rigidity in the formed macrocycle, it required much harsher conditions than HC[6] for high-yielding synthesis. In the same conditions, its more rigid analogue, norbornahemicucurbit[6]uril (norHC[6]), was formed in significantly lower yield (*30*). Together with norHC[6], traces of 4-, 5-, 7- and 8-membered norborna-hemicucurbiturils were detected by mass-spectrometric analysis (*30*). The only presently known chiral analogue of substituted hemicucurbiturils, (*all-S*) or (*all-R*)-cyclohexylhemicucurbit[6]uril (*chiral*-cycHC[6]) (*18*), has cyclohexyl and urea cycles joined in *trans*-fashion. High-yielding synthesis of the latter required a much longer (24 h) reaction time at the same temperature, compared with other substituted hemicucurbiturils (Figure 1).

In this paper, we report the isolation of a new chiral homologue of substituted hemicucurbituril, enantiomerically pure (*all-R*)-cyclohexylhemicucurbit[8]uril ((*all-R*)-cycHC[8]) and analytical evidence of the existence of its 7-, 9- and 10-membered homologues ((*all-R*)-cycHC[7], (*all-R*)-cycHC[9] and (*all-R*)-cycHC[10]). The calculated geometries of all reported macrocycles are also presented.

Results and discussion

The formation of hemicucurbiturils occurs as a result of a polymerisation reaction; therefore, in addition to the most favourable 6-membered macrocycles, the existence of homologues was expected. A reaction mixture of previously reported (*all-R*)-cycHC[6] was carefully examined by reverse-phase (RP)-HPLC–MS analysis, and 7-, 8-,

*Corresponding author. Email: riina@chemnet.ee

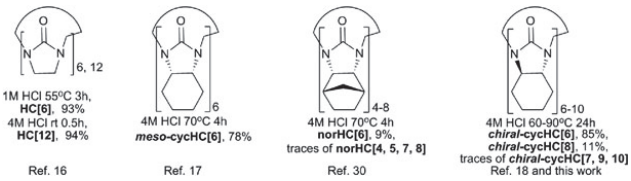

Figure 1. Hemicucurbit[*n*]urils structures and reaction conditions for their synthesis from Refs (*16–18*, *30*) and this work.

9- and 10-membered homologues of (*all-R*)-cycHC[6] were found. A chromatogram of cycHC[6–10] is shown in Figure 2, in which peaks were detected by ultraviolet (UV) light and positive ion mode high-resolution mass spectrometry. The order of homologue elution in RP column was cycHC[9], cycHC[8] and cycHC[7] as one cluster, followed by cycHC[6] and cycHC[10] further apart from each other. The elution order shows that 10- and 6-membered homologues were less polar than their 7-, 8- and 9-membered homologues.

Preliminary attempts were made to increase the degree of formation of higher homologues, by varying the reaction temperature of cyclisation between 60 and 90°C. According to the ^{1}H NMR analysis, cycHC[6] still remained the main product in all reactions performed in 4 M HCl solution and the reaction temperature did not influence significantly the content of crude product. Additional study is necessary to find out conditions that could drive macrocyclisation towards formation of higher homologues. Nevertheless, the purification of crude product by RP flash chromatography afforded (*all-R*)-cycHC[8] in 11% yield. NMR spectra of (*all-R*)-cycHC[8] showed high symmetry; therefore, signals belonging to all monomers of the macrocycle were identical, adopting the same averaged conformation as in the case of *chiral*-cycHC[6] (*18*). The chemical shifts of relevant atoms of *chiral*-cycHC[6] and (*all-R*)-cycHC[8] were distinguishable and their assignment is presented in Figure 3.

NMR observations are in good agreement with the calculated geometry of (*all-R*)-cycHC[8] (Figure 4).

The equatorial belt of the macrocycle adopted a square-like shape, having methylene bridges with carbon number C9 (Figure 3) on the corners of the macrocycle. Carbon C9 is situated between the stereogenic carbons C2, in which protons H(in) point inside the cavity. According to the optimised structure, all cyclohexyl rings were in chair conformation, which was also supported by the high value of $^{3}J_{(HH)}$-coupling constants (>11 Hz) between the cyclohexyl axial protons. Monomers were in zigzag orientation and cyclohexyl rings leaned slightly over the opening, as in the case of cycHC[6]. The diameter of (*all-R*)-cycHC[8] opening was 4.6 Å, which is within the corresponding values of normal cucubiturils (*31*) CB[6] (3.9 Å) and CB[7] (5.4 Å). The cavity diameter at the equator of cycHC[8] macrocycle was 8.5 Å, which is comparable to the 8.8 Å of the CB[8] cavity size. (*all-R*)-cycHC[8] had a barrel shape as do normal cucurbiturils, and its cavity dimensions were comparable to the most widely applied normal cucurbiturils. In the negative ion mode of MS analysis, complexes of (*all-R*)-cycHC[8] with chloride and formate anions were detected, confirming that the new substituted hemicucurbituril can bind anions as do other zigzag-oriented cucurbituril family members.

To get a better understanding of the structures of other existing chiral cyclohexylhemicucurbiturils, geometries of

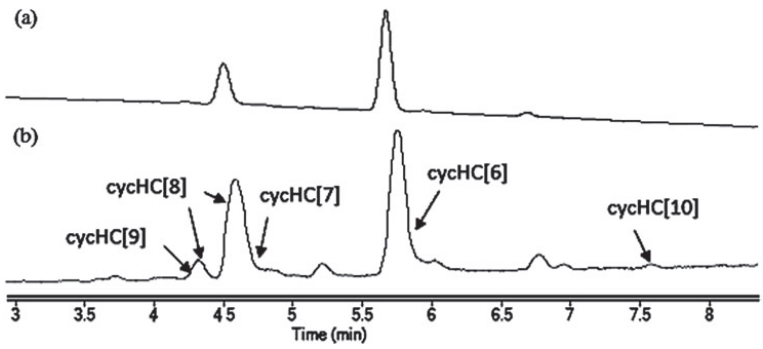

Figure 2. RP-HPLC–MS chromatograms of (*all-R*)-cycHC[9], (*all-R*)-cycHC[8], (*all-R*)-cycHC[7], (*all-R*)-cycHC[6] and (*all-R*)-cycHC[10] (a) detected by UV at 210 nm and (b) detected by (+)ESI-MS.

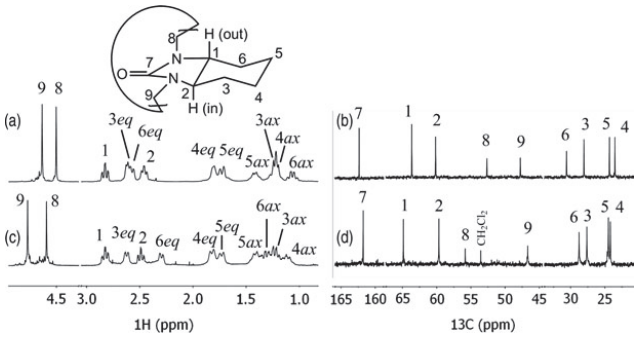

Figure 3. Assigned ^{1}H and ^{13}C NMR spectra of (a), (b) *chiral*-cycHC[6] and (c), (d) (*all-R*)-cycHC[8], respectively.

7-, 9- and 10-membered homologues were also calculated (Figure 5).

Macrocycles with odd numbers of monomers (cycHC[7], cycHC[9]) still formed almost barrel-like shapes. Cyclohexyl rings of zigzag-oriented monomers leaned over the openings, but two aligned urea cycles distorted the symmetry of the macrocycle, leading to two different sized openings (Table 1). The 10-membered homologue was a symmetrical five-cornered barrel. In 7-, 9- and 10-membered macrocycles, the cyclohexyl rings adopted both twisted and chair conformations. The dimensions describing the sizes of the cavities of the chiral hemicucurbiturils are outlined in Table 1.

Conclusions

As a result of RP liquid chromatography of the crude product of previously known *chiral*-cycHC[6], new 7-, 8-, 9- and 10-membered homologues of chiral cyclohexylhemicucurbituril were found. The barrel-shaped (*all-R*)-cyclohexylhemicucurbit[8]uril was isolated and its complexes with anions were detected in negative ion mode MS. Here, 7-, 9- and 10-membered homologues were detected by HPLC–HRMS. The geometries of all reported macrocycles were calculated using the density functional theory, which showed that even-numbered homologues were barrel-shaped and odd-numbered homologues were asymmetrical barrel-shaped with unequal dimensions of the openings. The isolated (*all-R*)-cycHC[8] was more polar than its 6-membered homologue. The cavity of (*all-R*)-cycHC[8] was comparable with CB[7] and CB[8]; therefore, it probably will serve as a chiral host for anions of small molecules.

Experimental section

General

All used instruments are located at Tallinn University of Technology, Department of Chemistry. RP-HPLC-MS was performed on an Agilent 6540 UHD Accurate-Mass Q-TOF LC/MS spectrometer (Agilent Technologies, Santa Clara, CA, USA) with AJ-ESI ionisation and a Zorbax

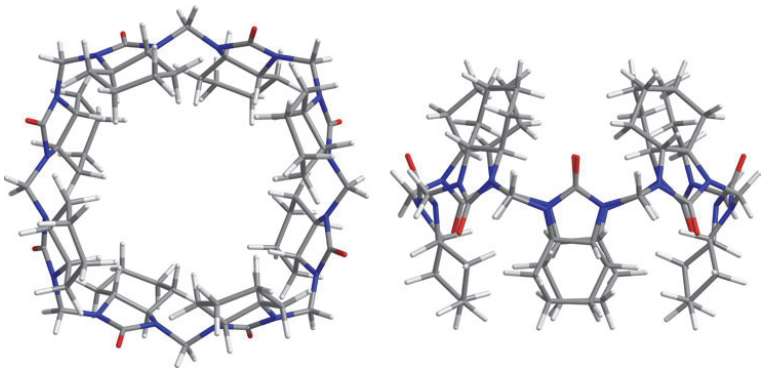

Figure 4. (Colour online) Calculated structures of (*all-R*)-cycHC[8].

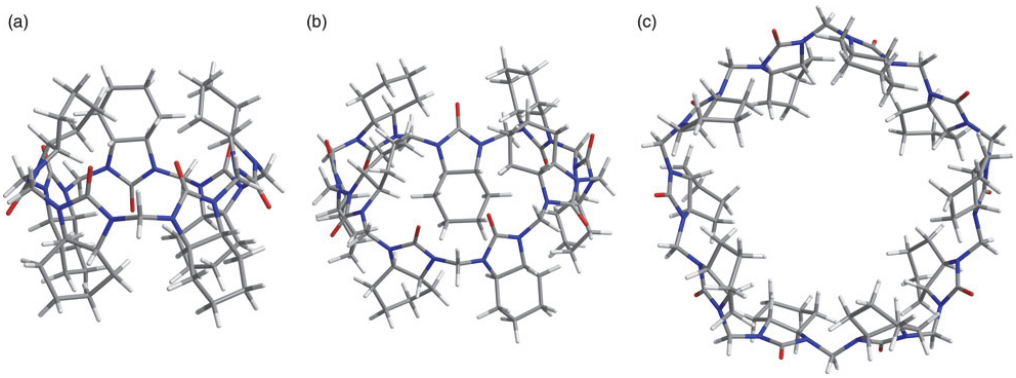

Figure 5. (Colour online) Calculated structures of (a) (*all-R*)-cycHC[7], (b) (*all-R*)-cycHC[9] and (c) (*all-R*)-cycHC[10].

Eclipse Plus C18 column (2.1 mm × 150 mm, 1.8 μm) and is reported as *m/z* ratios. RP flash column chromatography was performed on a Biotage Isolera™ Prime purification system using a Biotage SNAP KP-C18-HS Cartridge (60 g, 50 μm) (Biotage®, Uppsala, Sweden). NMR spectra were recorded using a Bruker Avance III 400 MHz spectrometer (Bruker BioSpin GmbH, Rheinstetten, Germany), and chemical shifts are referenced in carbon spectrum by $CDCl_3$ at 77.16 ppm and proton spectrum by $CDCl_3$ at 7.26 ppm. Infrared (IR) spectra were obtained on a Bruker Tensor 27 FT-IR spectrometer (Bruker Optik GmbH, Ettlingen, Germany) and are reported in wave numbers. The intensities of the peaks are reported using the following abbreviations: s: strong, m: medium and w: weak. Optical rotation was measured using an Anton Paar MCP 500 polarimeter (Anton Paar GmbH, Graz, Austria). The melting point was detected using a Nagema melting point microscope.

Experimental procedures

Synthesis of (*all-R*)-cyclohexylhemicucurbiturils was performed as described in an earlier publication (*18*), except for varying the temperature between 60 and 90°C.

An RP-HPLC-MS analysis of 1 mg/mL crude sample in 0.1% formic acid in acetonitrile was performed using a 10-min gradient from 70% to 100% of eluent A, which was acetonitrile, and eluent B was a 0.1% formic acid aqueous solution. The flow rate was set at 0.4 mL/min and the UV detection at 210 nm. Mass-to-charge ratios were measured using ESI-Q-TOF MS.

RP flash chromatography was performed with 200 mg of crude product (*18*), which was dissolved in 1 ml of formic acid before loading it into the column. The sample was purified using gradient from 50% to 100% of eluent A with the same eluents as described in the HPLC conditions. The flow rate was adjusted to 40 ml/min, and the sample detection was measured at 210 nm. Here, 22 mg of cycHC[8] was obtained in 11% yield.

Characterisation data

Compound (*all-R*)-cycHC[8]: It is a white solid (22 mg, 0.018 mmol, yield 11%). Mp = 245–250°C (dec). IR (KBr, cm^{-1}) 3502 w, 2936 m, 2858 m, 1711 s, 1435 m, 1359 s, 1332 m, 1232 s, 1134 w, 1058 w, 1014 w, 988 w, 919 w, 830 w, 774 m, 667 w, 628 w, 532 w, 516 w, 476 w. ^{1}H NMR (400 MHz, $CDCl_3$) δ = 1.18–1.05 (m, **H**4*ax*, 1H), 1.23 (qd, **H**3*ax*, *J* = 11.0, 2.9, 1H), 1.29 (qd, H6*ax*,

Table 1. Dimensions[a] of (*all-R*)-cyclohexylhemicucurbit[6–10]urils in Å.

	cycHC[6][b]	cycHC[7][c]	cycHC[8][c]	cycHC[9][c]	cycHC[10][c]
Diameter at the opening	2.2	2.3 4.2	4.6	4.9 7.3	6.6
Diameter at the equator of the cavity	5.3	6.8	8.5	9.8	11.5
Height	12.1	12.8	12.5	12.7	12.4

[a] Taking van der Waals radii into account.
[b] From Ref. (*18*).
[c] From calculated structures.

$J = 11.3, 3.3, 1H$), 1.47–1.35 (m, **H**5*ax*, 1H), 1.73 (bd, **H**5*eq*, $J = 12.7$, 1H), 1.82 (bd, **H**4*eq*, $J = 12.5$, 1H), 2.30 (dd, $J = 11.5, 2.7$, **H**6*eq*, 1H), 2.49 (td, $J = 11.0, 2.9$, **H**2 (in), 1H), 2.62 (dd, $J = 11.6, 2.7$, **H**3*eq*, 1H), 2.83 (td, $J = 11.1, 3.1$, **H1**(out), 1H), 4.59 (s, **H**8, 8H), 4.77 (s, **H**9, 8H). ^{13}C NMR (101 MHz, $CDCl_3$) $\delta = 161.77$ (C7), 64.86 (C1), 59.68 (C2), 55.83 (C8), 46.69 (C9), 28.76 (C6), 27.63 (C3), 24.48 (C5), 24.19 (C4). HRMS (ESI +): calculated for $(C_{64}H_{97}N_{16}O_8)^+$ $[M + H]^+$ 1217.7670, found 1217.7670. HRMS (ESI −): calculated for $(C_{65}H_{97}N_{16}O_{10})$ $[M + HCOO]$ 1261.7579, found 1261.7607. HRMS: calculated for $C_{64}H_{96}N_{16}O_8Cl$ $[M + Cl]$ 1251.7291, found 1251.7283. $[\alpha]_D^{25} = 60°$ (*c* 0.62, $CDCl_3$/$CHCl_3$).

Compound (*all-R*)-cycHC[7]: HRMS (ESI +): calculated for $(C_{56}H_{85}N_{14}O_7)^+$ $[M + H]^+$1065.6720, found 1065.6720. HRMS (ESI −): calculated for $(C_{57}H_{85}N_{14}O_9)$ $[M + HCOO]$ 1109.6341, found 1109.6621.

Compound (*all-R*)-cycHC[9]: HRMS (ESI +): calculated for $(C_{72}H_{109}N_{18}O_9)^+$ $[M + H]^+$1369.8619, found 1369.8621. HRMS (ESI −): calculated for $(C_{73}H_{109}N_{18}O_{11})$ $[M + HCOO]$ 1413.8529, found 1413.8490.

Compound (*all-R*)-cycHC[10]: HRMS (ESI +): calculated for $(C_{80}H_{121}N_{20}O_{10})^+$ $[M + H]^+$1521.9569, found 1521.9551.

Calculation studies

All structures were built and optimised on an MMFF94 (*32*) level of theory, using the programme Avogadro (*33*). Further geometry optimisations were conducted using density functional theory, combining BP86 (*34–38*) functional with a def2-SV(P) (*39*) basis set. Density functional theory calculations were performed with the program package Turbomole 6.4 (*40*).

The dimensions of (*all-R*)-cyclohexylhemicucurbiturils were measured using the lengths from the chosen atoms to the centre of the opening or to the centre of the cavity. For the opening, a hydrogen atom closest to the centre was chosen from each monomer. For the cavity, the carbonyl carbon of each monomer was chosen. Next, the average radius for both atom sets was found. For both dimensions, the Van der Waals radius was subtracted from the average radius and the diameter was obtained by multiplying the radius by two. The centre points were arithmetic averages of the Cartesian coordinates of chosen atom sets. Heights are distances between opening centres, positioned closest to the edge with two added Van der Waals radii of the hydrogens.

Funding

This work was supported by Estonian Science Foundation [grant number 8698], Tallinn University of Technology base financing [grant number B25], the Ministry of Education and Research [grant numbers IUT19-32, IUT19-9] and the EU European Regional Development Fund [grant number 3.2.0101.08-0017].

Supplementary data

Supplementary data for this article can be accessed at http://dx.doi.org/10.1080/10610278.2014.926362.

References

(1) Freeman, W.A.; Mock, W.L.; Shih, N.-Y. *J. Am. Chem. Soc.* **1981**, *103*, 7367–7368.
(2) Isaacs, L. *Chem. Commun.* **2009**, *6*, 619–629.
(3) Lagona, J.; Mukhopadhyay, P.; Chakrabarti, S.; Isaacs, L. *Angew. Chem. Int. Ed.* **2005**, *44*, 4844–4870.
(4) Day, A.; Arnold, A.P.; Blanch, R.J.; Snushall, B. *J. Org. Chem.* **2001**, *66*, 8094–8100.
(5) Kim, J.; Jung, I.-S.; Kim, S.-Y.; Lee, E.; Kang, J.-K.; Sakamoto, S.; Yamaguchi, K.; Kim, K. *J. Am. Chem. Soc.* **2000**, *122*, 540–541.
(6) Day, A.I.; Blanch, R.J.; Arnold, A.P.; Lorenzo, S.; Lewis, G.R.; Dance, I. *Angew. Chem. Int. Ed.* **2002**, *41*, 275–277.
(7) Lagona, J.; Fettinger, J.C.; Isaacs, L. *Org. Lett.* **2003**, *5*, 3745–3747.
(8) Flinn, A.; Hough, G.C.; Stoddart, J.F.; Williams, D. *J. Angew. Chem.* **1992**, *31*, 1475–1477.
(9) Isobe, H.; Sato, S.; Nakamura, E. *Org. Lett.* **2002**, *4*, 1287–1289.
(10) Zhao, Y.J.; Xue, S.F.; Zhu, Q.J.; Tao, Z.; Zhang, J.X.; Wei, Z.B.; Long, L.S.; Hu, M.L.; Xiao, H.P.; Day, A.I. *Chin. Sci. Bull.* **2004**, *49*, 1111–1116.
(11) Zhao, J.; Kim, H.-J.; Oh, J.; Kim, S.-Y.; Lee, J.W.; Sakamoto, S.; Yamaguchi, K.; Kim, K. *Angew. Chem. Int. Ed.* **2001**, *40*, 4233–4235.
(12) Lucas, D.; Minami, T.; Iannuzzi, G.; Cao, L.; Wittenberg, J. B.; Anzenbacher, Jr, P.; Isaacs, L. *J. Am. Chem. Soc.* **2011**, *133*, 17966–17976.
(13) Ma, D.; Zavalij, P.Y.; Isaacs, L. *J. Org. Chem.* **2010**, *75*, 4786–4795.
(14) Masson, E.; Ling, X.; Joseph, R.; Kyeremeh-Mensah, L.; Lu, X. *RSC Adv.* **2012**, *2*, 1213–1247.
(15) Chernikova, E.Yu; Fedorov, Yu.V.; Fedorova, O.A. *Russ. Chem. Bull. Int. Ed.* **2012**, *61*, 1363–1390.
(16) Miyahara, Y.; Goto, K.; Oka, M.; Inazu, T. *Angew. Chem. Int. Ed.* **2004**, *43*, 5019–5022.
(17) Li, Y.; Lin, L.; Zhu, Y.; Meng, X.; Wu, A. *Cryst. Growth Des.* **2009**, *9*, 4255–4257.
(18) Aav, R.; Shmatova, E.; Reile, I.; Borissova, M.; Topic, F.; Rissanen, K. *Org. Lett.* **2013**, *15*, 3786–3789.
(19) Buschmann, H.-J.; Cleva, E.; Schollmeyer, E. *Inorg. Chem. Commun.* **2005**, *8*, 125–127.
(20) Buschmann, H.-J.; Zielesny, A.; Schollmeyer, E. *J. Incl. Phenom. Macrocyc. Chem.* **2006**, *54*, 181–185.
(21) Svec, J.; Necas, M.; Sindelar, V. *Angew. Chem. Int. Ed.* **2010**, *49*, 2378–2381.
(22) Svec, J.; Dusek, M.; Fejfarova, K.; Stacko, P.; Klán, P.; Kaifer, A.E.; Li, W.; Hudeckova, E.; Sindelar, V. *Chem. Eur. J.* **2011**, *17*, 5605–5612.
(23) Havel, V.; Sindelar, V.; Necas, M.; Kaifer, A.E. *Chem. Commun.* **2014**, *50*, 1372–1374.
(24) Révész, Á.; Schröder, D.; Svec, J.; Wimmerov, M.; Sindelar, V. *J. Phys. Chem. A* **2011**, *115*, 11378–11386.
(25) Havel, V.; Svec, J.; Wimmerova, M.; Dusek, M.; Pojarova, M.; Sindelar, V. *Org. Lett.* **2011**, *13*, 4000–4003.

(26) Cheng, X.-J.; Liang, L.-L.; Chen, K.; Ji, N.-N.; Xiao, X.; Zhang, J.-X.; Zhang, Y.-Q.; Xue, S.-F.; Zhu, Q.-J.; Ni, X.-L.;, et al.. *Angew. Chem. Int. Ed.* **2013**, *52*, 7252−7255.
(27) Cong, H.; Yamato, T.; Feng, X. *J. Mol. Catal. A Chem.* **2012**, 181−185.
(28) Cong, H.; Yamato, T.; Zhu Tao *J. Mol. Catal. A Chem.* **2013**, 287−293.
(29) Cong, H.; Yamato, T.; Zhu Tao *New J. Chem.* **2013**, *37*, 3778−3783.
(30) Fiala, T.; Sindelar, V. *Synlett* **2013**, *24*, 2443−2445.
(31) Lee, J.W.; Samal, S.; Selvapalam, N.; Kim, H.-J.; Kim, K. *Acc. Chem. Res.* **2003**, *36*, 621−630.
(32) Halgren, T.A. *J. Comput. Chem.* **1998**, *17*, 490−519.
(33) Hanwell, M.D.; Curtis, D.E.; Lonie, D.C.; Vandermeersch, T.; Zurek, E.; Hutchison, G.R. *J. Cheminform.* **2012**, *4* (1), 17−33.
(34) Dirac, P.A.M. *Proc. Roy. Soc. (Lond.) A* **1929**, *123*, 714−733.
(35) Slater, J.C. *Phys. Rev.* **1951**, *81*, 385−390.
(36) Vosko, S.H.; Wilk, L.; Nusair, M.; Can *J. Phys.* **1980**, *58*, 1200−1211.
(37) Becke, A.D. *Phys. Rev. A* **1988**, *38*, 3098−3100.
(38) Perdew, J.P. *Phys. Rev. B* **1986**, *33*, 8822−8824.
(39) Weigend, F.; Ahlrichs, R. *Phys. Chem. Chem. Phys.* **2005**, *7*, 3297−3305.
(40) Ahlrichs, R.; Bär, M.; Häser, M.; Horn, H.; Kölmel, C. *Chem. Phys. Lett.* **1989**, *162*, 165−169.

Publication II

Prigorchenko, E.; Öeren, M.; Kaabel, S.; Fomitšenko, M.; Reile, I.; Järving, I.; Tamm, T.; Topic, F.; Rissanen, K.; Aav, R. "Template-controlled synthesis of chiral cyclohexylhemicucurbit[8]uril" Chemical Communications, 2015, **51**, 10921-10924.

ChemComm

COMMUNICATION

View Article Online
View Journal | View Issue

Cite this: *Chem. Commun.*, 2015, 51, 10921

Received 18th May 2015,
Accepted 3rd June 2015

DOI: 10.1039/c5cc04101e

www.rsc.org/chemcomm

Template-controlled synthesis of chiral cyclohexylhemicucurbit[8]uril†

E. Prigorchenko,[a] M. Öeren,[a] S. Kaabel,[a] M. Fomitšenko,[a] I. Reile,[b] I. Järving,[a] T. Tamm,[a] F. Topić,[c] K. Rissanen[c] and R. Aav*[a]

Enantiomerically pure cyclohexylhemicucurbit[8]uril (cycHC[8]), possessing a barrel-shaped cavity, has been prepared in high yield on a gram scale from either (*R*,*R*,*N*,*N*′)-cyclohex-1,2-diylurea and formaldehyde or cycHC[6]. In either case, a dynamic covalent library is first generated from which the desired cycHC can be amplified using a suitable anion template.

Research on new and selective host–guest systems and their applications is currently progressing very quickly.[1] Along with the search for new selective host–guest pairs, new and more efficient synthesis methods for hosts are being developed. Based on the recent success in the field of reversible non-covalent interactions in supramolecular chemistry,[2] the concept of dynamic covalent chemistry (DCC) has been established.[3] Controlling covalent bond formation by non-covalent interactions can serve as an excellent tool for developing efficient adaptive systems, where the formation of the host molecule is based on the structure of the guest.

Cucurbit[*n*]urils[4] (CB) are non-toxic host molecules[5] with a wide range of applications.[1a,d,6] Mechanistic studies have shown that the formation of oligomers and larger CBs proceeds reversibly, indicating that the principles of DCC are applicable in CB chemistry.[7] Hemicucurbiturils[8] (HC) are a sub-group of the cucurbituril family (Fig. 1). HCs are known to form complexes with anions[9] and unsubstituted HCs have been applied as catalysts in organic reactions.[10] It has been shown that biotin[6]uril esters can be applied as transmembrane anion carriers.[9g] Miyahara *et al.*[8a] were the first to describe an efficient synthesis of HC[6] and HC[12].

Fig. 1 Generalized shapes of normal CB, HC and chiral cycHC.

High selectivity towards the HC[6] was explained by the template effect of the chloride anion, which was recently confirmed in a biotin[6]uril synthesis.[8f] The halogen anion is also the necessary template in the synthesis of bambus[6]urils (BU),[11] which can be classified as substituted HCs. Presently, besides HC[12], only 6-membered HCs[8] and 4- and 6-membered BUs[11] have been isolated as main products. Until now, there has not been an efficient synthetic method available for the synthesis of 8-membered HCs. The existence of norbornahemicucurbit[8]uril[8d] has been detected only by mass-spectrometry and (all-*R*)-cyclohexylhemicucurbit[8]uril (cycHC[8]) has only been isolated as a by-product in low yield.[8e]

Herein we report an efficient synthesis of enantiomerically pure cycHC[8], starting either from its homologue cycHC[6] or (*R*,*R*,*N*,*N*′)-cyclohex-1,2-diylurea **1a** and paraformaldehyde. A mechanism of the transformation of cycHC[6] to cycHC[8] is proposed and proof of complexation with carboxylic acids is presented.

CycHC[6] was synthesized earlier in our group.[8c] Subsequently, a small amount of its homologue cycHC[8][8e] was isolated from the crude product of cycHC[6]. Moreover, we noticed that in the chromatographic sample of cycHC[6] containing formic acid the amount of cycHC[8] gradually increased over time. The screening of reaction conditions for this conversion showed that cycHC[6] was transformed to cycHC[8] in the presence of sulphuric, formic and trifluoroacetic acid, but not acetic acid (S4, ESI†). The conversion of cycHC[6] to cycHC[8] by trifluoroacetic acid catalysis is approximately ten times faster than by formic acid (Table 1, entries 1 and 2). Nevertheless, the isolated yield of cycHC[8] was in both cases 71% in gram scale.

[a] *Department of Chemistry, Tallinn University of Technology, Akadeemia tee 15, 12618 Tallinn, Estonia. E-mail: riina.aav@ttu.ee*
[b] *National Institute of Chemical Physics and Biophysics, Akadeemia tee 23, 12618 Tallinn, Estonia*
[c] *University of Jyvaskyla, Department of Chemistry, Nanoscience Center, P.O. Box. 3 , FI-40014 Jyvaskyla, Finland*

† Electronic supplementary information (ESI) available: A detailed description of synthesis, MS, NMR, crystallographic and computational details. CCDC 1053111. For ESI and crystallographic data in CIF or other electronic format see DOI: 10.1039/c5cc04101e

Table 1 Selected reaction conditions and the list of templates for cycHC synthesis

No.	Starting comp.	(Additive)/acid/solvent[a]	Template	Time (h), T	Ratio[b] of cycHC[8] to cycHC[6]	Product	Isolated yield of product (%)
1	cycHC[6]	$HCOOH/CH_3CN$	HCO_2^-	24, rt	92 : 8	cycHC[8]	71
2	cycHC[6]	CF_3COOH/CH_3CN	$CF_3CO_2^-$	1.5, rt	95 : 5	cycHC[8]	71
3	cycHC[6]	$NaPF_6$ (50 eq.)/CH_3COOH/CH_3CN	PF_6^-	24, rt	99 : 1	cycHC[8]	90
4	**1a**	$HCOOH/CH_3CN$	HCO_2^-	24, rt	92 : 8	cycHC[8]	7
5	**1a**	$NaPF_6$ (50 eq.)/CH_3COOH/CH_3CN	PF_6^-	24, rt	95 : 5	cycHC[8]	55
6	**1a**	CF_3COOH/CH_3CN	$CF_3CO_2^-$	2, rt	96 : 4	cycHC[8]	73
7[c]	**1a**	HCl/H_2O	Cl^-	24, 70 °C	0 : 100	cycHC[6] + HCl	85
8	cycHC[8]	HCl/H_2O	Cl^-	24, 70 °C	5 : 95	cycHC[6] + HCl	71
9	cycHC[8]	NaCl (50 eq.)/CH_3COOH	Cl^-	24, 70 °C	40 : 60	cycHC[6] + HCl	21

[a] Generally 300 eq. of organic acid or 4 M HCl were used. [b] Determined by HPLC. [c] Described previously in ref. 8*c*.

The kinetic data for the conversion of cycHC[6] to cycHC[8] revealed that the overall reaction was pseudo first-order, with a plateau. The fact, that the transformation of cycHC[6] to cycHC[8] proceeds faster in stronger acids (Table 1, compare entries 1 and 2) in combination with the results from DFT computational study of model structures (S29, ESI†) allows us to state, that the rate-limiting step of this process is protonation of the macrocycle. Occurrence of side reactions was minimal and no intermediates were detected by NMR (S16, ESI†).

Pittelkow *et al.* have shown that dimers are the main intermediates in the formation of biotin[6]uril.[8f] Also, since cycHC[6] and cycHC[8] differ from each other by a dimer unit, we wanted to examine whether the cycHC[8] formation proceeds *via* dimer addition. We thus introduced ^{13}C labels to methylene bridges of cycHC[6][8c] and subsequently used a 1 : 1 mixture of ^{13}C-labelled and non-labelled cycHC[6] in cycHC[8] synthesis. The number of ^{13}C-labelled methylene groups in isolated cycHC[8] varied from 0 to 8, following a normal distribution, thus confirming that beside dimers, other oligomers or monomers are involved in the reaction (S7, ESI†).

HRMS analysis of the reaction mixture showed the presence of cycHC[6–10][12] and various oligomers (up to an octamer, S14, ESI†). The large number of observed intermediates pointed to the presence of a dynamic combinatorial library (DCL).[3b]

According to DFT-calculated Gibbs' energies of cycHCs it is not the cycle strain, but the inclusion complex with formate anions that induces a preference towards the formation of cycHC[8] (S27, ESI†). Based on the experimental observations described above and the energy calculations on a model system (S29, ESI†), we propose that the transformation of cycHC[6] to cycHC[8] proceeds through the key steps outlined in Scheme 1. First, a reaction rate-limiting protonation of cycHC[6] occurs, then breakage of the first methylene bridge of cycHC[6]H^+ takes place, forming the iminium **3f**. The DCL, whose members have been observed by HRMS, is generated through depropagation and propagation reactions. A formate acts as an anionic template and shifts the thermodynamic equilibrium between DCL members towards the formation of cycHC[8].

To verify that an anionic template is necessary to drive the reaction towards the formation of cycHC, we selected an anion that possessed the size and shape suitable for the cavity of cycHC[8], the hexafluorophosphate, in combination with acetic acid. Acetic acid alone was shown not to facilitate the formation of cycHC[8] (S4, ESI†). As expected, in the presence of $NaPF_6$ in acetic acid/acetonitrile, cycHC[6] was efficiently converted to cycHC[8] (Table 1, entry 3). This observation confirmed that even though reaction rate depends on the acid strength, the macrocycle formation is controlled by the anion, acting as a template.

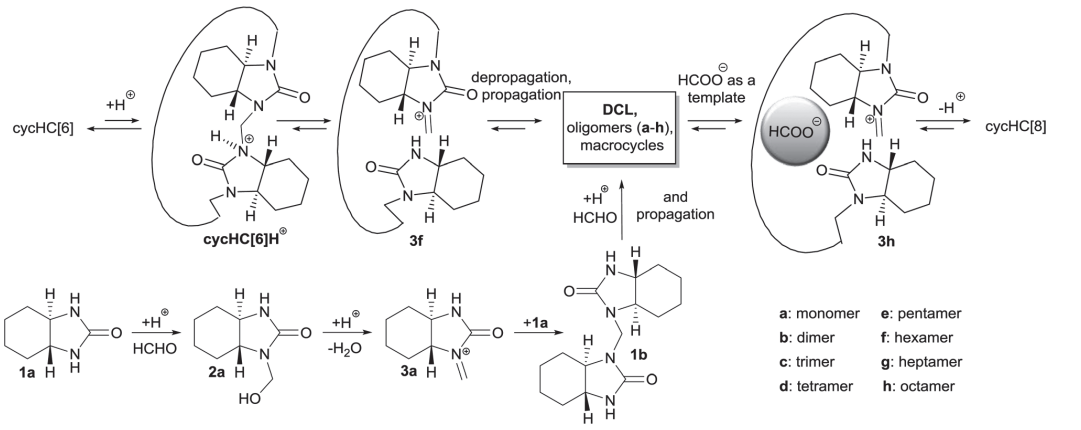

Scheme 1 Proposed reaction mechanism of the cycHC[8] formation catalysed by formic acid.

And with catalysis of formic and trifluoroacetic acid, their conjugate anions act as templates (Table 1, entries 1 and 2).

Next, based on the proposed mechanism, we envisioned that the DCL members could be generated starting from monomers **1a**. Indeed, using either formic acid, trifluoroacetic acid, or $NaPF_6$/acetic acid as catalysts afforded cycHC[8] (Table 1, entries 4–6). The lower rate of formation of cycHC[8] from **1a** than from cycHC[6], was due to the additional acid-promoted reactions necessary for building methylene bridges. The best yield and selectivity were achieved with trifluoroacetic acid, giving the cycHC[8] from **1a** on a gram scale in 73% yield. This synthetic method allowed for the preparation of enantiopure chiral macrocycle cycHC[8] very efficiently, in only two steps, starting from commercially available 1,2-cyclohexanediamine.[13]

According to the proposed mechanism, the conversion of cycHC[8] to cycHC[6] in the presence of a halide template, should also be possible. Indeed, using the classic conditions of CB formation (Table 1, entry 8), cycHC[8] was efficiently converted to cycHC[6] with the aid of the chloride anion. Similarly, using NaCl as a templating additive in acetic acid at elevated temperature, cycHC[8] was also converted to cycHC[6] (Table 1, entry 9), again highlighting the role of the templating anion in the reaction.

The crystal structure confirmed the barrel-like shape of cycHC[8] (Fig. 2). According to the crystal structure, the cavity of cycHC[8], similar in size to that of CB[6], is of sufficient size for the encapsulation of a number of organic and inorganic guests (Table 2).

Complexation studies of the cycHC[8] with carboxylic acids were performed by diffusion NMR in $CDCl_3$. The comparative results of the complexation of cycHC[6] and cycHC[8] are presented in Table 3. The association constants of simple carboxylic acids – acetic, formic and trifluoroacetic acids – follow the order of their acidity (Table 3, entries 1–3) for both hosts.

Analogously to small carboxylic acids, complexation with the more acidic α-methoxy-α-trifluoromethylphenylacetic acid (MTPA) was stronger than with α-methoxyphenylacetic acid (MPA) (Table 3, entries 5 and 6). The opposite preference of complexation of *R*-handed cycHC[6] and cycHC[8] toward MPA enantiomers may suggest different geometries of complexes in these cases. Nevertheless *R*-handed cycHC[8] showed nearly double affinity for *S*-MPA, compared to the *R*-MPA. This result confirms that cycHC[8] forms complexes enantioselectively.

In conclusion, we have presented the first highly efficient synthesis of an 8-membered representative of the cucurbituril family, the (all-*R*)-cyclohexylhemicucurbit[8]uril. We have shown that the reversibility of the methylene bridge formation allows the size of the cycHC macrocycles to be controlled by the anionic templates, with halides driving the equilibrium towards the formation of cycHC[6], while carboxylates and PF_6^- promoted the formation of cycHC[8].

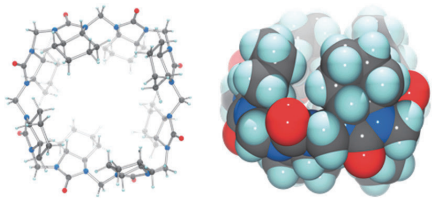

Fig. 2 Crystal structure of cycHC[8]: top view in ball and stick (left) and side view in CPK (right) representations (colour code: C grey, N blue, O red, H turquoise).

Table 2 Dimensions of cycHC[6,8] and CB[6,8]

Parameters[a]	CycHC[6][b]	CycHC[8]	CB[6][c]	CB[8][c]
Opening diameter (Å)	2.2	4.6	3.9	6.9
Cavity diameter (Å)	5.3	8.5	5.8	8.8
Height (Å)	12.1	12.5	9.1	9.1
Cavity volume (Å^3)	35[d]	123[d]	119 ± 21	356 ± 16

[a] Dimensions account for the van der Waals radii of the various atoms. [b] Opening, cavity and height values are from ref. 8*c*. [c] Opening, cavity and height values are from ref. 14*a* and cavity volume from ref. 14*b*. [d] Cavity volume of cycHC[6] from ref. 8*c* and cycHC[8] calculated by analysing the solvent accessible voids in the respective crystal structures using PLATON[15] with a probe radius of 1.2 Å^3 and grid steps of 0.2 Å.

Table 3 Association constants K_a (M^{-1}) of carboxylic acids with cycHC[6] and cycHC[8] in 1 : 1 mixtures in $CDCl_3$

No.	Guest	CycHC[6] K_a	CycHC[8] K_a
1	CH_3COOH	8.0 ± 0.5[a]	17 ± 2
2	HCOOH	97 ± 1	72.6 ± 0.5
3	CF_3COOH	21(±3) × 10^3	29(±1) × 10^3
4	*R*-MPA	27.2 ± 0.8[a]	27.0 ± 0.5
5	*S*-MPA	20.1 ± 0.2[a]	53 ± 3
6	*R*-MTPA	n.d.	3.3(±0.1) × 10^2
7	*S*-MTPA	n.d.	3.0(±0.1) × 10^2

[a] Association constants from ref. 8*c*; n.d. - not determined.

Chiral cycHC[8] and cycHC[6] were obtained very efficiently in one step, starting from enantiomerically pure (*R*,*R*,*N*,*N*′)-cyclohex-1,2-diylurea **1a** or either homologue. (all-*R*)-cycHC[8] enantioselectively formed complexes with chiral carboxylic acids, demonstrating chiral discrimination ability. CycHC[8] shows potential for application in host–guest chemistry.[9g,10,16]

In the present study, DCL members were formed from identical monomeric units. It can be envisioned that by utilizing a mixture of different monomeric ureas and suitable templates, a very efficient yet diverse library of useful hemicucurbituril hosts could become accessible *via* dynamic covalent chemistry.

The authors would like to thank Tiina Aid, Marina Kudrjašova and Jasper Adamson for experimental assistance and Aivar Lõokene, Mart Reimund and Omar Parve for help with the manuscript. This research was supported by the Academy of Finland (KR, grants 263256 and 265328), the Estonian Ministry of Education and Research through Grants IUT19-32, IUT19-9, IUT23-7 and PUT692, TUT grant no. B25, the ESF DoRa, and the EU European Regional Development Fund (3.2.0101.08-0017). Computations were performed on the HPC cluster at TUT, which is part of the ETAIS. FT acknowledges support from NGS-NANO through a PhD fellowship.

Notes and references

1 (*a*) X. Ma and Y. Zhao, *Chem. Rev.*, 2015, DOI: 10.1021/cr500392w; (*b*) Special Issue: Responsive Host–Guest Systems, *Acc. Chem. Res.*, 2014, **47**, 1923; (*c*) G. Ghale and W. M. Nau, *Acc. Chem. Res.*, 2014, **47**, 2150; (*d*) J. Hu and S. Liu, *Acc. Chem. Res.*, 2014, **47**, 2084.

2 (*a*) C. J. Pedersen, *Angew. Chem., Int. Ed. Engl.*, 1988, **27**, 1021; (*b*) J.-M. Lehn, *Angew. Chem., Int. Ed. Engl.*, 1988, **27**, 89; (*c*) D. J. Cram, *Angew. Chem., Int. Ed. Engl.*, 1988, **27**, 1009; (*d*) J.-M. Lehn, *Angew. Chem., Int. Ed.*, 2013, **52**, 2836.
3 (*a*) J.-M. Lehn, *Chem. – Eur. J.*, 1999, **5**, 2455; (*b*) S. J. Rowan, S. J. Cantrill, G. R. L. Cousins, J. K. M. Sanders and J. F. Stoddart, *Angew. Chem., Int. Ed.*, 2002, **41**, 898; (*c*) P. T. Corbett, J. Leclaire, L. Vial, K. R. West, J. L. Wietor, J. K. M. Sanders and S. Otto, *Chem. Rev.*, 2006, **106**, 3652; (*d*) Y. Jin, C. Yu, R. J. Denman and W. Zhang, *Chem. Soc. Rev.*, 2013, **42**, 6634; (*e*) Y. Jin, Q. Wang, P. Taynton and W. Zhang, *Acc. Chem. Res.*, 2014, **47**, 1575; (*f*) A. Herrmann, *Chem. Soc. Rev.*, 2014, **43**, 1899; (*g*) M. Matache, E. Bogdan and N. D. Hădade, *Chem. – Eur. J.*, 2014, **20**, 2106.
4 (*a*) E. Masson, X. Ling, R. Joseph, L. Kyeremeh-Mensah and X. Lu, *RSC Adv.*, 2012, **2**, 1213; (*b*) K. I. Assaf and W. M. Nau, *Chem. Soc. Rev.*, 2015, **44**, 394.
5 (*a*) R. Oun, R. S. Floriano, L. Isaacs, E. G. Rowan and N. J. Wheate, *Toxicol. Res.*, 2014, **3**, 447; (*b*) U. Hoffmann, M. Grosse-Sundrup, K. Eikermann-Haerter, S. Zaremba, C. Ayata, B. Zhang, D. Ma, L. Isaacs and M. Eikermann, *Anesthesiology*, 2013, **119**, 317; (*c*) V. D. Uzunova, C. Cullinane, K. Brix, W. M. Nau and A. I. Day, *Org. Biomol. Chem.*, 2010, **8**, 2037.
6 (*a*) S. Walker, R. Oun, F. J. McInnes and N. J. Wheate, *Isr. J. Chem.*, 2011, **51**, 616; (*b*) A. I. Day and J. G. Collins, Cucurbituril receptors and drug delivery, in *Supramolecular Chemistry: From Molecules to Nanomaterials*, ed. J. W. Steed and P. A. Gale, John Wiley & Sons, Ltd, 2012, vol. 3, p. 983; (*c*) L. Peng, A. Feng, M. Huo and J. Yuan, *Chem. Commun.*, 2014, **50**, 13005; (*d*) V. Mandadapu, A. I. Day and A. Ghanem, *Chirality*, 2014, **26**, 712; (*e*) A. A. Elbashir and H. Y. Aboul-Enein, *Crit. Rev. Anal. Chem.*, 2015, **45**, 52; (*f*) S. Gürbüz, M. Idrisa and D. Tuncel, *Org. Biomol. Chem.*, 2015, **13**, 330.
7 (*a*) A. Day, A. P. Arnold, R. J. Blanch and B. Snusball, *J. Org. Chem.*, 2001, **66**, 8094; (*b*) A. Chakraborty, A. Wu, D. Witt, J. Lagona, J. C. Fettinger and L. Isaacs, *J. Am. Chem. Soc.*, 2002, **124**, 8297; (*c*) W.-H. Huang, P. Y. Zavalij and L. Isaacs, *J. Am. Chem. Soc.*, 2008, **130**, 8446; (*d*) L. Isaacs, *Chem. Commun.*, 2009, 619; (*e*) L. Isaacs, *Isr. J. Chem.*, 2011, **51**, 578; (*f*) D. Lucas, T. Minami, G. Iannuzzi, L. Cao, J. B. Wittenberg, P. Anzenbacher Jr. and L. Isaacs, *J. Am. Chem. Soc.*, 2011, **133**, 17966.
8 (*a*) Y. Miyahara, K. Goto, M. Oka and T. Inazu, *Angew. Chem., Int. Ed.*, 2004, **43**, 5019; (*b*) Y. Li, L. Li, Y. Zhu, X. Meng and A. Wu, *Cryst. Growth Des.*, 2009, **9**, 4255; (*c*) R. Aav, E. Shmatova, I. Reile, M. Borissova, F. Topić and K. Rissanen, *Org. Lett.*, 2013, **15**, 3786; (*d*) T. Fiala and V. Sindelar, *Synlett*, 2013, 2443; (*e*) M. Fomitšenko, E. Shmatova, M. Öeren, I. Järving and R. Aav, *Supramol. Chem.*, 2014, **26**, 698; (*f*) M. Lisbjerg, B. M. Jessen, B. Rasmussen, B. Nielsen, A. U. Madsen and M. Pittelkow, *Chem. Sci.*, 2014, **5**, 2647.
9 (*a*) For anion binding of hemicucurbiturils see ref. 8 and H.-J. Buschmann, E. Cleva and E. Schollmeyer, *Inorg. Chem. Commun.*, 2005, **8**, 125; (*b*) H.-J. Buschmann, A. Zielesny and E. Schollmeyer, *J. Inclusion Phenom. Macrocyclic Chem.*, 2006, **54**, 181; (*c*) M. Sundararajan, R. V. Solomon, S. K. Ghosh and P. Venuvanalingam, *RSC Adv.*, 2011, **1**, 1333; (*d*) H.-J. Buschmann and A. Zielesny, *Comput. Theor. Chem.*, 2013, **1022**, 14; (*e*) M. Öeren, E. Shmatova, T. Tamm and R. Aav, *Phys. Chem. Chem. Phys.*, 2014, **16**, 19198; (*f*) A. M. Lisbjerg, B. E. Nielsen, B. O. Milhøj, S. P. A. Sauer and M. Pittelkow, *Org. Biomol. Chem.*, 2015, **13**, 369; (*g*) M. Lisbjerg, H. Valkenier, B. M. Jessen, H. Al-Kerdi, A. P. Davis and M. Pittelkow, *J. Am. Chem. Soc.*, 2015, **137**, 4948.
10 (*a*) H. Cong, T. Yamato and X. Feng, *J. Mol. Catal. A: Chem.*, 2012, 181; (*b*) H. Cong, T. Yamato and Z. Tao, *J. Mol. Catal. A: Chem.*, 2013, 287; (*c*) H. Cong, T. Yamato and Z. Tao, *New J. Chem.*, 2013, **37**, 3778.
11 (*a*) J. Svec, M. Necas and V. Sindelar, *Angew. Chem., Int. Ed.*, 2010, **49**, 2378; (*b*) V. Havel, J. Svec, M. Wimmerova, M. Dusek, M. Pojarova and V. Sindelar, *Org. Lett.*, 2011, **13**, 4000; (*c*) J. Rivollier, P. Thuéry and M.-P. Heck, *Org. Lett.*, 2013, **15**, 480; (*d*) M. A. Yawer, V. Havel and V. Sindelar, *Angew. Chem., Int. Ed.*, 2015, **54**, 276; (*e*) M. Singh, E. Solel, E. Keinan and O. Reany, *Chem. – Eur. J.*, 2015, **21**, 536.
12 ref. 8*e* and ESI† for detailed MS data.
13 (*a*) Enantiopure 1,2-cyclohexanediamine can also be isolated from racemic mixture: J. F. Larrow, E. N. Jacobsen, Y. Gao, Y. Hong, X. Nie and C. M. Zepp, *J. Org. Chem.*, 1994, **59**, 1939; (*b*) J. F. Larrow and E. N. Jacobsen, *Org. Syn., Coll.*, 2004, **10**, 96.
14 (*a*) J. Kim, I.-S. Jung, S.-Y. Kim, E. Lee, J.-K. Kang, S. Sakamoto, K. Yamaguchi and K. Kim, *J. Am. Chem. Soc.*, 2000, **122**, 540; (*b*) W. M. Nau, M. Florea and K. I. Assaf, *Isr. J. Chem.*, 2011, **51**, 559.
15 A. L. Spek, *Acta Crystallogr.*, 2009, **D65**, 148.
16 (*a*) P. A. Gale, *Acc. Chem. Res.*, 2011, **44**, 216; (*b*) J. Lacour and D. Moraleda, *Chem. Commun.*, 2009, 7073; (*c*) R. J. Phipps, G. L. Hamilton and F. D. Toste, *Nat. Chem.*, 2012, **4**, 603; (*d*) K. Wichmann, B. Antonioli, T. Söhnel, M. Wenzel, K. Gloe, K. Gloe, J. R. Price, L. F. Lindoy, A. J. Blake and M. Schröder, *Coord. Chem. Rev.*, 2006, **250**, 2987; (*e*) T. J. Wenzel, *J. Inclusion Phenom. Macrocyclic Chem.*, 2014, **78**, 1.

Publication III

Fomitšenko, M.; Peterson, A.; Reile, I.; Cong, H.; Kaabel, K.; Prigorchenko, E.; Järving I.; Aav R. "A quantitative method for analysis of mixtures of homologues and stereoisomers of hemicucurbiturils that allows us to follow their formation and stability" *New Journal of Chemistry*, 2017, **41**, 2490-2497

NJC

PAPER

View Article Online
View Journal | View Issue

Cite this: *New J. Chem.*, 2017, 41, 2490

A quantitative method for analysis of mixtures of homologues and stereoisomers of hemicucurbiturils that allows us to follow their formation and stability†

Maria Fomitšenko,[a] Anna Peterson,[a] Indrek Reile,[b] Hang Cong,[c] Sandra Kaabel,[a] Elena Prigorchenko,[a] Ivar Järving[a] and Riina Aav*[a]

Received 28th September 2016,
Accepted 13th February 2017

DOI: 10.1039/c6nj03050e

rsc.li/njc

Hemicucurbiturils are a sub-group of macrocyclic compounds within the cucurbit[*n*]uril family. The ability of unsubstituted and substituted hemicucurbiturils to form host–guest complexes allows selective binding of anions, application in catalysis and chiral discrimination between enantiomeric guests. Herein we demonstrate the separation of hemicucurbituril homologues and diastereomers by reverse phase HPLC and the quantitative analysis of hemicucurbit[6]uril, (all-*R*,*R*)-cyclohexanohemicucurbit[6]uril, (all-*R*,*S*)-cyclohexanohemicucurbit[6]uril and (all-*R*,*R*)-cyclohexanohemicucurbit[8]uril. The applicability of the developed quantitative analysis is demonstrated by the estimation of the reaction yields of cyclohexanohemicucurbiturils and by following the depolymerisation of hemicucurbit[6]uril under acidic conditions. Analysis of the studied set of compounds – monomers, oligomers and macrocycles – reveals that the number of repeating units and UV extinction coefficients are not proportional; also, the UV absorbance of a macrocycle is 10-fold higher compared to its linear isomer. The possibility of a drastic difference in the ultraviolet absorbance of oligomeric analogues should also be considered in quantification of other classes of polymeric macrocycles.

Introduction

Single bridged cucurbituril[1] (CB) family members, the hemicucurbiturils[2] (HCs) (Fig. 1A and B), are macrocycles that selectively bind anions into their hydrophobic cavity.[3–13] HCs have been reported to act as anion channels,[14] amino acid extracting agents,[15] and catalysts[16–19] and (all-*R*,*R*)-cyclohexanohemicucurbit[*n*]urils (cycHC[*n*], n = 6, 8) show chiral recognition toward carboxylic acids.[8,10] The focus of our group has been on the synthesis and analysis of cycHC[*n*]. We have developed an efficient templated synthesis of (all-*R*,*R*)-cycHC[6][8] and (all-*R*,*R*)-cycHC[8],[10] and established the conditions for the analytical separation of cycHC[6–10] homologues by RP-HPLC.[9] Our very recent study revealed the unique ability of cycHC[8] to encapsulate large anions with high affinity in a competitive protonic media,[13] highlighting the potential of these hosts as anion receptors.

CB family members are all formed in a polymerisation reaction, and the isolation of one particular macrocycle is achieved through careful control of the reaction and/or separation conditions. The most colourful example from CB chemistry is the isolation of CB[14] in 1% yield, where the chromatographic eluting period was approximately three months based on 12 h column running per day.[20] Demand for such an esoteric isolation procedure arises from the unavoidable similarity of partitioning behavior between linear and cyclic oligomeric homologues. A method that allows reliable estimation of the composition of the reaction mixture is therefore essential for the development of an efficient synthesis. An ineffective method can lead to underestimation of the number of compounds in a sample and overestimation of product yields. Widely applied NMR is a powerful technique for the structural determination of pure compounds, but for a mixture consisting of similar cucurbituril homologues and derivatives, it gives overlapping signals, which may lead to ambiguous results, such as those seen in the case of the synthesis of monohydroxy-CBs.[21,22] A method for assessing the purity and stability of the isolated macrocyclic compounds is also of crucial importance in the follow-up studies on the applications of CB family members. While many analytical methods have been developed to understand and describe the host–guest chemistry of CBs,[23–27] there are only a limited number of examples

[a] *Department of Chemistry and Biotechnology, Tallinn University of Technology, Akadeemia tee 15, 12618 Tallinn, Estonia. E-mail: riina.aav@ttu.ee*
[b] *National Institute of Chemical Physics and Biophysics, Akadeemia tee 23, 12618 Tallinn, Estonia*
[c] *Key Laboratory of Macrocyclic and Supramolecular Chemistry of Guizhou Province, Guizhou University, Guiyang 550025, P. R. China*

† Electronic supplementary information (ESI) available: UV spectra, HRMS data and NMR spectra. See DOI: 10.1039/c6nj03050e

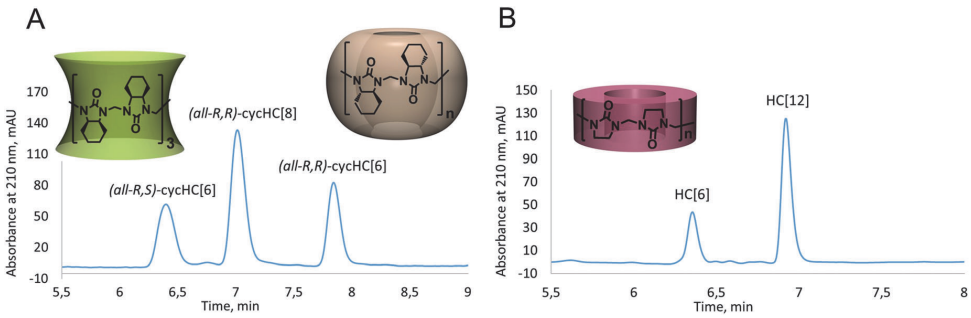

Fig. 1 Structures and RP-HPLC chromatograms of (A) (all-*R*,*S*)-cyclohexanohemicucurbit[6]uril, (all-*R*,*R*)-cyclohexanohemicucurbit[8]uril, (all-*R*,*R*)-cyclohexanohemicucurbit[6]uril and (B) hemicucurbit[6]uril and hemicucurbit[12]uril.

published for simultaneous screening and quantifying of several derivatives or isomers of CBs themselves.[11,28] Heck and Huber *et al.* synthesised substituted cucurbit[6]uril derivatives and measured their solubility in water by HPLC-ESI-MS, where mass detection was used to identify the CBs undetectable by UV spectroscopy. In their study an assumption was made, that the ionization efficiency of all studied CB[6] isomers is the same as that for unsubstituted CB[6]. Quantification of the content of alkyl substituted CB[6] isomers in the reaction mixture was based on relative MS intensity to CB[7] as the internal standard.[28] Pittelkow *et al.* applied RP-HPLC-ESI-MS and -UV analyses for the quantification of the observed linear oligomers and biotin[6]uril, calibrating the UV signal at 209 nm of biotin, its dimer and biotin[6]uril.[11] In their study, the slope of the biotin[6]uril calibration graph divided by six, and the slope of the biotin dimer divided by two corresponded to the slope of the monomer absorbance; therefore, a reasonable assumption was made that the UV intensity response was linear to the number of monomers in biotin[6]uril and in all oligomers.

Herein we present a HPLC method for simultaneous separation and quantification of 6- and 8-membered homologues and 6-membered diastereoisomers of cycHCs (Fig. 1A) as well as separation of unsubstituted 6- and 12-membered HCs (Fig. 1B). We also demonstrate the applicability of the quantification on two examples, for the estimation of the reaction yields of cycHCs and the degradation of unsubstituted HC[6] in acidic media. In addition, we point out the disproportionality of UV absorbance compared to the number of repeating units in the studied compounds.

Materials and methods

Chemicals and materials

All solvents used for HPLC analysis were of LC-MS grade. D_2O (99.8 atom% D) and $CDCl_3$ (99.8 atom% D) were obtained from Armar Chemicals (Switzerland), concentrated HCl from Penta (Czech Republic), $CF_3CF_2CO_2H$ (China) and $HO(CH_2O)_nH$ (Germany) from Sigma Aldrich and silica gel (40–63 μm) from ThoMar (Germany). Solvents for flash chromatography were dried and distilled according to standard laboratory procedures.

HC[6] and HC[12],[2] (all-*R*,*R*)-cycHC[6],[8] (all-*R*,*R*)-cycHC[8],[10] (all-*R*,*S*)-cycHC[6][4] and (*R*,*R*)-cyclohex-1,2-diylurea[29] were synthesised according to known literature procedures. (*R*,*S*)-Cyclohex-1,2-diylurea was synthesized from (1*R*,2*S*)-cyclohexanediamine analogously to its (*R*,*R*)-stereoisomer. Unsubstituted HCs were additionally purified over silica gel by simple flash chromatography (CH_2Cl_2/MeOH, 20 : 1).

Procedures

Chromatographic and mass spectrometric procedures. The calibration procedures and monitoring of the reactions were conducted using an Agilent Technologies HPLC 1200 system with a multiple wavelength detector, separating compounds on a Kinetex C18 column (2.1 × 100 mm, 2.6 μm). Eluents A (CH_3CN), B (H_2O) and C (H_2O with 0.1% CF_3CO_2H) were used in the gradient mode from 50A/50B to 100A/0B within 10 minutes for cycHCs and from 5A/95C to 100A/0C for HCs. For the quantification of cyclohex-1,2-diylurea isomers, a 5 minute gradient from 1A/99B to 80A/20B was used. The column temperature was set at 30 °C, the flow rate at 0.25 ml min^{-1}, the injection volume at 5 μl and the UV-detection at 210 nm. For the collection of oligomers slower flow rate (0.2 ml min^{-1}) and wider gradient (40A/60B to 100A/0B) were used.

The identification of compounds was performed on an Agilent 6540 UHD Accurate-Mass Q-TOF LC/MS system with AJ-ESI ionization and Zorbax Eclipse Plus C18 column (2.1 × 150 mm, 1.8 μm). Eluents D (CH_3CN with 0.1% HCO_2H and 1.0% H_2O) and E (H_2O with 0.1% HCO_2H) in a 10 minute gradient from 50D/50E to 100D/0E were used for cycHCs and 20D/80E to 100D/0E for HCs, respectively. The flow rate was 0.4 ml min^{-1}, the temperature was 30 °C and the injection volume was varied depending on the concentration of analytes.

Preparation of oligomers. 150 mg of cycHC[8] was dissolved in 3.9 ml (300 eq.) of $CF_3CF_2CO_2H$. The reaction was followed by RP-HPLC using 20 μl of the crude reaction mixture and diluting it in a $CHCl_3/CH_3CN$ (1 : 4) mixture. After 5 hours, the reaction was stopped by addition of H_2O and the precipitated product was subjected to column chromatography (CH_2Cl_2/MeOH, 100 : 1 to 1 : 5). Isolation of the 9 mg fraction containing mainly cycHC[6] and cycHC[8] and the 111 mg fraction of

oligomers (up to 18 units) was achieved. Both fractions were analysed using HPLC and the compounds were identified using HRMS.

The stock solution (50 mg ml^{-1}) of the oligomeric mixture was prepared in a CH_3CO_2H and HCO_2H mixture (1 : 1) and diluted 2 times in CH_3CN before injection. The single oligomers were separated by HPLC by collection of fractions directly from the detector outlet and right after the appearance of the signal. Three fractions containing single oligomers, according to HPLC-MS analysis (Fig. S1 and S2, ESI†), were chosen for UV measurements. The solvent was evaporated and the constant weights of 4-membered (0.094 mg), 6-membered (0.136 mg) and 7-membered (0.223 mg) oligomers were determined on microscales with a precision of 0.006 mg (Radwag MYA 11.4Y, Poland).

UV spectra measurements. UV spectra from 190 to 260 nm were measured on a Jasco V-730 spectrophotometer (Japan). The type S15-UV-10 quartz cuvettes were used (GL Sciences Inc., Japan). All compounds were measured in CH_3CN in the concentration range of 10^{-6}–10^{-4} M and referenced to the solvent absorption. The accuracy of concentrations of measured samples was within the range of ±4%. The extinction coefficients (ε_λ) were calculated according to Lambert–Beer's law:

$$\varepsilon_{210} = \frac{A_{210}}{l \cdot C_M},$$

where ε_{210} is the molar absorption coefficient (M^{-1} cm^{-1}) at 210 nm, A_{210} is the absorption at 210 nm, l is the width of the detector cell (cm), which is 1 cm, and C_M is the molar concentration (mol L^{-1}).

Determination of the purity of macrocycles. ^{1}H-NMR experiments were performed on a Bruker Avance III 400 MHz spectrometer. Spectra were measured under quantitative conditions (scans = 16, relaxation delay = 60 seconds, acquisition time = 4 seconds, and flip angle = 30°).

Each macrocycle was weighed (1–5 mg) with a precision of 0.001 mg (Mettler Toledo scales) and dissolved in $CDCl_3$, where a 1,3,5-tris(trifluoromethyl)benzene internal standard was added in an equimolar ratio. The procedure was repeated in three separate parallels. The purities for the macrocycles were calculated using the following equation:

$$P_x(\%) = \frac{I_x}{I_{st}} + \frac{N_{st}}{N_x} + \frac{M_x}{M_{st}} + \frac{W_{st}}{W_x} \cdot P_{st},$$

where I, N, M, W and P are the integral area, number of nuclei, molecular weight (mg $mmol^{-1}$), gravimetric weight (mg) and purity of the analyte (x) and standard (st), respectively.

The purity of the macrocycles used for calibration was as follows: (all-*R*,*R*)-cycHC[8] 84.4 ± 0.7%, (all-*R*,*R*)-cycHC[6] 85.2 ± 0.7%, (all-*R*,*S*)-cycHC[6] 87.7 ± 0.6% and HC[6] 80 ± 3%.

Calibration procedure. For the preparation of standard solutions, Mettler Toledo scales with a precision of 0.001 mg and Hamilton gas-tight syringes with accuracies of 0.5–2% were used. The overall uncertainty in all of the dilutions did not exceed 4%.

To calibrate the signal against each macrocycle content, two six-point calibration curves were analysed using linear regression analysis. The concentration ranges from the limit of detection to 200 μg ml^{-1} for cycHCs and to 400 μg ml^{-1} for HCs were analysed. Stock solutions of cycHCs and HC[6] were made by weighing the macrocycle and dissolving it in $CHCl_3$; for HC[12], 5% DMSO in $CHCl_3$ was used. Dilutions of (all-*R*,*R*)-cycHC homologues were made in CH_3CN and (all-*R*,*S*)-cycHC[6], HC[6] and HC[12] were diluted with CH_3OH. To determine the slopes of cyclohex-1,2-diylurea stereoisomers, the linear equations were found with three points at concentrations of 10, 100 and 200 μg ml^{-1}. The preparation of standard solutions was the same as that for the corresponding cycHC stereoisomers. Standard solutions were made directly before analysis to avoid precipitation of HCs upon storage at room temperature. Each solution was prepared in three parallels, which were measured once. The parallels were used to calculate the standard deviations of peak areas. The accuracies for standard solutions were calculated by the square root of the sum of the squares of accuracies corresponding to weights or syringes during preparation. The limit of detection (LoD) and limit of quantification (LoQ) were found experimentally by diluting samples until the signal to noise ratio was 3 and 10, respectively.

Yield calculation of formed cycHCs from crude reaction mixtures. 62 mg of (all-*R*,*R*)-cycHC[8] was obtained as a white solid with an isolated yield of 53% from a mixture of (*R*,*R*)-cyclohex-1,2-diylurea (108 mg, 0.8 mmol) and $HO(CH_2O)_nH$ (24 mg, 0.8 mmol) in 3 ml of CF_3CO_2H/CH_3CN (1 : 1) mixture.

790 mg of (all-*R*,*R*)-cycHC[6] was obtained as a white solid with an isolated yield of 68% from a mixture of (*R*,*R*)-cyclohex-1,2-diylurea (700 mg, 5.0 mmol) and $HO(CH_2O)_nH$ (150 mg, 5.0 mmol) in 20 ml of 4 M HCl aqueous solution.

(all-*R*,*S*)-cycHC[6] was obtained as a white solid (54 mg, 51%) from a mixture of (*R*,*S*)-cyclohex-1,2-diylurea (100 mg, 0.71 mmol) and $HO(CH_2O)_nH$ (22 mg, 0.74 mmol) in 3 ml of 4 M HCl aqueous solution.

For chromatographic analysis three samples (20 μl) of the reaction mixture were taken for three parallels and diluted in $CHCl_3/CH_3CN$ (1 : 4) or $CHCl_3$/MeOH (1 : 4) mixture. The concentrations were found using the $y = ax + b$ equation from the calibration curve and yields were calculated according to the following formula:

$$\text{Yield } \% = \frac{\overline{C_{sample}} \cdot f_{sample} \cdot n \cdot V_{reaction}}{mmol_{reagent} \cdot M_{product}} \cdot 100\%,$$

where $\overline{C_{sample}}$ is the average concentration (mg ml^{-1}) determined from the three parallels and calculated using the calibration curve equation; f_{sample} is the dilution factor; $mmol_{reagent}$ is millimoles of the limiting starting reagent; $M_{product}$ is the molecular weight of the product (cycHC[n]) (mg $mmol^{-1}$); n is the stoichiometry factor (number of monomeric units in the product) and $V_{reaction}$ is the volume of the reaction mixture (ml).

Stability analysis of HCs. For the qualitative analysis of HC[6] and HC[12], macrocycles were weighed in NMR tubes and 0.1 M HCl in D_2O was added (2.6 and 3.1 mg ml^{-1}, respectively). Suspensions were sonicated for 15 min, 50 μl of the solution was taken and diluted six times in CH_3OH to

analyse using HPLC and the rest of the sample was simultaneously analysed using ^{1}H-NMR. Then the NMR samples were heated in an oil bath at 65 °C for 3 hours and analysed again firstly by ^{1}H-NMR and secondly by HPLC by diluting the same sample in CH_3OH two times.

To quantify the rate of degradation of HC[6] in acidic media, three separate parallels of a homogeneous saturated solution (0.14 mg ml^{-1}) of the macrocycle in 0.1 M HCl were prepared and placed in an oil bath at 65 °C. After each hour batches of 200 µl were taken, diluted two times in CH_3OH and analysed by HPLC. The rate of HC[6] degradation was found by fitting the HC[6] quantification results with an exponential decay function using Sigmaplot 13™.

Results and discussion

UV absorption of cycHCs, linear oligomers and monomers

During the ongoing search for larger homologues of cycHCs $CF_3CF_2CO_2H$ was used as media with the hope to direct the reaction toward formation of larger macrocycles. The RP-HPLC-UV chromatogram suggested that the crude product contained mainly a mixture of (all-*R*,*R*)-cycHC[6,8,10,11,12] homologues (Fig. 2A). Unfortunately purification of the product by column chromatography gave 74% of the mixture of oligomers (Fig. 2B) along with 6% of the mixture of macrocycles mainly consisting of cycHC[6] and cycHC[8]. New macrocycles were not isolated.

The unexpected disproportionality between the chromatogram of crude (Fig. 2A) and isolated products (Fig. 2B) encouraged us to look closer into the UV absorption of (all-*R*,*R*)-cycHC macrocycles and their intermediates. Determining the relationship between the extinction coefficient of the monomer, oligomers and macrocycles and the number of repeating units in these compounds would be beneficial for the deduction of concentration of new HCs.

The correlation between the molar absorption coefficients of aromatic chromophores such as tryptophans, tyrosines and cysteines and their number in proteins is a widely used approach in biochemistry.[30] Codari *et al.* quantified poly(lactic acid) chains up to 9 units, which all correlated linearly with UV absorption at 210 nm using only monomer and dimer calibration.[31] And as noted before the UV absorption of biotin, its dimer and biotin[6]uril was proportional to the number of repeating units.[11]

UV spectra of (all-*R*,*R*)-cycHC[6], (all-*R*,*S*)-cycHC[6], (all-*R*,*R*)-cycHC[8], 4-, 6- and 7-membered oligomers, (*R*,*R*)-cyclohex-1,2-diylurea and (*R*,*S*)-cyclohex-1,2-diylurea, which structures are shown in Fig. 3, were analysed. The absorption maximum (λ_{max}) of the studied compounds, with the only exception of (all-*R*,*S*)-cycHC[6], is between 191 and 197 nm (Table 1).

The extinction coefficients (ε_λ of the analyzed compounds) are plotted in Fig. 4 and ε_λ values for λ_{max} and λ_{210} are shown in Table 1. Full UV experimental data are given in the ESI.†

One can clearly see that ε values of diastereomeric cyclohex-1,2-diylureas (Table 1, lines 7 and 8) and 4-, 6- and 7-membered oligomers (Table 1, lines 4–6) lie within the same order of magnitude at λ_{max}.

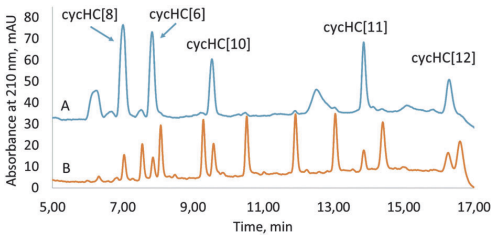

Fig. 2 HPLC-UV chromatograms of (A) the crude reaction mixture formed from (*R*,*R*)-cyclohex-1,2-diylurea and (B) the mixture of oligomers as the main product of this reaction.

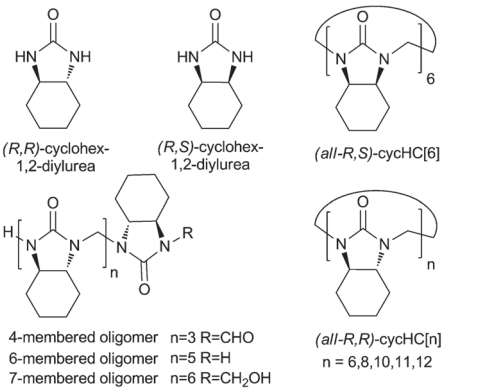

Fig. 3 Structures of cycHCs, linear oligomers and monomers.

Table 1 Absorption maximum (λ_{max}) and extinction coefficients (ε_λ) of cycHCs, oligomers and cyclohex-1,2-diylureas at λ_{max} and λ_{210}

No.	Compound	λ_{max} (nm)	$\varepsilon_{\lambda_{max}}{}^a$ (M^{-1} cm^{-1}) × 1000	$\varepsilon_{210}{}^a$ (M^{-1} cm^{-1}) × 1000
1	(all-*R*,*R*)-cycHC[8]	197	94.2 ± 0.2	19.2 ± 0.4
2	(all-*R*,*R*)-cycHC[6]	196	64 ± 4	17 ± 2
3	(all-*R*,*S*)-cycHC[6]	n.d.^{b}	145.0 ± 0.2^c	18.4 ± 0.2
4	4-membered oligomer	192	7 ± 4	3 ± 2
5	6-membered oligomer	192	6 ± 2	2 ± 1
6	7-membered oligomer	192	6 ± 3	3 ± 1
7	(*R*,*R*)-cyclohex-1,2-diylurea	191	4.3 ± 0.4	0.33 ± 0.07
8	(*R*,*S*)-cyclohex-1,2-diylurea	191	4.1 ± 0.4	0.5 ± 0.1

^{a} Values are given with standard deviation of ε determined at 5 different concentrations (see ESI). ^{b} The maximum was out of the range of measurement, below 190 nm. ^{c} Determined at 190 nm.

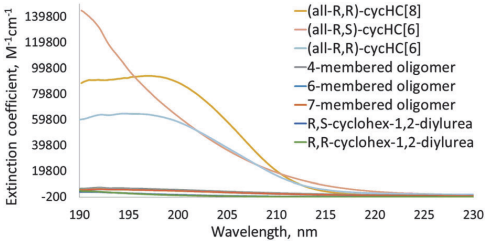

Fig. 4 UV extinction coefficients of cycHCs, oligomers and cyclohex-1,2-diylureas.

This and the relatively high deviation of extinction coefficient values of oligomers do not allow correlation between the number of repeating units in oligomers and UV absorption. The macrocycle ε values at 210 nm are very close and are not correlated with the number of monomers. In addition, the extinction coefficient of the 6-membered macrocycle (Table 1, line 2) is 10 times larger than that of the 6-membered linear isomer (Table 1, line 5). This clearly shows that the rigidly positioned urea functional groups in a macrocycle have significantly higher UV absorption compared to ureas in the linear isomers. These results explain the misleading signature of the HPLC chromatogram of the crude reaction mixture (Fig. 2A). Therefore, it can be concluded that there is no simple proportionality between the number of chromophores and UV absorbance in the studied oligomeric analogues and separate calibration is necessary for every compound of interest.

Calibration curves of cycHCs and their application in yield determination

Plotting the concentration in μg ml^{-1} of (all-*R*,*R*)-cycHC[8], (all-*R*,*R*)-cycHC[6] and (all-*R*,*S*)-cycHC[6] and monomers against their UV response at 210 nm showed accurate linear correlations for each macrocycle and monomer (Fig. 5). LoD, LoQ, the repeatability of the peak areas, linear equations, and correlation coefficients (R^2) are presented in Table 2 for each macrocycle. Also, the linear equations and correlation coefficients of diastereomeric cyclohex-1,2-diylureas are listed in Table 2.

The differences in calibration graph slopes between monomers and macrocycles are consistent with the disproportionality of their extinction coefficients (Tables 1 and 2), and as already stated macrocycles possess significantly higher absorption. The obtained calibration curves of cycHCs were applied for the calculation of yields of macrocycles from crude reaction mixtures (Table 3). The yields calculated from the reaction mixture through HPLC calibration curves were close to the isolated ones. A sufficiently accurate estimation of the cycHC yield for the reaction mixture by the presented HPLC methodology reflects the low impact of the reaction mixture matrix on the quantification. The presented method is robust and can be utilized for synthetic reaction screening or host concentration quantification.

Qualitative HPLC and NMR analyses of the stability of HCs and quantification of HC[6]

The co-author of this study Cong *et al.* previously described the changes in NMR spectra of unsubstituted HCs during their action as catalysts in acidic media.[19]

This raised a question about the stability of HCs in an aqueous acid and to determine that, the calibration of UV absorbance against concentrations of HC[6] and HC[12] was attempted. Unfortunately, due to the very low solubility of HC[12] in $CHCl_3$, CH_2Cl_2, DMSO, MeOH, EtOAc, H_2O and 0.1 M HCl, reliable quantification of the latter was not achieved. The calibration of the HC[6] signal was successful, but unlike cycHCs the UV response was not linear in the range of concentrations from LoD to 400 μg ml^{-1} (Fig. 6B). Nevertheless, a linear correlation

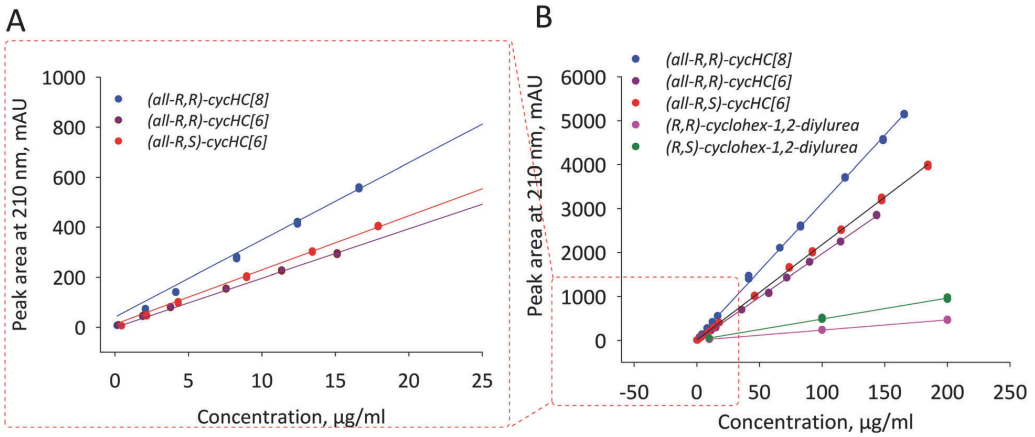

Fig. 5 Calibration graphs of cycHCs and their monomers (A) in the range from LoD to 20 μg ml^{-1} and (B) up to 200 μg ml^{-1}. The color code of the calibration curves is as follows: (all-*R*,*R*)-cycHC[8] is blue, (all-*R*,*S*)-cycHC[6] is red, (all-*R*,*R*)-cycHC[6] is purple, (*R*,*S*)-cyclohex-1,2-diylurea is green and (*R*,*R*)-cyclohex-1,2-diylurea is pink.

Table 2 Characteristic parameters for calibration of cycHCs and linear equations of diastereomeric monomers

No.	Parameter	(all-*R*,*R*)-cycHC[8]	(all-*R*,*R*)-cycHC[6]	(all-*R*,*S*)-cycHC[6]	(*R*,*R*)-cyclohex-1,2-diylurea	(*R*,*S*)-cyclohex-1,2-diylurea
1	LoD (μg ml^{-1})	0.149 ± 0.004	0.274 ± 0.004	0.446 ± 0.003		
2	LoQ (μg ml^{-1})	0.50 ± 0.01	0.91 ± 0.01	1.49 ± 0.01		
3	Repeatability[a]	≤6%	≤5%	≤6%	≤8%	≤5%
4	R^2	0.9993	0.9979	0.9997	0.9987	0.9977
5	Equation	$y = (30.2 \pm 0.1)x + (40 \pm 10)$	$y = (19.73 \pm 0.07)x - (1 \pm 4)$	$y = (21.7 \pm 0.1)x + (13 \pm 6)$	$y = 2.33x + 2.70$	$y = 4.79x + 8.53$

[a] Determined from 12 parallels for macrocycles and 3 for monomer isomers.

Table 3 Comparison of isolated yields and yields calculated using HPLC

Macrocycle	HPLC yield ± SD[a] (%)	Isolated yield (%)
(all-*R*,*R*)-cycHC[6]	77 ± 4	68
(all-*R*,*R*)-cycHC[8]	50 ± 2	53
(all-*R*,*S*)-cycHC[6]	54 ± 4	51

[a] Standard deviation of peak areas within three parallels.

in the lower range (LoD to 80 μg ml^{-1}) was found (Fig. 6A) HC[6] calibration parameters are given in Table 4.

Screening the solution before and after heating in 0.1 M HCl showed the decomposition of HC[6] to the linear oligomers (Fig. S11, ESI†). The HPLC-MS chromatogram of the reaction mixture is shown in Fig. 7A. Depolymerisation of HC[6] was also observed at room temperature, although the rate of decay was very slow. At room temperature, the half-life of HC[6] was 3 days *versus* 3 hours when heated at 65 °C. The formation of HCs occurs in 1–4 M HCl[16] whereas in low concentrations of HCl dynamic covalent methylene bridges are broken. HC[12] degraded at 65 °C to the same oligomeric products as HC[6], though twice faster. The products formed in heated samples of HC[6] and HC[12] showed a similar pattern in ^{1}H-NMR spectra, which supports the HPLC results (Fig. S12, ESI†). A homogeneous solution of HC[6] depolymerises in a heated 0.1 M HCl solution at the rate of 1.15 ± 0.02 h^{-1}. Contrary to the almost full decomposition of dissolved HC[6] in 3 hours, in a saturated solution only a 50% decrease of HC[6] within the same time frame was observed. This is explained by the continuous dissolution of the solid HC[6] into the saturated solution, which slows down the apparent degradation rate.

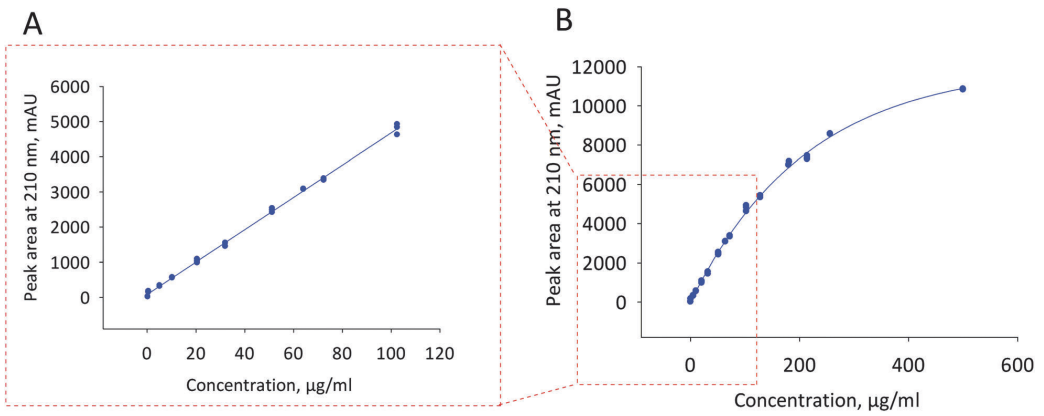

Fig. 6 Calibration graphs of HC[6]: (A) linear range from LoD to 80 μg ml^{-1} and (B) nonlinear range up to 400 μg ml^{-1}. Calibration of HC[12] was not successful.

Table 4 Characteristic parameters of calibration for two concentration ranges, HC[6], and molar absorption coefficients

	Linear range LoD to 80 μg ml^{-1}	Nonlinear range up to 400 μg ml^{-1}	Parameters from linear range	
Equation	$y = ax + b$	$y = a\cdot(1 - b^x)$	Repeatability[a]	≤9%
	$a = 46.0 \pm 0.4$	$a = (12.1 \pm 0.1) \times 10^3$	LoD (μg ml^{-1})	0.220 ± 0.004
	$b = 80 \pm 20$	$b = 0.9953 \pm 0.0001$	LoQ (μg ml^{-1})	0.73 ± 0.01
R^2	0.998	0.998	λ_{max}	197 nm

[a] 10 parallels.

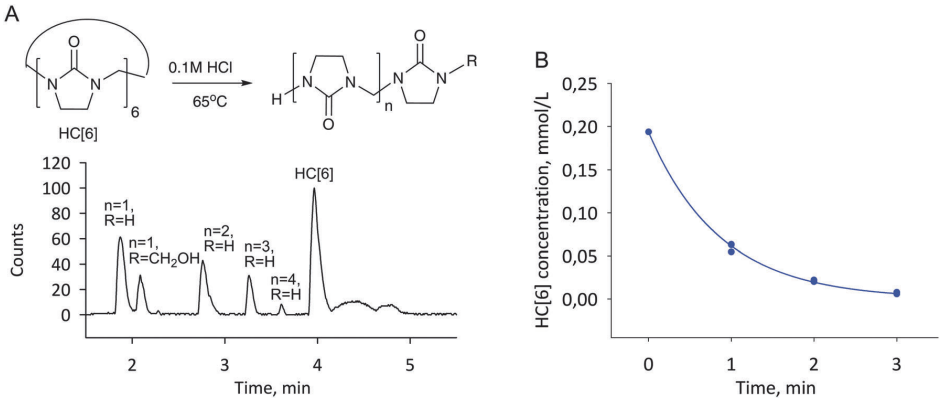

Fig. 7 (A) The HPLC-MS chromatogram of oligomers detected in the heated (3 h) HC[6] sample. (B) The degradation of HC[6] in 0.1 M HCl at 65 °C fits with the function $f = a \cdot e^{(-b \cdot x)}$ with an R^2 value of 0.9979, where a is the initial concentration (0.193 ± 0.002 mmol L^{-1}), b is the decomposition rate (1.15 ± 0.02 h^{-1}) and x is time (h).

Conclusions

The first comparative study of the quantification of hemicucurbituril homologues and isomers and their UV responses was conducted, and a quantitative RP-HPLC method for the reliable analysis of (all-*R*,*S*)-cycHC[6], (all-*R*,*R*)-cycHC[6], (all-*R*,*R*)-cycHC[8] and HC[6] was developed. The extinction coefficients of cycHC homologues could not be tied to each other through the number of repeating units. The cyclic 6-membered cycHC[6] has a 10-fold higher UV absorption compared to its 6-membered linear isomer. These differences are accounted for by the rigid geometries of hemicucurbiturils. The possibility of a drastic difference in the ultraviolet absorbance of linear and cyclic oligomeric analogues may also occur in other classes of macrocycles. For accurate quantitative analysis it is therefore necessary to calibrate the UV response of each cyclic homologue independently. Such method was successfully used in this study for the estimation of the yields of the cycHCs from reaction mixtures and to follow the degradation of unsubstituted HCs in acidic media. The correlation of UV absorbance of HC[6] was linear in a smaller concentration range, compared to cycHC macrocycles. It was confirmed that unsubstituted HCs that are dissolved in an aqueous acidic environment depolymerise to linear oligomers, although HCs in the solid phase are resistant to hydrolysis, and therefore it is proposed that HCs can be used as heterogeneous catalysts even at elevated temperatures in acidic media. The presented results uncover the possibilities of UV-detection of HCs and their oligomeric isomers and will support the development of synthesis of new isomers and their application.

Acknowledgements

The authors thank Dr. Victor Borovkov and Dr. Mohhamed Hasan from Tallinn University of Technology for assistance in UV measurements and bachelor students Karin Kreekman and Anastassia Baškir for performing cycHC synthesis reactions. This research was supported by the Estonian Ministry of Education and Research through Grants IUT23-7 and PUT692, TUT grant no. B25, and the EU European Regional Development Fund projects 3.2.0101.08-0017 and TK134. and EU FP7 for research, technological development and demonstration under grant agreement no. 621364 (TUTIC-Green) and "National Natural Science Foundation of China (NO. 21662007), Natural Science Foundation of Guizhou Province (No. [2016]1031), the Project of Talent Introduction of Guizhou University (NO. (2014)24)."

References

1 W. Freeman, W. L. Mock and N.-Y. Y. Shih, *J. Am. Chem. Soc.*, 1981, **103**(24), 7367–7368.
2 Y. Miyahara, K. Goto, M. Oka and T. Inazu, *Angew. Chem., Int. Ed.*, 2004, **43**(38), 5019–5022.
3 H.-J. Buschmann, E. Cleve and E. Schollmeyer, *Inorg. Chem. Commun.*, 2005, **8**, 125–127.
4 Y. Li, L. Li, Y. Zhu, X. Meng and A. Wu, *Cryst. Growth Des.*, 2009, **9**(10), 4255–4257.
5 J. Svec, M. Necas and V. Sindelar, *Angew. Chem., Int. Ed.*, 2010, **49**(13), 2378–2381.
6 V. Havel, J. Svec, M. Wimmerova, M. Dusek, M. Pojarova and V. Sindelar, *Org. Lett.*, 2011, **13**(15), 4000–4003.
7 J. Rivollier, P. Thuéry and M. P. Heck, *Org. Lett.*, 2013, **15**(3), 480–483.
8 R. Aav, E. Shmatova, I. Reile, M. Borissova, F. Topi and K. Rissanen, *Org. Lett.*, 2013, **15**(14), 3786–3789.
9 M. Fomitšenko, E. Shmatova, M. Öeren, I. Järving and R. Aav, *Supramol. Chem.*, 2014, **26**(9), 698–703.
10 E. Prigorchenko, M. Öeren, S. Kaabel, M. Fomitšenko, I. Reile, I. Järving, T. Tamm, F. Topić, K. Rissanen and R. Aav, *Chem. Commun.*, 2015, **51**(54), 10921–10924.
11 M. Lisbjerg, B. M. Jessen, B. Rasmussen, B. E. Nielsen, A. Ø. Madsen and M. Pittelkow, *Chem. Sci.*, 2014, **5**(7), 2647–2650.

12 M. Singh, E. Solel, E. Keinan and O. Reany, *Chem. – Eur. J.*, 2015, **21**(2), 536–540.
13 S. Kaabel, J. Adamson, F. Topić, A. Kiesilä, E. Kalenius, M. Öeren, M. Reimund, E. Prigorchenko, A. Lõokene, H. J. Reich, K. Rissanen and R. Aav, *Chem. Sci.*, 2017, DOI: 10.1039/C6SC05058A.
14 M. Lisbjerg, H. Valkenier, B. M. Jessen, H. Al-Kerdi, A. P. Davis and M. Pittelkow, *J. Am. Chem. Soc.*, 2015, **137**(15), 4948–4951.
15 E. I. Cucolea, H.-J. Buschmann and L. Mutihac, *Supramol. Chem.*, 2016, **28**(9–10), 727–732.
16 H. Cong, J. Yu, T. Yamato and Z. Tao, *3rd International Conference on Cucurbiturils*, Program and Abstract Book, 2013, p. 19.
17 H. Cong, T. Yamato, X. Feng and Z. Tao, *J. Mol. Catal. A: Chem.*, 2012, **365**, 181–185.
18 H. Cong, T. Yamato and Z. Tao, *New J. Chem.*, 2013, **37**(11), 3778–3783.
19 H. Cong, T. Yamato and Z. Tao, *J. Mol. Catal. A: Chem.*, 2013, **379**, 287–293.
20 X.-J. Cheng, L.-L. Liang, K. Chen, N.-N. Ji, X. Xiao, J.-X. Zhang, Y.-Q. Zhang, S.-F. Xue, Q.-J. Zhu, X.-L. Ni and Z. Tao, *Angew. Chem., Int. Ed.*, 2013, **52**(28), 7252–7255.
21 M. M. Ayhan, H. Karoui, M. Hardy, A. Rockenbauer, L. Charles, R. Rosas, K. Udachin, P. Tordo, D. Bardelang and O. Ouari, *J. Am. Chem. Soc.*, 2015, **137**(32), 10238–10245.
22 M. M. Ayhan, H. Karoui, M. Hardy, A. Rockenbauer, L. Charles, R. Rosas, K. Udachin, P. Tordo, D. Bardelang and O. Ouari, *J. Am. Chem. Soc.*, 2016, **138**(6), 2060.
23 I. W. Wyman and D. H. Macartney, *Org. Biomol. Chem.*, 2010, **8**(1), 247–252.
24 J. M. Chinai, A. B. Taylor, L. M. Ryno, N. D. Hargreaves, C. A. Morris, P. J. Hart and A. R. Urbach, *J. Am. Chem. Soc.*, 2011, **133**(23), 8810–8813.
25 G. Y. Tonga, Y. Jeong, B. Duncan, T. Mizuhara, R. Mout, R. Das, S. T. Kim, Y.-C. Yeh, B. Yan, S. Hou and V. M. Rotello, *Nat. Chem.*, 2015, **7**(7), 597–603.
26 Y. Huang, S. F. Xue, Q. J. Zhu and T. Zhu, *Supramol. Chem.*, 2008, **20**(3), 279–287.
27 X. X. Zhang, K. E. Krakowiak, G. P. Xue, J. S. Bradshaw and R. M. Izatt, *Ind. Eng. Chem. Res.*, 2000, **39**(10), 3516–3520.
28 V. Lewin, J. Rivollier, S. Coudert, D. A. Buisson, D. Baumann, B. Rousseau, F. X. Legrand, H. Kouřilová, P. Berthault, J. P. Dognon, M. P. Heck and G. Huber, *Eur. J. Org. Chem.*, 2013, (18), 3857–3865.
29 Á. L. Fuentes De Arriba, D. G. Seisdedos, L. Simón, V. Alcázar, C. Raposo and J. R. Morán, *J. Org. Chem.*, 2010, **75**(23), 8303–8306.
30 S. C. Gill and P. H. von Hippel, *Anal. Biochem.*, 1989, **182**(2), 319–326.
31 F. Codari, D. Moscatelli, G. Storti and M. Morbidelli, *Macromol. Mater. Eng.*, 2010, **295**(1), 58–66.

ACKNOWLEDGEMENTS

This research was carried out in the Department of Chemistry, recently renamed the Department of Chemistry and Biotechnology, at Tallinn University of Technology.
I would like to express my gratitude to all of the people connected with this work or who somehow affected me during my PhD study.
Firstly, I will be forever thankful to my supervisor Riina Aav, who saw potential in me when we first met, took me into her group and helped me to become a stronger person. I am also really thankful for the opportunity to teach, which took up almost half of my time. So, thank you, Riina, for everything, for teaching me and giving me critical feedback and believing in me through all these years.
Secondly, I want to thank all of my lab-mates from the fourth floor: Elena, Madli, Anna, Nastja, Sandra, Karin, Oliver, Kamini, Mario and Nele, our cucurbituril research group, who made me feel important and gave me a sense of belonging. Thank you for letting me be a part of the group.
I want to also express my gratitude to some people who really helped me with my work by sharing their professional experience: Marina Kudrašova for helping me with NMR experiments, and Ivar Järving, who showed me how to use and interpret mass spectrometric data, Mohhamed Hasan, who helped with the UV analysis, and Victor Borovkov, for the very helpful consultation on spectrometry.
I want also thank my 3rd floor younger lab-mates – Heidi Lees, Piia Jõul, Tiina Aid and Piret Saar-Reismaa for your friendship and time during our master's and PhD studies.
I am also grateful to colleagues from the Chair of Analytical Chemistry, Jelena Gorbatšova, Maria Kuhtinskaja, Merike Vaher, Aini Vaarmann, Mihkel Kaljurand and Mihkel Koel, my supervisors Anne Orav and Maria Kulp for creating great memories and experiences during my bachelor's and master's studies and for giving me professional knowledge and educational interest in the field of analytical chemistry.
I want to thank all of the financial supporters, including the Estonian Science Foundation, the Ministry of Education and Research, Tallinn University of Technology and the EU European Regional Development Fund. Part of the work was also supported by ASTRA "TUT Institutional Development Programme for 2016-2022" Graduate school of functional materials and technologies (2014-2020.4.01.16-0032), and Dora's activities are also acknowledged.

ABSTRACT

Host-guest chemistry as a part of supramolecular chemistry is an attractive field since it offers potential opportunities to develop different types of molecular systems which can be controlled by external stimuli and is held together by non-covalent interactions. This makes possible the design of host molecules which can mimic biological systems, and moreover they can be selective and tunable. The study of these systems will lead to a better understanding of involved reactions, which will lead to improved specificity and better treatment for illnesses.

Cucurbiturils (CBs) are host molecules that have a wide range of applications, through complexation with cationic guests. Hemicucurbiturils (HC), to the contrary, have a preference for binding negatively charges species. Anion sensing is important in biological processes, but it is more difficult to achieve. Fortunately HCs have shown promising results in that field owing to the strongest bindings for some anions both in water and in organic solvents at this time.

The development of new approaches for the analysis of HCs was the main goal of this thesis. During this study, the formation of the first 8-membered HC occurred. A RP-HPLC protocol for the quantitative analysis of 6- and 8-membered (*R,R*)-cycHC homologues and 6-membered isomers ((*R,R*)-, (*R,S*)- and inverted-(*R,S*)-cycHC[6]) was developed. The UV signal at 210 nm was calibrated against the concentrations of the compounds and the developed technique was applied to follow the reaction rates and quantify the yields of the HCs routinely, making it possible to also optimize reaction conditions on a small scale. The calibration procedure of the cycHC macrocycles revealed disproportionality between UV absorbance and the number of chromophoric units. The UV-analysis of cycHC macrocycles and their linear oligomers showed that the extinction coefficient of the latter is about one order of magnitude lower than macrocycle coefficients. This is an important observation, as in the majority of polymers the signal is assumed to be proportional to the number of chromophoric units.

RP-HPLC-HRMS analysis of the mixture of the dynamic combinatorial library members was essential for revealing the mechanism of the reversible macrocyclisation of cycHCs.

Unsubstituted HC[6] and HC[12] were analyzed with the RP-HPLC and their behavior in acidified media was examined in order to study the reversibility of their formation. In the presence of hydrochloric acid, the degradation of HC[6] and HC[12] to open-chain oligomers was noted.

This is the first comprehensive study on the chromatographic analysis of HCs and contributes significantly to the development of new host molecules.

KOKKUVÕTE

Võõrustaja-külaline komplekside keemia, mis hõlmab suure osa supramolekulaarsest keemiast, on aktuaalne ja atraktiivne valdkond, kuna see pakub laialdasi võimalusi disainida molekulaarseid süsteeme, mis on seotud läbi mitte-kovalentsete interaktsioonide ja seetõttu lihtsasti kontrollitavad väliste stiimulite abil. Seetõttu saab võimalikuks selliste võõrustaja molekulide disain, mis suudavad jäljendada bioloogilisi protsesse ning on samas ka kontrollitavad ja timmitavad. Uuringud selles valdkonnas aitavad kaasa selektiivsemate protsesside mõistmisele, et parendada näiteks teatud haiguste ravi tulevikus.

Kukurbituriilid (CB) on võõrustaja molekulid, mis on leidnud väga laialdast kasutust erinevates valdkondades. CB-de rakendus põhineb võimel siduda katioonseid külalismolekule. Hemikukurbituriilid (HC) seovad see eest eelistatult anioone. Anioonide poolt reguleeritud protsessid meie kehas on sama tähtsad, kuid võrreldes katioonidega on nende selektiivne komplekseerimine oluliselt keerulisem. Hetkel kuulub anioonide sidumiskonstandi rekord just asendatud HC-dele nii vees kui ka orgaanilistes lahustes.

Antud töö eesmärk oli välja töötada uued lahendused HC-de analüüsiks. Selle töö raames tuvastati esimest korda 8-ühikulise cycHC teke. Töötati välja HPLC tingimused järgnevatele tsükloheksano-asendatud hemikukurbituriilide kvantitatiivseks analüüsiks: 6- ja 8-liikmelised (*R,R*)-cycHC homoloogid ja 6-liikmelised isomeerid ((*R,R*)-, (*R,S*)- ja pööratud-(*R,S*)-cycHC[6]). Näidati et väljatöötatud meetodit saab rakendada reaktsioonide kineetika ja produktide saagiste määramisel. Seda meetodit kasutatakse rutiinselt ja see võimaldab optimeerida reaktsioonitingimusi väikestemahulistes sünteesides. Antud makrotsüklite ja nende avatud ahelaga oligomeeride analüüsi käigus täheldati, et korrelatsioon kromofooride hulga ja UV absorbtsiooni vahel ei ole proportsionaalne. UV-analüüs makrotsüklite ja avatud ahelaga oligomeeridest näitas, et viimaste molaarne neeldumiskoefitsient on ligilaudu ühe suurusjärgu võrra madalam kui makrotsüklite neeldumiskoefitsiendid. Leitud nähtus on oluline, sest üldiselt eeldatakse polümeeridekeemias UV neeldumise proportsionaalsust korduvate ühikute arvuga.

(*R,R*)-cycHC pöörduva makrotsükliseerumise mehhanism tõestati dünaamiliste vaheühendite indentifitseerimisega RP-HPLC-HRMS analüüsil.

Töötati välja asendamata hemikukurbituriilide HC[6] and HC[12] kromatograafiline analüüs ja uuriti nende stabiilsust happelistes tingimustes.

Käesolev töö on esimene nii laiaulatuslik uurimus hemikukurbituriilide kromatograafilise analüüsi valdkonnas, mis rikastab makrotsükliliste võõrustaja-molekulide uurimise valdkonda.

ORIGINAL PUBLICATIONS

Kobrin, E-G.; Lees, H.; Fomitšenko, M.; Kubáň, P.; Kaljurand, M. Fingerprinting postblast explosive residues by portable capillary electrophoresis with contactless conductivity detection. *Electrophoresis*, **2014**, 35 (8), 1165−1172.

Fomitšenko, M.; Shmatova, E.; Öeren, M.; Järving, I.; Aav, R. New homologues of chiral cyclohexylhemicucurbit[n]urils. *Supramolecular Chemistry*, **2014**, 26 (9), 698−703.

Prigorchenko, E.; Öeren, M.; Kaabel, S.; Fomitšenko, M.; Reile, I.; Järving, I.; Tamm, T.; Topic, F.; Rissanen, K.; Aav, R. Template-controlled synthesis of chiral cyclohexylhemicucurbit[8]uril. *Chemical Communications*, **2015**, 51 (54), 10921−10924.

Aav, R.; Kaabel, S.; Fomitšenko, M. Cucurbiturils: Synthesis, Structures, Formation Mechanisms, and Nomenclature. Comprehensive Supramolecular Chemistry II, **2017**, 3, 203−220.

Fomitšenko, M.; Peterson, A.; Reile, I.; Cong, H.; Kaabel, K.; Prigorchenko, E.; Järving I.; Aav R. A quantitative method for analysis of mixtures of homologues and stereoisomers of hemicucurbiturils that allows us to follow their formation and stability. *New Journal of Chemistry*, **2017**, 41, 2490-2497.

CURRICULUM VITAE

Personal Data

Name	Maria Fomitšenko
Date an place of birth	26.07.1989, Tallinn
Sitizenship	estonian
Email address	maria.fomitsenko@ttu.ee

Education

Tallinn University of Technology	2013	Applied Chemistry and Biotechnology / M.Sc.
Tallinn University of Technology	2011	Applied Chemistry and Biotechnology / B.Sc.
Avinurme Secondary School	2008	Secondary education

Language commpetence

Estonian	Native
Russian	Fluent
English	Fluent

Special Courses

2013-2014	Graduate School „ Functional materials and technologies“
2013-2014	Online course „Estimation of Measurement Uncertainty in Chemical Analysis“
2016-2017	Graduate School „ Functional materials and technologies“

Proffessional employment

01.01.2014-31.12.2014.	Tallinn University of Technology, young researcher
01.01.2015-31.05.2015.	Tallinn University of Technology, young researcher
01.09.2015-31.12.2015.	Tallinn University of Technology, teaching in the field of analytical chemistry

Research activity

Bachelor's thesis was done in 2011 on the GC Analysis of essential oils in parsley, supervisor Anne Orav, TUT, Chair of Analytical Chemistry.

Participation in Project of Ministry of Defence, Analysis of postblast explosive residues by portable capillary electrophoresis in 2014 at TUT, Chair of Analytical Chemistry.

Master's thesis was done in 2013, supervisor Maria Kulp, Determination of adenylate energy charge (AEC) in normal and cancer cells by different analytical methods, TUT, Chair of Analytical Chemistry.

The main are in the PhD study (2013-2017) was analysis of cucurbiturils and their host-guest complexes of in TUT, Chair of Organic Chemistry.

ELULOOKIRJELDUS

Isikuandmed

Nimi	Maria Fomitšenko
Sünniaeg ja –koht	26.07.1989, Tallinn
Kodakondsus	eesti
E-posti aadress	maria.fomitsenko@ttu.ee

Haridus

Tallinna Tehnikaülikool	2013	Rakenduskeemia ja Biotehnoloogia /M.Sc.
Tallinna Tehnikaülikool	2011	Rakenduskeemia ja Biotehnoloogia /B.Sc.
Avinurme Keskkool	2008	Keskharidus

Keelteoskus

Eesti keel	Emakeel
Vene keel	Kõrgtase
Inglise keel	Kõrgtase

Täiendusõpe

2013-2014	Funktsionaalsete materjalide ja tehnoloogiate doktorikool
2013-2014	E-kursus „Keemilise analüüsi mõõtemääramatuse hindamine“
2016-2017	Funktsionaalsete materjalide ja tehnoloogiate doktorikool

Teenistuskäik

01.01.2014-31.12.2014.	Tallinn Tehnikaülikool, nooremteadur
01.01.2015-31.05.2015.	Tallinn Tehnikaülikool, nooremteadur
01.09.2015-31.12.2015.	Tallinn Tehnikaülikool, õpetamine

Teadustegevus

Bakalaureuse töö oli sooritatud 2011 aastal teemal „Eeterlike õlide gaasikromatograafiline analüüs petersellis Anne Orava juhendamise all TTÜ-s Analüütilise keema õppetoolis.

Kaitseministeeriumi projektis osalemine, kus põhiülesandeks oli plahvatusjärgsete jälgede analüüs portatiivse kapillarelektroforeesi masinaga. Aasta 2014, TTÜ, Analüütilise keema õppetool.

Magistrikraad, aasta 2013, Adenülaatse energeetilise taseme määramine normaalsetes ning vähirakkudes erinevate lahutusmeetoditega, juhendaja Maria Kulp, TTÜ, Analüütilise keema õppetool.

Põhiline uurimisvaldkond doktoriõppes (2013-2017) oli kukurbituriilide ja nende võõrustaja-külalise kompleksite analüüs, TTÜ, Orgaanilise keema õppetool.

DISSERTATIONS DEFENDED AT TALLINN UNIVERSITY OF TECHNOLOGY ON *NATURAL AND EXACT SCIENCES*

1. **Olav Kongas**. Nonlinear Dynamics in Modeling Cardiac Arrhytmias. 1998.
2. **Kalju Vanatalu**. Optimization of Processes of Microbial Biosynthesis of Isotopically Labeled Biomolecules and Their Complexes. 1999.
3. **Ahto Buldas**. An Algebraic Approach to the Structure of Graphs. 1999.
4. **Monika Drews**. A Metabolic Study of Insect Cells in Batch and Continuous Culture: Application of Chemostat and Turbidostat to the Production of Recombinant Proteins. 1999.
5. **Eola Valdre**. Endothelial-Specific Regulation of Vessel Formation: Role of Receptor Tyrosine Kinases. 2000.
6. **Kalju Lott**. Doping and Defect Thermodynamic Equilibrium in ZnS. 2000.
7. **Reet Koljak**. Novel Fatty Acid Dioxygenases from the Corals *Plexaura homomalla* and *Gersemia fruticosa.* 2001.
8. **Anne Paju**. Asymmetric oxidation of Prochiral and Racemic Ketones by Using Sharpless Catalyst. 2001.
9. **Marko Vendelin**. Cardiac Mechanoenergetics *in silico*. 2001.
10. **Pearu Peterson**. Multi-Soliton Interactions and the Inverse Problem of Wave Crest. 2001.
11. **Anne Menert**. Microcalorimetry of Anaerobic Digestion. 2001.
12. **Toomas Tiivel**. The Role of the Mitochondrial Outer Membrane in *in vivo* Regulation of Respiration in Normal Heart and Skeletal Muscle Cell. 2002.
13. **Olle Hints**. Ordovician Scolecodonts of Estonia and Neighbouring Areas: Taxonomy, Distribution, Palaeoecology, and Application. 2002.
14. **Jaak Nõlvak**. Chitinozoan Biostratigrapy in the Ordovician of Baltoscandia. 2002.
15. **Liivi Kluge**. On Algebraic Structure of Pre-Operad. 2002.
16. **Jaanus Lass**. Biosignal Interpretation: Study of Cardiac Arrhytmias and Electromagnetic Field Effects on Human Nervous System. 2002.
17. **Janek Peterson**. Synthesis, Structural Characterization and Modification of PAMAM Dendrimers. 2002.
18. **Merike Vaher**. Room Temperature Ionic Liquids as Background Electrolyte Additives in Capillary Electrophoresis. 2002.
19. **Valdek Mikli**. Electron Microscopy and Image Analysis Study of Powdered Hardmetal Materials and Optoelectronic Thin Films. 2003.
20. **Mart Viljus**. The Microstructure and Properties of Fine-Grained Cermets. 2003.
21. **Signe Kask**. Identification and Characterization of Dairy-Related *Lactobacillus.* 2003.
22. **Tiiu-Mai Laht**. Influence of Microstructure of the Curd on Enzymatic and Microbiological Processes in Swiss-Type Cheese. 2003.

23. **Anne Kuusksalu**. 2–5A Synthetase in the Marine Sponge *Geodia cydonium*. 2003.
24. **Sergei Bereznev**. Solar Cells Based on Polycristalline Copper-Indium Chalcogenides and Conductive Polymers. 2003.
25. **Kadri Kriis**. Asymmetric Synthesis of C_2-Symmetric Bimorpholines and Their Application as Chiral Ligands in the Transfer Hydrogenation of Aromatic Ketones. 2004.
26. **Jekaterina Reut**. Polypyrrole Coatings on Conducting and Insulating Substracts. 2004.
27. **Sven Nõmm**. Realization and Identification of Discrete-Time Nonlinear Systems. 2004.
28. **Olga Kijatkina**. Deposition of Copper Indium Disulphide Films by Chemical Spray Pyrolysis. 2004.
29. **Gert Tamberg**. On Sampling Operators Defined by Rogosinski, Hann and Blackman Windows. 2004.
30. **Monika Übner**. Interaction of Humic Substances with Metal Cations. 2004.
31. **Kaarel Adamberg**. Growth Characteristics of Non-Starter Lactic Acid Bacteria from Cheese. 2004.
32. **Imre Vallikivi**. Lipase-Catalysed Reactions of Prostaglandins. 2004.
33. **Merike Peld**. Substituted Apatites as Sorbents for Heavy Metals. 2005.
34. **Vitali Syritski**. Study of Synthesis and Redox Switching of Polypyrrole and Poly(3,4-ethylenedioxythiophene) by Using *in-situ* Techniques. 2004.
35. **Lee Põllumaa**. Evaluation of Ecotoxicological Effects Related to Oil Shale Industry. 2004.
36. **Riina Aav**. Synthesis of 9,11-Secosterols Intermediates. 2005.
37. **Andres Braunbrück**. Wave Interaction in Weakly Inhomogeneous Materials. 2005.
38. **Robert Kitt**. Generalised Scale-Invariance in Financial Time Series. 2005.
39. **Juss Pavelson**. Mesoscale Physical Processes and the Related Impact on the Summer Nutrient Fields and Phytoplankton Blooms in the Western Gulf of Finland. 2005.
40. **Olari Ilison**. Solitons and Solitary Waves in Media with Higher Order Dispersive and Nonlinear Effects. 2005.
41. **Maksim Säkki**. Intermittency and Long-Range Structurization of Heart Rate. 2005.
42. **Enli Kiipli**. Modelling Seawater Chemistry of the East Baltic Basin in the Late Ordovician–Early Silurian. 2005.
43. **Igor Golovtsov**. Modification of Conductive Properties and Processability of Polyparaphenylene, Polypyrrole and polyaniline. 2005.
44. **Katrin Laos**. Interaction Between Furcellaran and the Globular Proteins (Bovine Serum Albumin β-Lactoglobulin). 2005.
45. **Arvo Mere**. Structural and Electrical Properties of Spray Deposited Copper Indium Disulphide Films for Solar Cells. 2006.

46. **Sille Ehala**. Development and Application of Various On- and Off-Line Analytical Methods for the Analysis of Bioactive Compounds. 2006.
47. **Maria Kulp**. Capillary Electrophoretic Monitoring of Biochemical Reaction Kinetics. 2006.
48. **Anu Aaspõllu.** Proteinases from *Vipera lebetina* Snake Venom Affecting Hemostasis. 2006.
49. **Lyudmila Chekulayeva**. Photosensitized Inactivation of Tumor Cells by Porphyrins and Chlorins. 2006.
50. **Merle Uudsemaa**. Quantum-Chemical Modeling of Solvated First Row Transition Metal Ions. 2006.
51. **Tagli Pitsi**. Nutrition Situation of Pre-School Children in Estonia from 1995 to 2004. 2006.
52. **Angela Ivask**. Luminescent Recombinant Sensor Bacteria for the Analysis of Bioavailable Heavy Metals. 2006.
53. **Tiina Lõugas**. Study on Physico-Chemical Properties and Some Bioactive Compounds of Sea Buckthorn (*Hippophae rhamnoides* L.). 2006.
54. **Kaja Kasemets**. Effect of Changing Environmental Conditions on the Fermentative Growth of *Saccharomyces cerevisae* S288C: Auxo-accelerostat Study. 2006.
55. **Ildar Nisamedtinov**. Application of ^{13}C and Fluorescence Labeling in Metabolic Studies of *Saccharomyces* spp. 2006.
56. **Alar Leibak**. On Additive Generalisation of Voronoï's Theory of Perfect Forms over Algebraic Number Fields. 2006.
57. **Andri Jagomägi**. Photoluminescence of Chalcopyrite Tellurides. 2006.
58. **Tõnu Martma**. Application of Carbon Isotopes to the Study of the Ordovician and Silurian of the Baltic. 2006.
59. **Marit Kauk**. Chemical Composition of $CuInSe_2$ Monograin Powders for Solar Cell Application. 2006.
60. **Julia Kois**. Electrochemical Deposition of $CuInSe_2$ Thin Films for Photovoltaic Applications. 2006.
61. **Ilona Oja Açik**. Sol-Gel Deposition of Titanium Dioxide Films. 2007.
62. **Tiia Anmann**. Integrated and Organized Cellular Bioenergetic Systems in Heart and Brain. 2007.
63. **Katrin Trummal**. Purification, Characterization and Specificity Studies of Metalloproteinases from *Vipera lebetina* Snake Venom. 2007.
64. **Gennadi Lessin**. Biochemical Definition of Coastal Zone Using Numerical Modeling and Measurement Data. 2007.
65. **Enno Pais**. Inverse problems to determine non-homogeneous degenerate memory kernels in heat flow. 2007.
66. **Maria Borissova**. Capillary Electrophoresis on Alkylimidazolium Salts. 2007.
67. **Karin Valmsen**. Prostaglandin Synthesis in the Coral *Plexaura homomalla*: Control of Prostaglandin Stereochemistry at Carbon 15 by Cyclooxygenases. 2007.

68. **Kristjan Piirimäe**. Long-Term Changes of Nutrient Fluxes in the Drainage Basin of the Gulf of Finland – Application of the PolFlow Model. 2007.
69. **Tatjana Dedova**. Chemical Spray Pyrolysis Deposition of Zinc Sulfide Thin Films and Zinc Oxide Nanostructured Layers. 2007.
70. **Katrin Tomson**. Production of Labelled Recombinant Proteins in Fed-Batch Systems in *Escherichia coli*. 2007.
71. **Cecilia Sarmiento**. Suppressors of RNA Silencing in Plants. 2008.
72. **Vilja Mardla**. Inhibition of Platelet Aggregation with Combination of Antiplatelet Agents. 2008.
73. **Maie Bachmann**. Effect of Modulated Microwave Radiation on Human Resting Electroencephalographic Signal. 2008.
74. **Dan Hüvonen**. Terahertz Spectroscopy of Low-Dimensional Spin Systems. 2008.
75. **Ly Villo**. Stereoselective Chemoenzymatic Synthesis of Deoxy Sugar Esters Involving *Candida antarctica* Lipase B. 2008.
76. **Johan Anton**. Technology of Integrated Photoelasticity for Residual Stress Measurement in Glass Articles of Axisymmetric Shape. 2008.
77. **Olga Volobujeva**. SEM Study of Selenization of Different Thin Metallic Films. 2008.
78. **Artur Jõgi**. Synthesis of 4'-Substituted 2,3'-dideoxynucleoside Analogues. 2008.
79. **Mario Kadastik**. Doubly Charged Higgs Boson Decays and Implications on Neutrino Physics. 2008.
80. **Fernando Pérez-Caballero**. Carbon Aerogels from 5-Methylresorcinol-Formaldehyde Gels. 2008.
81. **Sirje Vaask**. The Comparability, Reproducibility and Validity of Estonian Food Consumption Surveys. 2008.
82. **Anna Menaker**. Electrosynthesized Conducting Polymers, Polypyrrole and Poly(3,4-ethylenedioxythiophene), for Molecular Imprinting. 2009.
83. **Lauri Ilison**. Solitons and Solitary Waves in Hierarchical Korteweg-de Vries Type Systems. 2009.
84. **Kaia Ernits**. Study of In_2S_3 and ZnS Thin Films Deposited by Ultrasonic Spray Pyrolysis and Chemical Deposition. 2009.
85. **Veljo Sinivee**. Portable Spectrometer for Ionizing Radiation "Gammamapper". 2009.
86. **Jüri Virkepu**. On Lagrange Formalism for Lie Theory and Operadic Harmonic Oscillator in Low Dimensions. 2009.
87. **Marko Piirsoo**. Deciphering Molecular Basis of Schwann Cell Development. 2009.
88. **Kati Helmja**. Determination of Phenolic Compounds and Their Antioxidative Capability in Plant Extracts. 2010.
89. **Merike Sõmera**. Sobemoviruses: Genomic Organization, Potential for Recombination and Necessity of P1 in Systemic Infection. 2010.

90. **Kristjan Laes**. Preparation and Impedance Spectroscopy of Hybrid Structures Based on $CuIn_3Se_5$ Photoabsorber. 2010.
91. **Kristin Lippur**. Asymmetric Synthesis of 2,2'-Bimorpholine and its 5,5'-Substituted Derivatives. 2010.
92. **Merike Luman**. Dialysis Dose and Nutrition Assessment by an Optical Method. 2010.
93. **Mihhail Berezovski**. Numerical Simulation of Wave Propagation in Heterogeneous and Microstructured Materials. 2010.
94. **Tamara Aid-Pavlidis**. Structure and Regulation of BDNF Gene. 2010.
95. **Olga Bragina**. The Role of Sonic Hedgehog Pathway in Neuro- and Tumorigenesis. 2010.
96. **Merle Randrüüt**. Wave Propagation in Microstructured Solids: Solitary and Periodic Waves. 2010.
97. **Marju Laars**. Asymmetric Organocatalytic Michael and Aldol Reactions Mediated by Cyclic Amines. 2010.
98. **Maarja Grossberg**. Optical Properties of Multinary Semiconductor Compounds for Photovoltaic Applications. 2010.
99. **Alla Maloverjan**. Vertebrate Homologues of Drosophila Fused Kinase and Their Role in Sonic Hedgehog Signalling Pathway. 2010.
100. **Priit Pruunsild**. Neuronal Activity-Dependent Transcription Factors and Regulation of Human *BDNF* Gene. 2010.
101. **Tatjana Knjazeva**. New Approaches in Capillary Electrophoresis for Separation and Study of Proteins. 2011.
102. **Atanas Katerski**. Chemical Composition of Sprayed Copper Indium Disulfide Films for Nanostructured Solar Cells. 2011.
103. **Kristi Timmo.** Formation of Properties of $CuInSe_2$ and $Cu_2ZnSn(S,Se)_4$ Monograin Powders Synthesized in Molten KI. 2011.
104. **Kert Tamm**. Wave Propagation and Interaction in Mindlin-Type Microstructured Solids: Numerical Simulation. 2011.
105. **Adrian Popp**. Ordovician Proetid Trilobites in Baltoscandia and Germany. 2011.
106. **Ove Pärn**. Sea Ice Deformation Events in the Gulf of Finland and This Impact on Shipping. 2011.
107. **Germo Väli**. Numerical Experiments on Matter Transport in the Baltic Sea. 2011.
108. **Andrus Seiman**. Point-of-Care Analyser Based on Capillary Electrophoresis. 2011.
109. **Olga Katargina**. Tick-Borne Pathogens Circulating in Estonia (Tick-Borne Encephalitis Virus, *Anaplasma phagocytophilum*, *Babesia* Species): Their Prevalence and Genetic Characterization. 2011.
110. **Ingrid Sumeri**. The Study of Probiotic Bacteria in Human Gastrointestinal Tract Simulator. 2011.
111. **Kairit Zovo**. Functional Characterization of Cellular Copper Proteome. 2011.

112. **Natalja Makarytsheva**. Analysis of Organic Species in Sediments and Soil by High Performance Separation Methods. 2011.
113. **Monika Mortimer**. Evaluation of the Biological Effects of Engineered Nanoparticles on Unicellular Pro- and Eukaryotic Organisms. 2011.
114. **Kersti Tepp**. Molecular System Bioenergetics of Cardiac Cells: Quantitative Analysis of Structure-Function Relationship. 2011.
115. **Anna-Liisa Peikolainen**. Organic Aerogels Based on 5-Methylresorcinol. 2011.
116. **Leeli Amon**. Palaeoecological Reconstruction of Late-Glacial Vegetation Dynamics in Eastern Baltic Area: A View Based on Plant Macrofossil Analysis. 2011.
117. **Tanel Peets**. Dispersion Analysis of Wave Motion in Microstructured Solids. 2011.
118. **Liina Kaupmees**. Selenization of Molybdenum as Contact Material in Solar Cells. 2011.
119. **Allan Olspert**. Properties of VPg and Coat Protein of Sobemoviruses. 2011.
120. **Kadri Koppel**. Food Category Appraisal Using Sensory Methods. 2011.
121. **Jelena Gorbatšova**. Development of Methods for CE Analysis of Plant Phenolics and Vitamins. 2011.
122. **Karin Viipsi**. Impact of EDTA and Humic Substances on the Removal of Cd and Zn from Aqueous Solutions by Apatite. 2012.
123. **David Schryer**. Metabolic Flux Analysis of Compartmentalized Systems Using Dynamic Isotopologue Modeling. 2012.
124. **Ardo Illaste**. Analysis of Molecular Movements in Cardiac Myocytes. 2012.
125. **Indrek Reile**. 3-Alkylcyclopentane-1,2-Diones in Asymmetric Oxidation and Alkylation Reactions. 2012.
126. **Tatjana Tamberg**. Some Classes of Finite 2-Groups and Their Endomorphism Semigroups. 2012.
127. **Taavi Liblik**. Variability of Thermohaline Structure in the Gulf of Finland in Summer. 2012.
128. **Priidik Lagemaa**. Operational Forecasting in Estonian Marine Waters. 2012.
129. **Andrei Errapart**. Photoelastic Tomography in Linear and Non-linear Approximation. 2012.
130. **Külliki Krabbi**. Biochemical Diagnosis of Classical Galactosemia and Mucopolysaccharidoses in Estonia. 2012.
131. **Kristel Kaseleht**. Identification of Aroma Compounds in Food using SPME-GC/MS and GC-Olfactometry. 2012.
132. **Kristel Kodar**. Immunoglobulin G Glycosylation Profiling in Patients with Gastric Cancer. 2012.
133. **Kai Rosin**. Solar Radiation and Wind as Agents of the Formation of the Radiation Regime in Water Bodies. 2012.

134. **Ann Tiiman**. Interactions of Alzheimer's Amyloid-Beta Peptides with Zn(II) and Cu(II) Ions. 2012.
135. **Olga Gavrilova**. Application and Elaboration of Accounting Approaches for Sustainable Development. 2012.
136. **Olesja Bondarenko**. Development of Bacterial Biosensors and Human Stem Cell-Based *In Vitro* Assays for the Toxicological Profiling of Synthetic Nanoparticles. 2012.
137. **Katri Muska**. Study of Composition and Thermal Treatments of Quaternary Compounds for Monograin Layer Solar Cells. 2012.
138. **Ranno Nahku**. Validation of Critical Factors for the Quantitative Characterization of Bacterial Physiology in Accelerostat Cultures. 2012.
139. **Petri-Jaan Lahtvee**. Quantitative Omics-level Analysis of Growth Rate Dependent Energy Metabolism in *Lactococcus lactis*. 2012.
140. **Kerti Orumets**. Molecular Mechanisms Controlling Intracellular Glutathione Levels in Baker's Yeast *Saccharomyces cerevisiae* and its Random Mutagenized Glutathione Over-Accumulating Isolate. 2012.
141. **Loreida Timberg**. Spice-Cured Sprats Ripening, Sensory Parameters Development, and Quality Indicators. 2012.
142. **Anna Mihhalevski**. Rye Sourdough Fermentation and Bread Stability. 2012.
143. **Liisa Arike**. Quantitative Proteomics of *Escherichia coli*: From Relative to Absolute Scale. 2012.
144. **Kairi Otto**. Deposition of In_2S_3 Thin Films by Chemical Spray Pyrolysis. 2012.
145. **Mari Sepp**. Functions of the Basic Helix-Loop-Helix Transcription Factor TCF4 in Health and Disease. 2012.
146. **Anna Suhhova**. Detection of the Effect of Weak Stressors on Human Resting Electroencephalographic Signal. 2012.
147. **Aram Kazarjan**. Development and Production of Extruded Food and Feed Products Containing Probiotic Microorganisms. 2012.
148. **Rivo Uiboupin**. Application of Remote Sensing Methods for the Investigation of Spatio-Temporal Variability of Sea Surface Temperature and Chlorophyll Fields in the Gulf of Finland. 2013.
149. **Tiina Kriščiunaite**. A Study of Milk Coagulability. 2013.
150. **Tuuli Levandi**. Comparative Study of Cereal Varieties by Analytical Separation Methods and Chemometrics. 2013.
151. **Natalja Kabanova**. Development of a Microcalorimetric Method for the Study of Fermentation Processes. 2013.
152. **Himani Khanduri**. Magnetic Properties of Functional Oxides. 2013.
153. **Julia Smirnova**. Investigation of Properties and Reaction Mechanisms of Redox-Active Proteins by ESI MS. 2013.
154. **Mervi Sepp**. Estimation of Diffusion Restrictions in Cardiomyocytes Using Kinetic Measurements. 2013.

155. **Kersti Jääger**. Differentiation and Heterogeneity of Mesenchymal Stem Cells. 2013.
156. **Victor Alari**. Multi-Scale Wind Wave Modeling in the Baltic Sea. 2013.
157. **Taavi Päll**. Studies of CD44 Hyaluronan Binding Domain as Novel Angiogenesis Inhibitor. 2013.
158. **Allan Niidu**. Synthesis of Cyclopentane and Tetrahydrofuran Derivatives. 2013.
159. **Julia Geller**. Detection and Genetic Characterization of *Borrelia* Species Circulating in Tick Population in Estonia. 2013.
160. **Irina Stulova**. The Effects of Milk Composition and Treatment on the Growth of Lactic Acid Bacteria. 2013.
161. **Jana Holmar**. Optical Method for Uric Acid Removal Assessment During Dialysis. 2013.
162. **Kerti Ausmees**. Synthesis of Heterobicyclo[3.2.0]heptane Derivatives *via* Multicomponent Cascade Reaction. 2013.
163. **Minna Varikmaa**. Structural and Functional Studies of Mitochondrial Respiration Regulation in Muscle Cells. 2013.
164. **Indrek Koppel**. Transcriptional Mechanisms of BDNF Gene Regulation. 2014.
165. **Kristjan Pilt**. Optical Pulse Wave Signal Analysis for Determination of Early Arterial Ageing in Diabetic Patients. 2014.
166. **Andres Anier**. Estimation of the Complexity of the Electroencephalogram for Brain Monitoring in Intensive Care. 2014.
167. **Toivo Kallaste**. Pyroclastic Sanidine in the Lower Palaeozoic Bentonites – A Tool for Regional Geological Correlations. 2014.
168. **Erki Kärber**. Properties of ZnO-nanorod/In_2S_3/$CuInS_2$ Solar Cell and the Constituent Layers Deposited by Chemical Spray Method. 2014.
169. **Julia Lehner**. Formation of Cu_2ZnSnS_4 and $Cu_2ZnSnSe_4$ by Chalcogenisation of Electrochemically Deposited Precursor Layers. 2014.
170. **Peep Pitk**. Protein- and Lipid-rich Solid Slaughterhouse Waste Anaerobic Co-digestion: Resource Analysis and Process Optimization. 2014.
171. **Kaspar Valgepea**. Absolute Quantitative Multi-omics Characterization of Specific Growth Rate-dependent Metabolism of *Escherichia coli*. 2014.
172. **Artur Noole**. Asymmetric Organocatalytic Synthesis of 3,3'-Disubstituted Oxindoles. 2014.
173. **Robert Tsanev**. Identification and Structure-Functional Characterisation of the Gene Transcriptional Repressor Domain of Human Gli Proteins. 2014.
174. **Dmitri Kartofelev**. Nonlinear Sound Generation Mechanisms in Musical Acoustic. 2014.
175. **Sigrid Hade**. GIS Applications in the Studies of the Palaeozoic Graptolite Argillite and Landscape Change. 2014.
176. **Agne Velthut-Meikas**. Ovarian Follicle as the Environment of Oocyte Maturation: The Role of Granulosa Cells and Follicular Fluid at Pre-Ovulatory Development. 2014.

177. **Kristel Hälvin**. Determination of B-group Vitamins in Food Using an LC-MS Stable Isotope Dilution Assay. 2014.
178. **Mailis Päri**. Characterization of the Oligoadenylate Synthetase Subgroup from Phylum Porifera. 2014.
179. **Jekaterina Kazantseva**. Alternative Splicing of *TAF4*: A Dynamic Switch between Distinct Cell Functions. 2014.
180. **Jaanus Suurväli**. Regulator of G Protein Signalling 16 (RGS16): Functions in Immunity and Genomic Location in an Ancient MHC-Related Evolutionarily Conserved Synteny Group. 2014.
181. **Ene Viiard**. Diversity and Stability of Lactic Acid Bacteria During Rye Sourdough Propagation. 2014.
182. **Kristella Hansen**. Prostaglandin Synthesis in Marine Arthropods and Red Algae. 2014.
183. **Helike Lõhelaid**. Allene Oxide Synthase-lipoxygenase Pathway in Coral Stress Response. 2015.
184. **Normunds Stivrinš**. Postglacial Environmental Conditions, Vegetation Succession and Human Impact in Latvia. 2015.
185. **Mary-Liis Kütt**. Identification and Characterization of Bioactive Peptides with Antimicrobial and Immunoregulating Properties Derived from Bovine Colostrum and Milk. 2015.
186. **Kazbulat Šogenov**. Petrophysical Models of the CO_2 Plume at Prospective Storage Sites in the Baltic Basin. 2015.
187. **Taavi Raadik**. Application of Modulation Spectroscopy Methods in Photovoltaic Materials Research. 2015.
188. **Reio Põder**. Study of Oxygen Vacancy Dynamics in Sc-doped Ceria with NMR Techniques. 2015.
189. **Sven Siir**. Internal Geochemical Stratification of Bentonites (Altered Volcanic Ash Beds) and its Interpretation. 2015.
190. **Kaur Jaanson**. Novel Transgenic Models Based on Bacterial Artificial Chromosomes for Studying BDNF Gene Regulation. 2015.
191. **Niina Karro**. Analysis of ADP Compartmentation in Cardiomyocytes and Its Role in Protection Against Mitochondrial Permeability Transition Pore Opening. 2015.
192. **Piret Laht**. B-plexins Regulate the Maturation of Neurons Through Microtubule Dynamics. 2015.
193. **Sergei Žari**. Organocatalytic Asymmetric Addition to Unsaturated 1,4-Dicarbonyl Compounds. 2015.
194. **Natalja Buhhalko**. Processes Influencing the Spatio-temporal Dynamics of Nutrients and Phytoplankton in Summer in the Gulf of Finland, Baltic Sea. 2015.
195. **Natalia Maticiuc**. Mechanism of Changes in the Properties of Chemically Deposited CdS Thin Films Induced by Thermal Annealing. 2015.
196. **Mario Öeren**. Computational Study of Cyclohexylhemicucurbiturils. 2015.
197. **Mari Kalda**. Mechanoenergetics of a Single Cardiomyocyte. 2015.

198. **Ieva Grudzinska**. Diatom Stratigraphy and Relative Sea Level Changes of the Eastern Baltic Sea over the Holocene. 2015.
199. **Anna Kazantseva**. Alternative Splicing in Health and Disease. 2015.
200. **Jana Kazarjan**. Investigation of Endogenous Antioxidants and Their Synthetic Analogues by Capillary Electrophoresis. 2016.
201. **Maria Safonova**. SnS Thin Films Deposition by Chemical Solution Method and Characterization. 2016.
202. **Jekaterina Mazina**. Detection of Psycho- and Bioactive Drugs in Different Sample Matrices by Fluorescence Spectroscopy and Capillary Electrophoresis. 2016.
203. **Karin Rosenstein**. Genes Regulated by Estrogen and Progesterone in Human Endometrium. 2016.
204. **Aleksei Tretjakov**. A Macromolecular Imprinting Approach to Design Synthetic Receptors for Label-Free Biosensing Applications. 2016.
205. **Mati Danilson**. Temperature Dependent Electrical Properties of Kesterite Monograin Layer Solar Cells. 2016.
206. **Kaspar Kevvai**. Applications of ^{15}N-labeled Yeast Hydrolysates in Metabolic Studies of *Lactococcus lactis* and *Saccharomyces Cerevisiae*. 2016.
207. **Kadri Aller**. Development and Applications of Chemically Defined Media for Lactic Acid Bacteria. 2016.
208. **Gert Preegel**. Cyclopentane-1,2-dione and Cyclopent-2-en-1-one in Asymmetric Organocatalytic Reactions. 2016.
209. **Jekaterina Služenikina**. Applications of Marine Scatterometer Winds and Quality Aspects of their Assimilation into Numerical Weather Prediction Model HIRLAM. 2016.
210. **Erkki Kask**. Study of Kesterite Solar Cell Absorbers by Capacitance Spectroscopy Methods. 2016.
211. **Jürgen Arund**. Major Chromophores and Fluorophores in the Spent Dialysate as Cornerstones for Optical Monitoring of Kidney Replacement Therapy. 2016.
212. **Andrei Šamarin**. Hybrid PET/MR Imaging of Bone Metabolism and Morphology. 2016.
213. **Kairi Kasemets**. Inverse Problems for Parabolic Integro-Differential Equations with Instant and Integral Conditions. 2016.
214. **Edith Soosaar**. An Evolution of Freshwater Bulge in Laboratory Scale Experiments and Natural Conditions. 2016.
215. **Peeter Laas**. Spatiotemporal Niche-Partitioning of Bacterioplankton Community across Environmental Gradients in the Baltic Sea. 2016.
216. **Margus Voolma**. Geochemistry of Organic-Rich Metalliferous Oil Shale/Black Shale of Jordan and Estonia. 2016.
217. **Karin Ojamäe**. The Ecology and Photobiology of Mixotrophic Alveolates in the Baltic Sea. 2016.
218. **Anne Pink**. The Role of CD44 in the Control of Endothelial Cell Proliferation and Angiogenesis. 2016.

219. **Kristiina Kreek**. Metal-Doped Aerogels Based on Resorcinol Derivatives. 2016.
220. **Kaia Kukk**. Expression of Human Prostaglandin H Synthases in the Yeast Pichia pastoris. 2016.
221. **Martin Laasmaa**. Revealing Aspects of Cardiac Function from Fluorescence and Electrophysiological Recordings. 2016.
222. **Eeva-Gerda Kobrin**. Development of Point of Care Applications for Capillary Electrophoresis. 2016.
223. **Villu Kikas**. Physical Processes Controlling the Surface Layer Dynamics in the Stratified Gulf of Finland: An Application of Ferrybox Technology. 2016.
224. **Maris Skudra**. Features of Thermohaline Structure and Circulation in the Gulf of Riga. 2017.
225. **Sirje Sildever**. Influence of Physical-Chemical Factors on Community and Populations of the Baltic Sea Spring Bloom Microalgae. 2017.
226. **Nicolae Spalatu**. Development of CdTe Absorber Layer for Thin-Film Solar Cells. 2017.
227. **Kristi Luberg**. Human Tropomyosin-Related Kinase A and B: from Transcript Diversity to Novel Inhibitors. 2017.
228. **Andrus Kaldma**. Metabolic Remodeling of Human Colorectal Cancer: Alterations in Energy Fluxes. 2017.
229. **Irina Osadchuk**. Structures and Catalytic Properties of Titanium and Iridium Based Complexes. 2017.
230. **Roman Borozнjak**. A Computational Approach for Rational Monomer Selection in Molecularly Imprinted Plolymer Synthesis. 2017.
231. **Sten Erm**. Use of Mother-Daughter Multi-Bioreactor Systems for Studies of Steady State Microbial Growth Space. 2017.
232. **Merike Kriisa**. Study of ZnO:In, Zn(O,S) and Sb_2S_3 Thin Films Deposited by Aerosol Methods. 2017.
233. **Marianna Surženko**. Selection of Functional Starter Bacteria for Type I Sourdough Process. 2017.
234. **Nkwusi God'swill Chimezie**. Formation and Growth of Cu_2ZnSnS_4 Monograin Powder in Molten CdI_2. 2017.
235. **Ruth Tomson**. Urea- and Creatinine-Based Parameters in the Optical Monitoring of Dialysis: The Case of Lean Body Mass and Urea Rebound Assessment. 2017.
236. **Natalja Jepihhina**. Heterogeneity of Diffusion Restrictions in Cardiomyocytes. 2017.
237. **Sophie Maria Teresa Marinucci de Reguardati**. High-Accuracy Reference Standards for Quantitative Two-Photon Absorption Spectroscopy. 2017.
238. **Martin Lints**. Optimised Signal Processing for Nonlinear Ultrasonic Nondestructive testing of Complex Materials and Biological Tissues. 2017.
239. **Maris Pilvet**. Study of $Cu_2(Zn,Cd)SnS_4$ Absorber Materials for Monograin Layer Solar Cells. 2017.